# UV/$TiO_2$ ASSISTED PHOTOCATALYTIC DEGRADATION OF SOME SELECTED VAT AND AZO PIGMENTS USING BOX BECKHEN DESIGN

**BY**

**SULEIMAN PENDO UKANAH**

**DEPARTMENT OF TEXTILE SCIENCE AND TECHNOLOGY,**
**FACULTY OF SCIENCE,**
**AHMADU BELLO UNIVERSITY, ZARIA.**
**NIGERIA.**

**SEPTEMBER, 2014.**

# UV/$TiO_2$ ASSISTED PHOTOCATALYTIC DEGRADATION OF SOME SELECTED VAT AND AZO PIGMENTS USING BOX BECKHEN DESIGN

**BY**

**Suleiman Pendo UKANAH, B.Sc. (A.B.U) 2010**
**M.Sc/Sci/1536/2011-2012**

**A THESIS SUBMITTED TO THE SCHOOL OF POSTGRADUATE STUDIES,**
**AHMADU BELLO UNIVERSITY, ZARIA**

**IN PARTIAL FULFILMENT OF THE REQUIREMENTS FOR THE AWARD**
**OF A**
**MASTER OF SCIENCE DEGREE**
**IN COLOUR CHEMISTRY AND TECHNOLOGY.**

**DEPARTMENT OF TEXTILE SCIENCE AND TECHNOLOGY,**
**FACULTY OF SCIENCE,**
**AHMADU BELLO UNIVERSITY, ZARIA**
**NIGERIA.**

**SEPTEMBER, 2014**

## DECLARATION

I hereby declare that this thesis entitled UV/$TiO_2$ Assisted Photocatalytic Degradation of Some Selected Vat and Azo Pigments Using Box- Beckhen Design was carried out by me in the Department of Textile Science and Technology, Ahmadu Bello University, Zaria, under the supervision of Prof. P.O. Nkeonye, Prof. M.K. Yakubu and Dr. A. Giwa.

The information derived from the literature has been duly acknowledged in the text and a list of references provided. No part of this thesis was previously presented for another degree or diploma in any Institution.

| Ukanah Suleiman Pendo | _____ | _____ |
|---|---|---|
| Name of Student | Signature | Date |

## CERTIFICATION

This thesis entitled **"UV/$TiO_2$ ASSISTED PHOTOCATALYTIC DEGRADATION OF SOME SELECTED VAT AND AZO PIGMENTS USING BOX-BECKHEN DESIGN"** by Suleiman Pendo Ukanah, meets the regulations governing the award of the degree of M.Sc in Colour Chemistry and Technology, and is approved for its contribution to knowledge and literary presentation.

| | | |
|---|---|---|
| Prof. P.O. Nkeonye | | |
| Chairman, Supervisory Committee | Signature | Date |
| Prof. M.K. Yakubu | | |
| Member, Supervisory Committee | Signature | Date |
| Dr. A. Giwa | | |
| Member, Supervisory Committee | Signature | Date |
| Dr. A. Danladi | | |
| Head of Department | Signature | Date |
| Prof. A.Z. Hassan | | |
| Dean, School of Postgraduate Studies | Signature | Date |

## DEDICATION

This research thesis is dedicated to the Almighty God for His protection over my life and for making this research work a success.

## ACKNOWLEDGEMENTS

Without any reservation, my profound gratitude goes to the Almighty God who has given me the opportunity of living to this day in good health and acquiring a postgraduate education. I say thank you God for without you, I really cannot define my niche on this ecosystem.

Also, my heartfelt gratitude goes to my supervisors; Prof. P. O. Nkeonye, Prof. M.K. Yakubu and Dr. A. Giwa without whose close supervision, accessibility and understanding, this work would not have been completed.

Indeed, I am most grateful to my parents; Mrs Rekiyatu Ukanah & Mr. S.A. Ukanah of blessed memory, Mr. & Mrs. J.O. Lawal and Pastor & Mrs. L.A. Lawal who through thick and thin were always there for me and never doubted my abilities to achieve my goals. Mummies and Daddies, thanks for your constant support and enthusiasm. I love you all and I pray God grant us prosperous long life to reap the fruits of our labour, amen.

I also appreciate the immeasurable love and kindness of my aunts and uncles among whom are: Aunty Sa'adat and family, Uncle Elliot and family and Bro. John Ogbodo and family.

Special thanks also go to my siblings for being there for me both spiritually and otherwise. They include: Ustaz Yunus Ukanah and family, Mrs Saiki Hajarat and family, Mrs Balogun Mariam and family, Mrs Gabriel Esther and family, Mrs Raji Hannah and family, Ozofu, Nuratu, Khadijat, Solomon, Ruth, Salamatu, Adams, Oke, Michael, Oiza, and Famous. I love you all.

I would like to appreciate the effort of my colleague and roommate in the person of Suleiman Mohammed Awalu who was always by my side encouraging me and also

very supportive. Indeed, you are one in a million and more than just a friend and colleague. I pray God rewards you immensely. Lets do it again in Ph.D.

My profound gratitude also goes to my one time tutor and friend in the person of Engr. Olowojoba Emmanuel Ofuje who showed me love and kindness wholeheartedly. I really cannot thank you completely but I pray God rewards you in manifold ways, amen.

I also appreciate the hall administrator of Suleiman Hostel in the person of Alh. S.A. Badamasi and my fellow prostgraduate students who reside in the aforementioned hostel for their co-operation and support accorded me during my tenure in office as the governor of Suleiman hostel – postgraduate students' domain.

Finally, I would like to thank the following for their generosity in helping to make this research as complete as possible. They include; Mr. Elijah Danladi, Pastor Victor Olabode, Mal. S.A. Ameuru, Mr. Emmanuel Okechukwu (Igwe), Sheik Abdulrahman Salisu, Mr. Ibrahim Oladimeji Kereem, Mal. Idris Danjuma, Mal. Zaharadeen Salisu, Miss Franker Imadegbor, Miss Blessing Daniel Enejo, Mr. Musa Azaido, Mr. Tajudeen Adekeye, Mr. S.O. Okeje, Mal. Abdullahi Baba, Mal. Salisu Lawal, Mal. Nuhu Lawal, Mr. Ijai Ayuba Thliza, all the staff of the Department of Textile Science and Technology, my friends and colleagues in and outside the department and all well wishers. I thank you all and I pray God reward you all.

For those whose names were not mentioned, take it as an oversight from me and pardon me for that meanwhile I also pray God rewards you all.

## ABSTRACT

In this study, photocatalytic degradation has been studied on four water insoluble colorants; two of these are commercial vat pigments; Caledon Khaki 2G (C.I Vat Green 8) and Caledon Green 2G (C.I Vat Green 2) while the other two were azo pigments synthesized in the laboratory in excellent yields via diazotization of p-nitroaniline and coupling with 2-hydroxy-3-naphthanilide and N,N-dimethylaniline respectively. The pigments samples were dissolved in dimethylformamide (DMF) to enhance solute-solvent interaction. The two synthesized azo pigments were characterized by melting point analysis, solubility test, uv-visible spectroscopy, infrared spectroscopy and mass spectroscopy. Suitable experimental design such as Box Beckhen design and multivariate analysis which allows adjustment of factor level to obtain an optimal response in experimental analysis was used for the optimization of colour removal from aqeous solution using UV radiation and $TiO_2$ as photocatalyst. The photodegradation studies were conducted by dissolving 0.1g of each pigment sample in 100ml of DMF contained in four separate volumetric flasks to make a stock solution. Several other concentrations as stipulated by the design of experiment (DOE) were prepared from the stock solution and used in the degradation studies. The photocatalytic degradation study of the dissolved pigments in DMF was then carried out using a laboratory scale photoreactor for both the synthesized azo pigments and commercial vat pigments under UV light as a function of irradiation time, catalyst loading, pigment concentration and pH using titanium dioxide as the photocatalyst. The effects of these various operational parameters were investigated during the process and the extent of colour disappearance was determined using UV-vis Spectrophotometer at the wavelength of maximum absorption of each pigment sample and decolorization performance of over 95% was achieved. The results for the optimization revealed the following optimum conditions for degradation: initial pigment concentration 18.34 mg/L, catalyst loading 1.47 g/L, pH of 8.71 and irradiation time of 88.36 min. for Caledon Khaki 2G. The optimum conditions for the Caledon Green 2G were: initial pigment concentration of 19.13 mg/L, catalyst loading of 1.17 g/L, pH of 8.40 and irradiation time of 81.28 min. For the first synthesized azo pigment (AP1), its optimum conditions for degradation were: initial pigment concentration of 20 mg/L, catalyst loading of 1.53 g/L, pH of 9.38 and irradiation time of 89.29 min. while the optimum conditions of the second synthesized azo pigment (AP2) were; initial pigment concentration of 18.14 mg/L, catalyst loading of 1.50 g/L, pH of 9.85 and irradiation time of 83.46 min. It can be concluded that UV/$TiO_2$ photocatalytic degradation of textile pigments using Box Beckhen design is a viable technique for the treatment of textile waste effluents since it is multivariate in approach which allows adjustment of factor level to obtain an optimal response in experimental analysis.



**Keywords: Photocatalytic, UV Irradiation, Titanium dioxide, Azo pigment, Vat Pigment, Degradation.**

## TABLE OF CONTENTS


Cover Page - - - - - - - - - i

Title Page - - - - - - - - - ii

Declaration - - - - - - - - - iii

Certification - - - - - - - - - iv

Dedication - - - - - - - - - v

Acknowledgement - - - - - - - - - vi

Abstract - - - - - - - - - viii

Table of contents - - - - - - - - - ix

List of Tables - - - - - - - - - - xiii

List of Figures - - - - - - - - - - xiv

List of Schemes - - - - - - - - - - xvii

List of Appendice - - - - - - - - - xviii

**CHAPTER ONE**

1.0 **INTRODUCTION** - - - - - - - **1**

1.1 Statement of Research Problem - - - - - - 4

1.2 Justification/Significance of the study - - - - - 4

1.3 Aim and Objectives of the research - - - - - 5

1.4 Scope of the study - - - - - - - - 5

**CHAPTER TWO**

**2.0 LITERATURE REVIEW** - - - - - - **6**

**2.1 Pigments** - - - - - - - - - **6**

2.2 Classification of pigments - - - - - - - 8

**2.3 Azo pigments** - - - - - - - - **8**

2.3.1 Classification of azo pigments - - - - - - 10

**2.4 Vat pigments - - - - - - - - 16**

2.4.1 Perylene pigments - - - - - - - 17

2.4.2 Perinone pigments - - - - - - - 19

2.4.3 Thioindigo pigments - - - - - - - 21

**2.5 Titanium dioxide - - - - - - - - 23**

2.5.1 Production of Titanium dioxide - - - - - - 23

2.5.2 Applications of Titanium dioxide - - - - - 26

**2.6 Pigment/Dye removal techniques from wastewater - - - 30**

2.6.1 Advance Oxidation Process (AOP's) - - - - - 31

2.6.2 Decolorization by fungi - - - - - - - 35

2.6.3 Membrane filtration - - - - - - - 36

2.6.4 Coagulation/Flocculation - - - - - - 37

2.6.5 Adsorption - - - - - - - - 37

2.6.6 Sedimentation - - - - - - - - 37

**CHAPTER THREE**

**3.0 MATERIALS AND METHODS - - -- - - 38**

3.1 Materials - - - - - - - - - 38

3.2 Equipments and Apparatus - - - - - - 39.

**3.3 The commercial vat and synthesized azo pigments - - - 39**

3.3.1 The commercial vat pigments - - - - - - 39

3.3.2 Synthesis of the azo pigments - - - - - - 41

3.3.3 Spectral analysis of the synthesized azo pigments - - - 42

**3.4 Determination of molar extinction coefficient of the synthesized azo pigments - - - - - - - - - - - 43**

**3.5 Photodegradation Studies of synthesized azo pigments and commercial vat pigment - - - - - - - - - 43**

**CHAPTER FOUR**

**4.0 RESULTS - - - - - - - - 51**

4.1 Structure and physical characteristics of the pigments - - - 51

4.2 Infrared Spectra of synthesized azo pigments - - - - 52

4.3 Gas Chromatography-Mass Spectroscopy (GC-MS) of synthesized azo pigments - - - - - - - - - - 52

4.4 Visible Absorption Spectra of synthesized azo pigment - - - 53

**CHAPTER FIVE**

**5.0 DISCUSSION - - - - - - - - 80**

**5.1 Synthesis of the diazonium salt - - - - - - 80**

5.2 Synthesis of the azo pigments - - - - - - 80

5.3 Visible Absorption Spectra of the pigments - - - - 81

5.4 Melting point determination of the pigments - - - - 81

**5.5 Spectra analysis of the pigments - - - - - 81**

5.5.1 Infrared spectra of the synthesized azo pigments - - - 81

5.5.2 Gas Chromatography-Mass Spectroscopy Spectra of Synthesized azo pigment - - - - - - - - - - 82

**5.6 Calibration curves of the pigment - - - - - 82**

**5.7 Photodegradation effects on the pigments solution - - - 83**

**5.8 Regression equation of percentage degradation versus pigment concentration, catalyst loading- - - - - - - - 95**

**CHAPTER SIX**

**6.0 Summary, Conclusion and Recommendations - - - 96**

6.1 Summary - - - - - - - - - 96

6.2 Conclusion - - - - - - - - 98

6.3 Recommendation - - - - - - - - 99

**REFERENCES - - - - - - - - 100**

**LIST OF APPENDICE - - - - - - - 111**

## LIST OF TAB LES

Table 3.1 Summary of experimental design for Caledon Khaki 2G and Caledon Green 2G - - - - - - - - 45

Table 3.2 Summary of experimental design for AP 1 and AP2 - - 46

Table 3.3 Design of experiment for Caledon Khaki 2G - - - 47

Table 3.4 Design of experiment for Caledon Green 2G - - - 48

Table 3.5 Design of experiment for AP 1 - - - - - 49

Table 3.6 Design of experiment for AP 2 - - - - - 50

Table 4.1 Physical Characteristics of the pigments - - - - 51

Table 4.2 Infrared Spectra analysis of the synthesized azo pigments- - 52

Table 4.3 GC-MS analysis of AP 1 - - - - - - 52

Table 4.4 Visible Absorption Spectra of synthesized azo pigment - - 53

Table 4.5 Design of experiment for Caledon Khaki 2G - - - 54

Table 4.6 Design of experiment for Caledon Green 2G - - - 55

Table 4.7 Design of experiment for AP 1 - - - - - 56

Table 4.8 Design of experiment for AP 2 - - - - - 57

## LIST OF FIGURES

Figure 2.1 Derivative of perylene and perinone pigments - - - 17

Figure 2.2 Preparation of perylene pigments - - - - - 18

Figure 2.3 General structure of perylene pigments - - - - 19

Figure 2.4 Preparation of perinone pigments - - - - - 20

Figure 2.5 Generation of cis and trans isomers of perinone pigments - 21

Figure 2.6 Structure of some selected vat pigment - - - - 22

Figure 2.7 Schematic diagram of photocatalytic process initiated by photon acting on semiconductor - - - - - - - 33

Figure 3.1 Structure of Caledon Khaki 2G (C.I Vat Green 8) VP1 - - 40

Figure 3.2 Structure of Caledon Green 2G (C.I Vat Green 2) VP2 - - 40

Figure 3.3 Schematic diagram of the laboratory scale photoreactor - - 45

Figure 4.1 Calibration curve for VP1 - - - - - - 58

Figure 4.2 Calibration curve for VP2 - - - - - - 58

Figure 4.3 Calibration curve for AP1 - - - - - - 59

Figure 4.4 Calibration curve for AP2 - - - - - - 59

Figure 4.1a Standard residual vs Fitted value (VP1) - - - - 60

Figure 4.1b Histogram of frequency vs Standard residuals (VP1) - - 60

Figure 4.1c Normal probability plot of residual (VP1) - - - 61

Figure 4.1d Standardized residual vs observation order (VP1)- - - 61

Figure 4.1e Contour plot of %degradation vs pH, time of exposure (min.) VP1 62

Figure 4.1f Contour plot of %degradation vs pH, catalyst loading (g/L) VP1 62

Figure 4.1g Contour plot of %degradation vs time of exposure (min.), pigment concentration(mg/L) VP1 - - - - - 63

Figure 4.1h Contour plot of %degradation vs time of exposure (min.), pigment concentration(mg/L) (VP1) - - - - - - 63

Figure 4.1i Contour plot of %degradation vs pH, pigment concentration (mg/L) VP1 - - - - - - - - - 64

Figure 4.1j Contour plot of %degradation vs Catalyst loading (g/L), pigment concentration(mg/L) VP1 - - - - - - 64

Figure 4.2a Standard residual vs Fitted value (VP2) - - - - 65

Figure 4.2b Histogram of frequency vs Standardized residuals (VP2) - 65

Figure 4.2c Normal probability plot of residual (VP2) - - - 66

Figure 4.2d Standardized residual vs observation order (VP2) - - 66

Figure 4.2e Contour plot of %degradation vs pH, time of exposure (min.) VP2 67

Figure 4.2f Contour plot of %degradation vs pH, catalyst loading (g/L) VP2 67

Figure 4.2g Contour plot of %degradation vs time of exposure (min.), catalyst loading (mg/L) VP2 - - - - - - - 68

Figure 4.2h Contour plot of %degradation vs pH, pigment concentration (mg/L) VP2 - - - - - -- - - 68

Figure 4.2i Contour plot of %degradation vs time of exposure (min.), pigment concentration(mg/L) VP2 - - - - - 69

Figure 4.2j Contour plot of %degradation vs Catalyst loading (g/L), pigment concentration(mg/L) VP2 - - - - - 69

Figure 4.3a Standardized residual vs Fitted value (AP1) - - - 70

Figure 4.3b Histogram of frequency vs Standardized residual (AP1) - 70

Figure 4.3c Normal probability plot of residual (AP1) - - - 71

Figure 4.3d Standardized residual vs observation order (AP1) - - 71

Figure 4.3e Contour plot of %degradation vs pH, time of exposure (min.) AP1 72

Figure 4.3f Contour plot of %degradation vs pH, catalyst loading (g/L) AP1 72

Figure 4.3g Contour plot of %degradation vs time of exposure (min.), catalyst loading (mg/L) AP1 - - - - - - - 73

Figure 4.3h Contour plot of %degradation vs pH, pigment concentration (mg/L) AP1 - - - - - - - -- - 73

Figure 4.3i Contour plot of %degradation vs time of exposure (min.), pigment concentration (mg/L) VP2 - - - - - 74

Figure 4.3j Contour plot of %degradation vs Catalyst loading (g/L), pigment concentration(mg/L) AP1 - - - - - 74

Figure 4.4a Standardized residual vs Fitted value (AP2) - - - 75

Figure 4.4b Histogram of frequency vs Standardized residual (AP2) - 75

Figure 4.4c Normal probability plot of residual (AP2) - - - 76

Figure 4.4d Standardized residual vs observation order (AP2) - - 76

Figure 4.4e Contour plot of %degradation vs pH, time of exposure (min.) AP2 77

Figure 4.4f Contour plot of %degradation vs pH, catalyst loading (g/L) AP2 77

Figure 4.4g Contour plot of %degradation vs time of exposure (min.), catalyst loading (mg/L) AP2 - - - - - - - 78

Figure 4.4h Contour plot of %degradation vs pH, pigment concentration (mg/L) AP2 - - - - - - - - - 78

Figure 4.4i Contour plot of %degradation vs time of exposure (min.), pigment concentration (mg/L) AP2 - - - - - 79

Figure 4.4j Contour plot of %degradation vs Catalyst loading (g/L), pigment concentration (mg/L) AP2 - - - - - - 79

Figure 5.1 Structures of the coupling components used - - - 81

## LIST OF SCHEMES

Scheme 5.1 Schematic route for the diazotization of p-nitroaniline - - 80

Scheme 5.2 Schematic route for coupling with N,N-dimethylaniline. - 80

Scheme 5.3 Schematic route for coupling Naphthol AS. - - - 80

## LIST OF APPENDICE

APPENDICE A: Infra red spectra of synthesized azo pigments - - 111

APPENDICE B: Gas Chromatography-Mass Spectroscopy of synthesized azo pigment (AP1) - - - - - - - 112

APPENDICE C: Absorbance and Concentration of Pigments samples - 112

APPENDICE D: Box-Beckhen design for commercial vat and synthesized azo pigment- - - - - - - - - - - 113

# CHAPTER ONE

## 1.0 INTRODUCTION

Dyes and pigments are essential organic compounds which are extensively used by industries to colour textiles, papers, plastics, leather, food and cosmetics. These dyes and pigment molecules usually consist of chromogen and there exist about 12 of these chromogens of which azo type is the most common making about 60 – 70% of textile colorants (Giwa *et al*., 2012). At present, more than 10,000 azo colorants have been effectively commercialized (Leena and Selva, 2008). Azo dyes and pigments represent a major group of colorants and have wide applications in textile industries because of their ease of synthesis, versatility and cost-effectiveness. Although, due to inefficiencies of the industrial dyeing processes, about 10 - 15% of these colorants are lost in the effluents of textile units which render them highly coloured (Olukani *et al*., 2006). This massive influx of untreated organic chemicals into the waterways not only introduces aesthetic concerns, but far more importantly, it promotes eutrophication and adversely affects the environmental health of the region by reducing light penetration, thereby affecting aquatic life and limiting utilization of the water media (Vautier *et al*., 2001).

Majority of these commercial azo colorants are chemically stable and are difficult to remove from wastewater as they are stable to light, heat and oxidizing agents (Mamdouh *et al*., 1997), causing environmental concern because of their intense colour, biorecalcitrance, potential toxicity and carcinogenicity to animals and human beings (Siddiqui *et al*., 2009; Raju *et al*., 2007). These colorants (dyes and pigments) are xenobiotics and their decolourization in nature is rather difficult. Textile wastewaters are known to comprise of an amalgam of dyes, surfactants, and additives that are acquired

throughout the application processes. Because of the extensive variation in type and distribution of chemicals found in the effluents, no single, comprehensive method of treatment has been developed (Moraes *et al*., 2000). It is worthy of mention that some chemical and physical techniques (e.g. coagulation, ultra-filtration, reverse osmosis, etc.) also remove certain dyes from water. However, these techniques merely transfer the dyes from one form of waste to another (e.g liquid to solid), and, therefore, cannot be considered to be a complete treatment of the waste (Al-Momani and Touraud, 2002). Moreover, the techniques based on coagulation are dye specific; water-insoluble dyes are easily removed because of their preferential partitioning onto suspended particulates, flocs, and biomass, whereas water-soluble dyes are not eliminated (Al-Degs *et al*., 2000). One concern about using azo dyes is their toxicity. There are three known ways by which azo dyes can be toxic (Brown and De Vito, 1993). First, azo dyes themselves may be carcinogenic, a characteristic determined by the structure. For example, of the different isomers of hydrophobic azo dyes containing amino groups, para-isomers are carcinogenic and ortho-isomers are not carcinogenic (Cancer, 2010). Second, reduced azo dyes and cleavage of the azo linkage produces toxic aromatic amines, which have one or more aromatic rings in their molecular structure. Some of these compounds have negative environmental or health-related effects (Pinheiro *et al*. 2004). Third, azo dyes can be activated via direct oxidation of the azo linkage to highly reactive electrophilic diazonium salts. Thus, there is an urgent need to develop effective methods to treat these toxic textile industrial effluents. The use of photochemical technologies has been shown to be a promising alternative for the detoxification of industrial effluents (Legrini *et al*., 1993; Parsons, 2004), especially from the environmental point of view (Munoz *et al*., 2005). Heterogeneous photocatalytic

treatment is a more attractive alternative for the removal of soluble organic compounds. Contrary to physical processes, it can facilitate the complete mineralization of organic compounds to carbon dioxide, water, and mineral acids. Moreover, photocatalysis does not require expensive oxidants and can be carried out at mild temperature and pressure. However, the obligation to separate the small $TiO_2$ particles from the suspension after treatment limits the process development. Alternatively, the catalyst may be immobilized onto a suitable solid inert material, which eliminates the catalyst-removal step (Fernandez *et al*., 1995; Guillard *et al*., 2003; Lachheb *et al*., 2002), and permits the reuse of the photocatalyst several times.

Photocatalysis is therefore a process by which a semiconducting material absorbs light energy more than or equal to its band gap, thereby generating holes and electrons, which can further generate free-radicals in the system to oxidize the substrate. The resulting free-radicals are very efficient oxidizers of organic matter. The degradation of organic compounds is the most widely used photocatalytic application of nanocrystalline particles (Ralph and Mathew, 1992; Xiaodan *et al*., 2006). The photocatalytic decolorization of many dyes has been extensively and prominently explored in many previous studies by using different nanoparticles (Akpan and Hameed, 2009; Konstantinou and Albanis, 2004; Wang *et al*., 2000). Many studies revealed the effects of operating parameters on the photocatalytic degradation of textile dyes/pigments using $TiO_2$-based photocatalysts and concluded that various parameters, such as the initial pH of the colorant solution, oxidizing agents and catalyst loading exert their individual influence on the photocatalytic degradation of many colorants in aqueous solution (Nishio *et al*., 2006).

## 1.1 STATEMENT OF RESEARCH PROBLEM

Although several workers have reported photocatalytic degradation of water soluble colorants in the presence of $TiO_2$ catalyst but there is still scanty literatures in the area of degradation of water insoluble colorants. These insoluble colorants in waste waters present a significant problem in the wastewater due to their complex and varied chemical structure alongside other residual chemical reagents and impurities. The complexities of these chemical structures of synthetic organic pigments make them resistant to breakdown and remain fast for the lifetime of the fabric. They will not break down on exposure to sunlight, water, soap, etc. and are therefore difficult to treat in wastewater. Colour in wastewater is an obvious indicator of water pollution (Anliker and Clarke, 1982). The discharges of dye house wastewater into the environment is aesthetically displeasing, impede light penetration, damage the quality of the receiving streams and may be toxic to treatment processes, to food chain organisms and to aquatic life. The degradation of molecules of dyes/pigments in the environment by microorganisms is likely to be slow (Meyer, 1981), which means that it is possible for high levels of dye/pigment to persist, and potentially accumulate. Furthermore, any degradation that does occur may produce smaller molecules equally unfamiliar to the environment, such as amines, and may also be toxic. Hence, the adoption of photocatalysis which ensures completes mineralization of these organic contaminants into $CO_2$ and $H_2O$ (Sahel et al., 2007; Wang, 2007 and Skoeb et al., 2008).

## 1.2 JUSTIFICATION/SIGNIFICANCE OF THE STUDY

The development of industries and improvement of human life, cause more use of and need for coloured compounds (Shaylinda, 2005). Colour is a visible pollutant and its presence not only hampers the aesthetic quality of surface waters but also affects and alters the

aquatic ecosystem by reducing the penetration of light, hence the need for photodegradation of these coloured substances (dyes and pigments) using an eco-friendly method. $TiO_2$-based photocatalysis is an emerging technology aimed at decolorizing textile based water effluents since it leads to complete mineralization of organic carbons into carbon dioxide and it can be done at ambient conditions by using atmospheric oxygen as the oxidant. In addition, $TiO_2$ photocatalyst is very easy to come by, very cheap and non-toxic.

## 1.3 AIM AND OBJECTIVES OF THE RESEARCH

The aim of this research is to carry out photocatalytic degradation on some selected vat and synthesized azo pigments using Box-Beckhen design. This aim is achieved through the following objectives.

i. To select two commercial anthraquinone vat pigments.
ii. To synthesize some selected azo pigments.
iii. To carry out photodegradation studies on the synthesized azo pigments and some selected vat pigments.
iv. To optimize the photodegradation process by varying operational parameters like pH, initial concentration and catalyst loading, for improving the effectiveness of the process.
v. To characterize the pigments using FTIR/GC-MS.

## 1.4 SCOPE OF THE STUDY

This research is restricted only to Photocatalytic degradation of some selected vat and azo pigments both of which are insoluble in water.

# CHAPTER TWO

## 2.0 LITERATURE REVIEW

## 2.1 PIGMENTS

A pigment is a finely divided solid coloring material which is essentially insoluble in its application medium (Herbst and Hunger, 2004). Pigments are used mostly in the coloration of paints, printing inks, and plastics. Although, they are applied to a certain extent in a much wider range of substrates, including papers, textiles, rubbers, glasses, ceramics, cosmetics, crayons, and building materials such as cement and concrete. In most cases, the application of pigments involves their incorporation into a liquid medium, for example a wet paint or ink or a molten thermoplastic material, by a dispersion process in which clusters or agglomerates of pigment particles are broken down into primary particles and small aggregates. The pigmented medium is then allowed to solidify, either by solvent evaporation, physical solidification or by polymerisation and the individual pigment particles become fixed mechanically in the solid polymeric matrix. In contrast to textile dyes where the individual dye molecules are strongly attracted to the individual polymer molecules of the fibres to which they are applied, pigments are considered to have only a weak affinity for their application medium and only at the surface where the pigment particle is in contact with the medium. Pigments are incorporated to modify the optical properties of a substrate, the most obvious effect being the provision of colour. However, this is not the only optical function of a pigment. Pigment may also be required to provide opacity, most critically in paints, which are generally designed to protect the surface to which they are applied.

In chemical terms, pigments are conveniently classified as either inorganic or organic. These two broad groups of pigments are of roughly comparable importance

industrially. In general, inorganic pigments are capable of providing excellent resistance to heat, light, weathering, solvents and chemicals, and in these respects they can offer technical advantage over most organic pigments (Herbst and Hunger, 2004). In addition, inorganic pigments are generally of significantly lower cost than organics. On the other hand, they commonly lack the intensity and brightness of colour of typical organic pigments. Organic pigments are characterized by high colour strength and brightness although the fastness properties which they offer are somewhat variable. The ability either to provide opacity or to ensure transparency provides a further contrast between inorganic and organic pigments. While the inorganic pigments are characterize by high refractive index materials capable of giving high opacity, the organic pigments are of low refractive index and consequently are transparent. Surface treatments are commonly used to improve the performance of pigments. For example, treatment with organic surface active agents may lead to an improvement in the ease of dispersion into organic application media, while coating the particles with inorganic oxides, such as silica, may be used to improve the light fastness and chemical stability of certain inorganic pigments.

Pigments are versatile colouring agents that come with all round features to give credence to its suitability in a variety of media. Below are some of the features of pigments:

i. Excellent light and weather fastness.
ii. A good baking stability that makes them suitable for automotive and other industrial paints.
iii. High tinting strength.
iv. Good over spray fastness when applied to paints.

v. Gives heat stability of around 300°C in the case of polyolefins plastics.

vi. Excellent solvent resistance properties

vii. Easily dispersible.

## 2.2 CLASSIFICATION OF PIGMENTS

As earlier stated, pigments are classified into organic and inorganic pigments but for the purpose of this research work, emphasis is made on azo pigment which is an organic pigment.

## 2.3 AZO PIGMENTS

Azo pigments constitute by far the most important chemical class of commercial organic colorants. They account for around 60 - 70% of the colorants used in traditional textile applications and they occupy a similarly prominent position in the range of classical organic pigments. Azo pigments, as the name implies, contain as their common structural feature the azo (—N=N—) linkage which is attached at either side to two $sp^2$ carbon atoms. The synthesis of azo pigments is economically attractive, because of the standard sequence of diazonium salt formation and subsequent reaction with a wide choice of coupling components allows access to a wide range of products (Christie, 2001). The majority of the commercially important azo pigments contain a single azo group and are therefore referred to as monoazo pigments, but there are many which contain two (disazo), three (trisazo) or more such groups. In terms of their colour properties, azo pigments are capable of providing virtually a complete range of hues. There is no doubt that they are significantly more important commercially in yellow, orange and red colours (i.e. absorbing at shorter wavelengths), than in blues and greens. However, as a result of relatively recent research, the range of longer wavelength absorbing azo pigments has been extended, leading to the

emergence of significant numbers of commercially important blue azo pigments and there are even a few specifically-designed azo compounds which absorb in the near-infrared region of the spectrum (Venkataraman, 1978). Azo pigments are capable of providing high intensity of colour, about twice that of the anthraquinone and reasonably bright colours (Christie, 2004). They are capable of providing reasonable to very good technical properties, for example fastness to light, heat, water and other solvents, although in this respect they are often inferior to other chemical classes, for example carbonyl and phthalocyanine pigments, especially in terms of light fastness. Perhaps the prime reason for the commercial importance of azo colorants is that they are the most cost-effective of all the chemical classes of organic dyes and pigments. The reasons for this may be found in the nature of the processes used in their manufacture. The synthesis of azo pigments brings together two organic components, a diazo component and a coupling component in a two-stage sequence of reactions known as diazotization and azo coupling (Christie, 2001). The versatility of the chemistry involved in this synthetic sequence means that an immense number of azo pigments may be prepared and this accounts for the fact that they have been adapted structurally to meet the requirements of most colour applications. On an industrial scale, the processes are straight forward, making use of simple multi-purpose chemical plant. They are usually capable of production in high, often virtually quantitative yields and the processes are carried out at or below ambient temperatures, thus presenting low energy requirements. The synthesis involves low cost, readily available organic starting materials such as aromatic amines and phenols etc.

### 2.3.1 Classification of azo pigments

Azo pigments are classified according to the number of azo groups or by the type of diazo or coupling component. These classifications are as follows:

#### 2.3.1.1 Monoazo Yellow and Orange Pigments

The monoazo yellow pigment obtained by coupling a diazonium salt with acetoaceticarylides as coupling components cover the spectral range between greenish and medium yellow; while coupling with 1-arylpyrazolones-5 affords reddishyellow to orange shades. All members of this pigment family share good light fastness, combined with poor solvent and migration resistance. These properties define and limit their application. Monoazo yellow pigments are used extensively in air-dried alkyd resin and in emulsion paints, and certain inks used in flexo and screen printing. Other applications are in letter press and offset inks, as well as in office articles. Examples of monoazo yellow and orange pigments are the structures shown below.

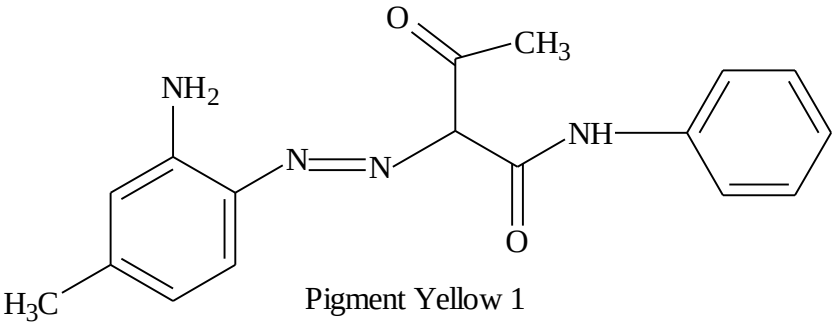


Pigment Yellow 1

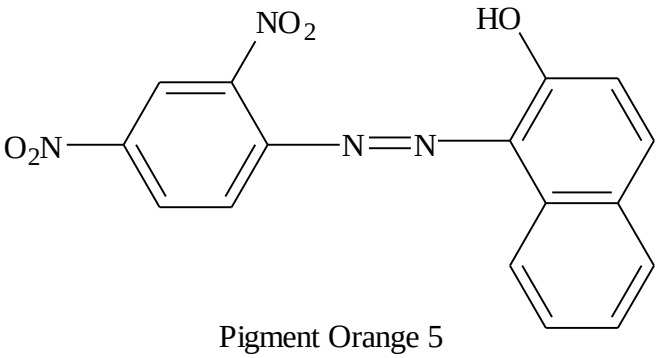


Pigment Orange 5

### 2.3.1.2 Disazo Pigments

There is a dual classification system based on differences in the starting materials. The first and most important group includes compounds whose synthesis involves the coupling of di- and tetra-substituted diaminodiphenyls as diazonium salts with acetoaceticarylides (diarylide yellows) or pyrazolones (disazo pyrazolones) as coupling components. The second group, bisacetoacetic arylide pigments, is obtained by diazotization of aromatic amines, followed by coupling onto bisacetoacetic arylides.The colour potential of disazo pigments covers the colour range from very greenish yellow to reddish yellow, orange and red. Most show poorer lightfastness and weather fastness; but better solvent and migration fastness than monoazo yellow and orange pigments. Their main applications are in printing inks and plastics, and to a lesser extent in coatings. Below is an example of disazo pigment.

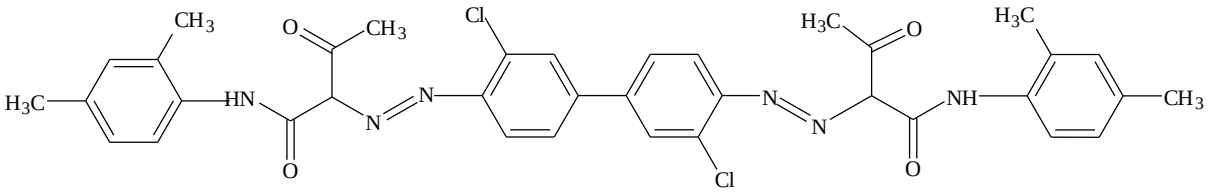


Pigment Yellow 13

### 2.3.1.3 β_Naphthol Pigments

β-Naphthol pigments provide colours in the range from orange to medium red. The typical coupling reaction with β-naphthol as a coupling component yields such well-known pigments as Toluidine Red and Dinitroaniline Orange. Their commercial application in paints requires good lightfastness. Solvent resistance, migration fastness and lightfastness are comparable to the monoazo yellow pigments.

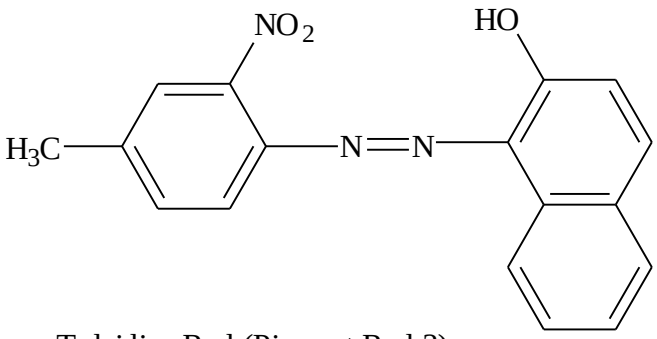


Toluidine Red (Pigment Red 3)

### 2.3.1.4 Naphtol AS Pigments (Naphtol Reds)

These pigments are obtained by coupling substituted aryl diazonium salts with arylides of 2-hydroxy-3-naphthoic acid (2-hydroxy-3-naphthoic acid anilide i.e. Naphtol AS). They provide a broad range of colors from yellowish and medium red to bordeaux, carmine, brown, and violet; their solvent fastness and migration resistance are only marginal. Naphtol AS pigments are used mainly in printing inks and paints.

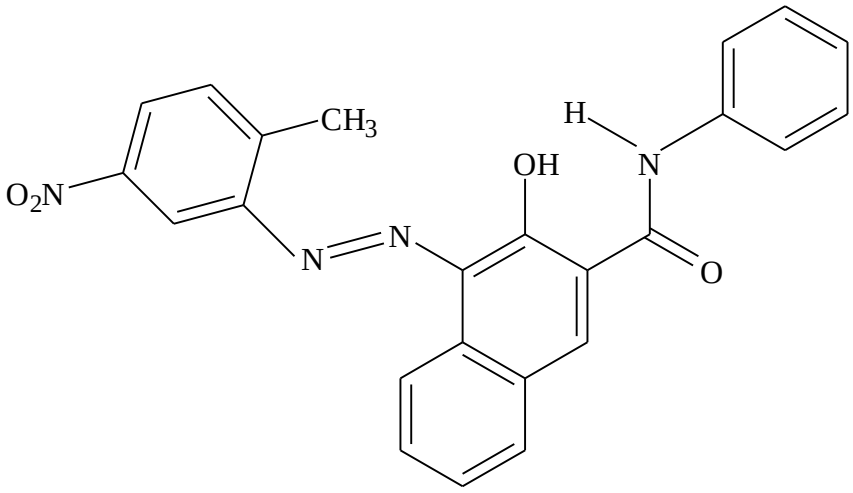


Pigment Red 22

### 2.3.1.5 Azo Pigment Lakes (Salt Type Pigments)

In Europe, pigments of this type are known as “toners”, but since this term is differently used elsewhere they can also be refer to as “lakes”, although a chemically correct description would be “salt type pigments”.

Historically, “lakes” refered to the first type of synthetic organic pigments made from water soluble dyes by precipitation onto alumina hydrate (aluminium hydroxide).

These pigments are formed by precipitating a monoazo compound which contains sulfo and/or carboxyl groups. The coupling component in the reaction may vary. β-naphthol lakes are derived from 2-naphthol, BONA pigment lakes use 2-hydroxy-3-naphthoic acid (Beta-Oxy-Naphthoic Acid); and Naphthol AS pigment lakes contain anilides of 2-hydroxy-3-naphthoic acid as a coupling component. Lakes may also be prepared from naphthalene sulfonic acids. Lake Red C is one of the commercially significant β-naphthol lakes. Limited lightfastness, which ranks far behind the non-laked β-naphthol counterparts, along with a tendency to migrate largely restricts their use mainly to the

printing inks field. Most BONA lake pigments provide an extra site for salt formation. Apart from the usual substituents, the diazo components of almost all BONA lake pigments contain a sulfonic acid functional group. Two acid substituents are thus available to form insoluble salts, which is the form in which these pigments are commercially available. Metal cations such as calcium, strontium, barium, magnesium, or manganese combine with the organic anion to produce shades between medium red and bluish red. Their use in printing inks exceeds their increasing use in plastics and paints. The organic acid group of Naphtol AS pigment lakes is part of the diazo component; a second site for salt formation can be provided by the coupling component. The plastics industry is the main user of such

lakes. Naphthalenesulfonic acid lake pigments are based on naphthalenesulfonic acid as a coupling component; introduction of an additional $SO_3H$ function as part of the diazo component is possible.

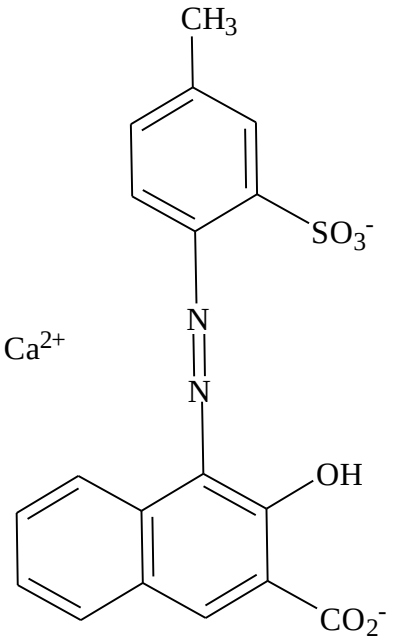


Lithol Rubine BK (Pigment Red 57)

**2.3.1.6 Benzimidazolone Pigments**

Benzimidazolone pigments feature the benzimidazolone structure, introduced aspart of the coupling component. The pigments that are obtained by coupling onto 5-acetoacetylaminobenzimidazolone cover the spectrum from greenish yellow to orange; while 5-(2b-hydroxy-3b-naphthoylamino)-benzimidazolone as a coupling component affords products that range from medium red to carmine, maroon, bordeaux, and brown shades. Pigment performance, including light fastness and weatherability, is generally excellent. Pigments that satisfy the specifications of the automobile industry are used to an appreciable extent in automotive finishes. Benzimidazolone pigments are also used extensively to colour plastics and high grade printing inks.

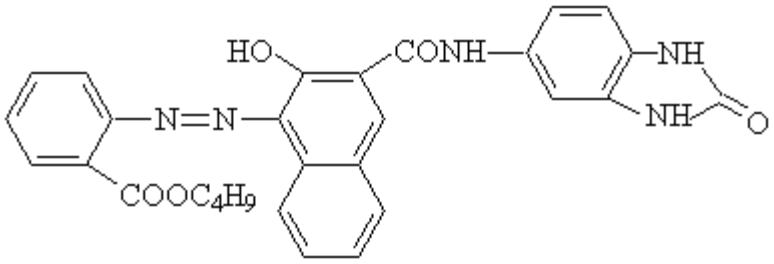


Pigment Red 208

**2.3.1.7 Disazo Condensation Pigments**

These pigments can formally be viewed as resulting from the condensation of two carboxylic monoazo components with one aromatic diamine. The resulting high molecular weight pigments show good solvent and migration resistance and generally provide good heat stability and lightfastness. Their main markets are in the plastics field and in spin dyeing. The spectral range of disazo condensation pigments extends from greenish yellow to orange and bluish red or brown.

**2.3.1.8 Metal Complex Pigments**

Only a few azo metal complexes are available as pigments. Most of these are very lightfast and weather fast. The chelating metal is usually nickel, and less commonly, cobalt or iron (II). The azo group (–N=N–) may be replaced by the analogous (–CH=N) moiety to form an azomethine complex pigment, usually with copper as a chelating metal. The number of commercially available products in this group is also restricted. They typically afford yellow shades. Those species that provide the required light fastness and weather resistance are used in automotive finishes and other industrial coatings.

**2.3.1.9 Isoindolinone and Isoindoline Pigments**

Although of comparatively good light and weather fastness, solvent and migration resistance, only a few members of the isoindolinone and isoindoline families' are

commercially available as pigments. Chemically classified as heterocyclic azomethines, these pigments produce greenish to reddish yellow hues. Isoindolinone pigments are preferably supplied for the pigmentation of plastics and high grade coatings.

## 2.4 VAT PIGMENTS

These are ancient pigments which include indigo and anthraquinone types that are chemically complexed and insoluble in water. They are usually reduced to the leuco form in alkaline solution of sodium hydrosulfite before application to the cotton or rayon fibre. Air oxidation fixes the pigment strongly on the fibre, resulting in excellent wash and light fastness. This class of pigment was one of the most important classes of pigment invented in the $20^{th}$ century. The first anthraquinone vat pigment, indanthrene was synthesized by Rene Bohn at BASF in Germany in 1901. He used synthetic indigo reaction conditions with β-aminoanthranquinone, fusing it with caustic potash, to obtain an insoluble blue substance resembling indigo both in appearance and the fact that it was rendered soluble by action of reducing agent in the presence of alkali. The substance proved to have the properties of a vat pigment and was introduced into the market under the trade name Indanthrene Blue. It was the first of a large number of anthraquinone vat piments which has vastly increased the range of shades and also the fastness of this group. Vat pigments are expensive and somewhat troublesome to apply, but their outstanding fastness makes them invaluable for many applications.

Some of the examples of vat dyes which are used as pigments are perylene, perinone and thioindigo. The perylene and perinone are chemically related and they follow the same synthetic route of production. While the groups of perylene pigments are derived from

perylene-3, 4, 9, 10-tetracarboxylic acid, the perinone pigments are derivatives of napthalene-1, 4, 5, 8-tetracarboxylic acid.

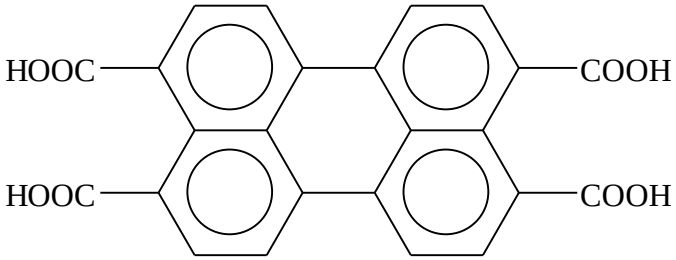


Perylene-3, 4, 9, 10-tetracarboxylic acid

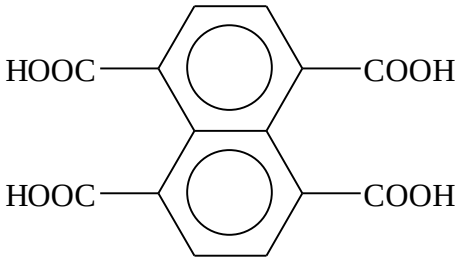


Napthalene-1, 4, 5, 8-tetracarboxylic acid

Figure 2.1: Derivative of perylene and perinone pigments

### 2.4.1 Perylene Pigments

These pigments are diimides of perylene tetracarboxylic acid. They are prepared by reaction of perylenetetracarboxylic dianhydride with primary aliphatic or aromatic amines in a high boiling solvent. The dianhydride which is the primary starting material for the synthesis of the perylene pigment is prepared by fusing 1,8-naphthalene dicarboxylic acid imide (naphthalic acid imide) with caustic alkali, for instance in sodium hydroxide/potassium hydroxide/sodium acetate at 190 to 220°C, followed by air oxidation of the molten reaction mixture or of the aqueous hydrolysate. The reaction initially affords

the bisimide (peryldiimide), which is subsequently hydrolyzed with concentrated sulfuric acid at 220°C to form the dianhydride:

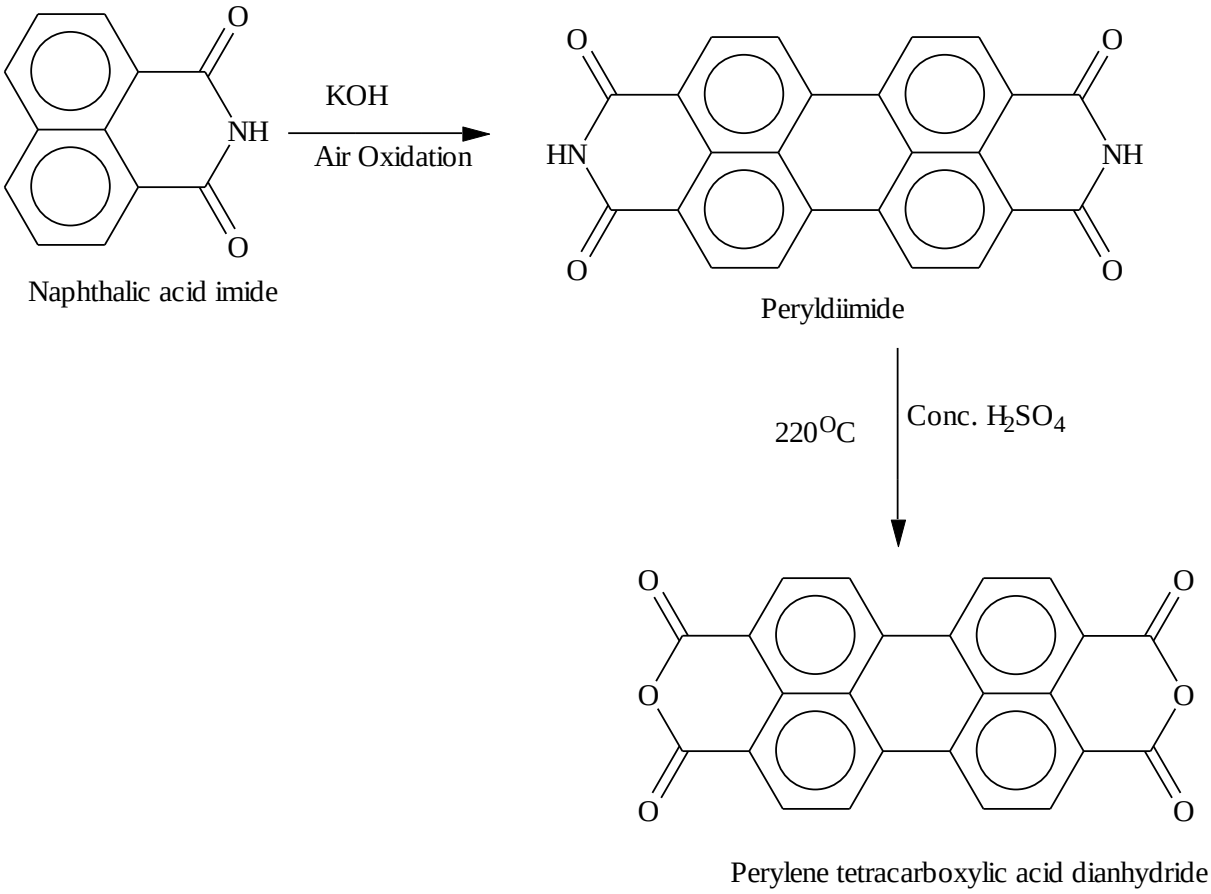


Figure 2.2: Preparation of perylene pigments

Heating perylene tetracarboxylic dianhydride, as described above from 150 to 250°C with a primary aliphatic or aromatic amine in a high boiling solvent affords the desired crude pigment. The reaction may be accelerated by adding agents such as sulfuric acid, phosphoric acid, or zinc salts. Perylene pigments are derivatives of the general structure shown below.

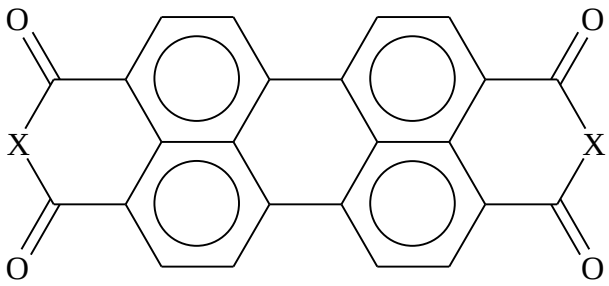


Figure 2.3: General structure of perylene pigments

In an industrially interesting pigment, X usually stands for O or N–R, and R represents H, $CH_3$, or possibly a substituted phenyl moiety. The phenyl ring may possess a methyl, a methoxy, an ethoxy, or an 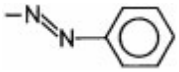 substituent.

**2.4.2 Perinone Pigments**

The yellowish red vat was one of the earliest commercial products of the perinone pigment which was discovered in 1924 by Eckert and Greune at Hoechst AG. It was used over a long time as vat dye on cotton until 1950 when it found recognition as pigment.

Perinone pigments are obtained from naphthalene-1, 4, 5, 8-tetracarboxylic acid or its monoanhydride. The acid, referred to as “tetra acid”, is prepared as follows by a Friedel–Crafts reaction, in which acenaphthene is reacted with malonic dinitrile and aluminum chloride. The resulting condensation product is oxidized with sodium chlorate/hydrochloric acid to form the dichloroacenaphthindandione. Oxidation with sodium hypochlorite solution/sodium permanganate affords naphthalene tetracarboxylic acid, mostly existing as the monoanhydride. The dianhydride, on the other hand, evolves only after drying at approximately 150°C.

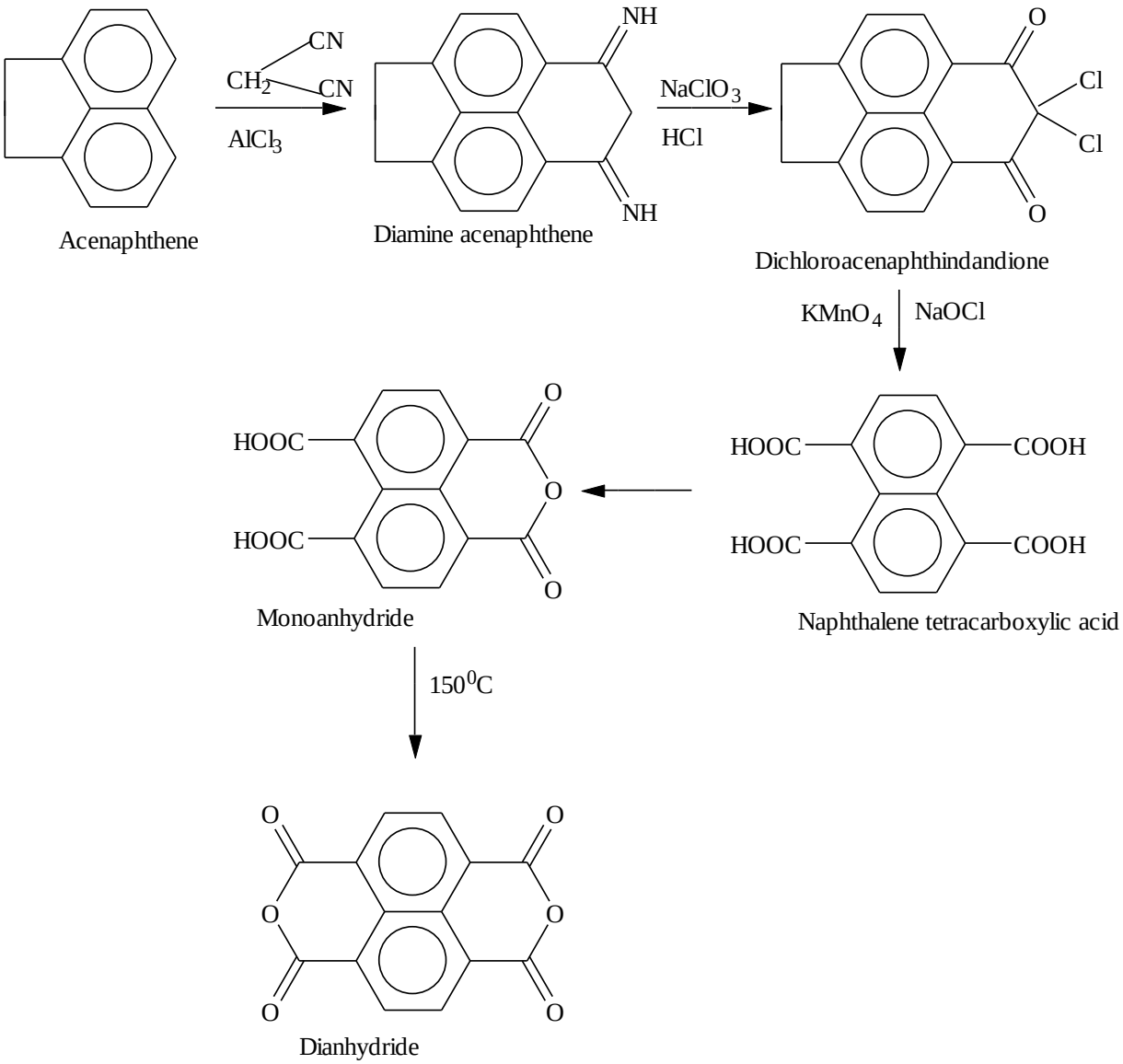


Figure 2.4: Preparation of perinone pigments

The perinone ring system is thus formed by condensation with aromatic o-diamines. Reaction of o-phenylenediamine with the monoanhydride is typically achieved in glacial acetic acid at 120°C. A mixture of the cis and trans isomers evolved which appeared as mixed crystals as shown in Figure 2.5.

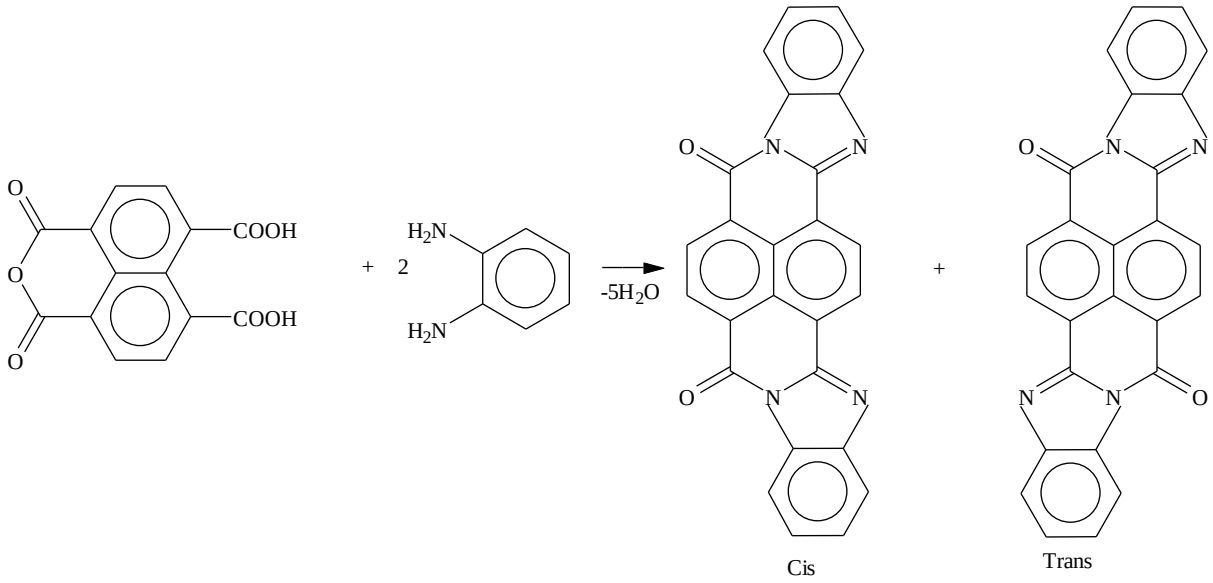


Figure 2.5: Generation of cis and trans isomers of perinone pigments

### 2.4.3 Thioindigo Pigments

4, 4', 7, 7'-Tetrachlorothioindigo with a reddish violet shade reigns supreme as a pigment among the derivatives of this indigo. It can be used for bordeaux shades in automotive refinishes. Thioindigo pigments are generally used in industrial coatings and plastics for their good lightfastness and weatherfastness in deeper shades.

Some other examples of vat pigments are shown below with their structures.

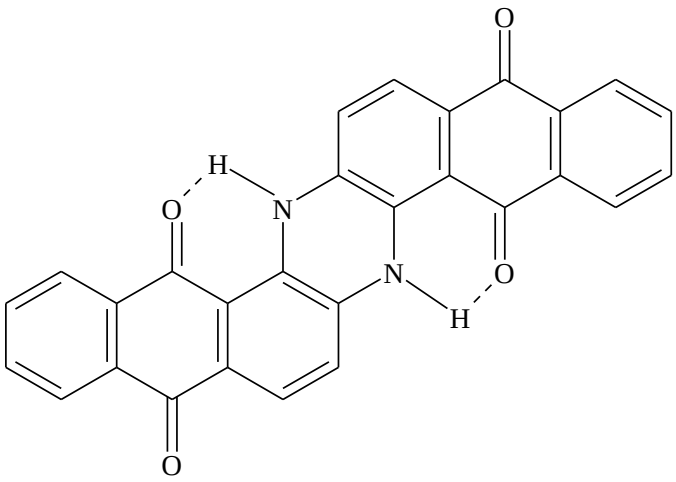


Indanthrone, C.I Vat Blue 4

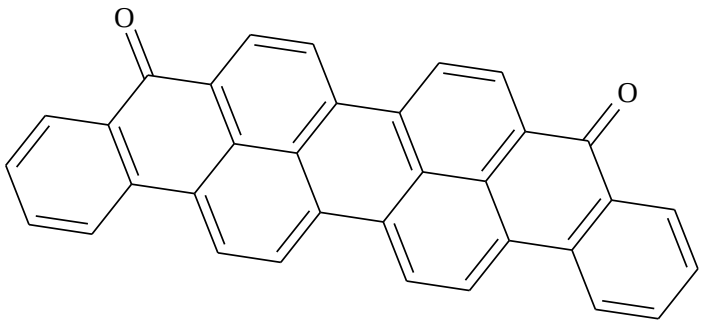


Violanthrone, C.I Vat Blue 20

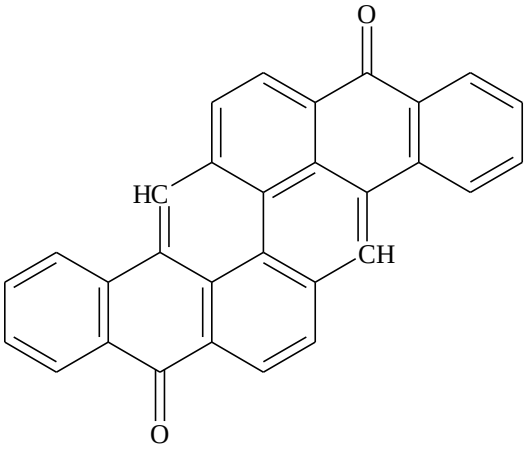


Pyranthrone, C.I Vat Orange 9

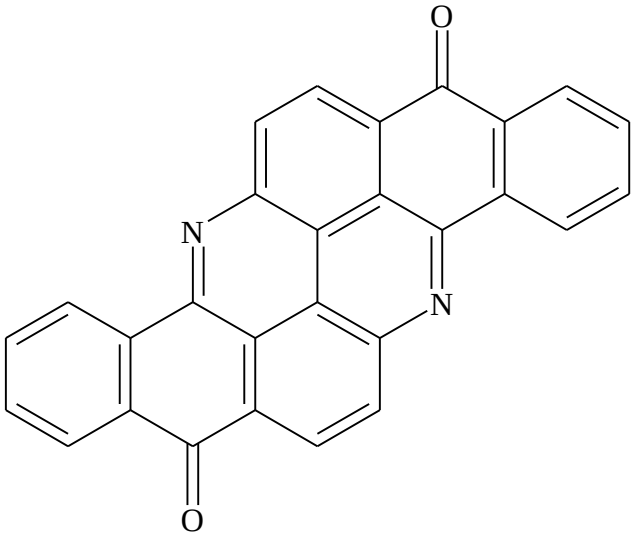


Flavanthrone, C.I Vat Yellow 1

Figure 2.6: Structures of some selected vat pigments

## 2.5 TITANIUM DIOXIDE

Titanium dioxide which is one of the most important white pigments finds widespread use in paints, plastics, printing inks, rubbers, papers, synthetic fibres, ceramics and cosmetics. It owes its dominant industrial position to its ability to provide a high degree of opacity and whiteness (maximum light scattering with minimum light absorption) and to its excellent durability and non-toxicity. The pigment is manufactured in two polymorphic forms, rutile and anatase, the former being far more important commercially because of its compactness and high density as compared to the latter. The rutile form has a higher refractive index (2.70) than the anatase form (2.55), a feature which is attributed to the particularly compact atomic arrangement in its crystal structure, and it is therefore more opaque. In addition, the rutile form is more durable (Nkeonye, 2012).

### 2.5.1 PRODUCTION OF TITANIUM DIOXIDE

Two processes are used in the manufacture of titanium dioxide pigments: the sulfate process and the chloride process. While the sulphate process is used for the production of anatase, the chloride process is used for the production of rutile.

#### 2.5.1.1 The sulphate process

The major portion of world's production of $TiO_2$ pigment is made by the sulphate process. The raw material mainly used is the ilmenite. The essential stages involved in this process are highlighted below (Nkeonye, 2012).

i. Drying and milling (ball–mill used) the ilmenite to reduce the particle size.

ii. Digesting the ground ore with $H_2SO_4$ to ensure uniform reaction rate. The reaction is done at 160°C and the mixture is converted to a porous cake containing ferric, ferrous and titanium sulphate. The cake is extracted with

water or dilute acid and the ferric iron in the mixture is reduced to ferrous by means of scrap iron. Thus, in the digester, we have:

$TiO_2 (SO_4)_3.FeSO_4$

(Tinyl sulphate and ferrous sulphate)

iii. Removing much of the iron impurities by crystallization as $FeSO_4.7H_2O$ (copperas) after cooling the solution to ≈10°C.

iv. Concentrating the solution by cooling.

v Precipitation of the titanium as hydrous titanium oxide (pulp):

$TiO (SO_4) \longrightarrow Ti (OH)$

Basic sulphate hydrous titanium oxide (pulp)

The pulp tends to consist of

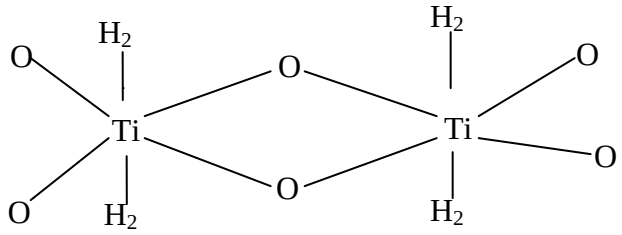


Pulp: particle size ≈100Å

Stage (v) is the most critical stage in the process. It must be carried out under carefully controlled conditions so as to produce a precipitate which can be readily filtered, and which will produce crystallites of the correct type on calcination.

vi Calcination in internally fired inclined rotary kilns, through which the pulp moves slowly under gravity.

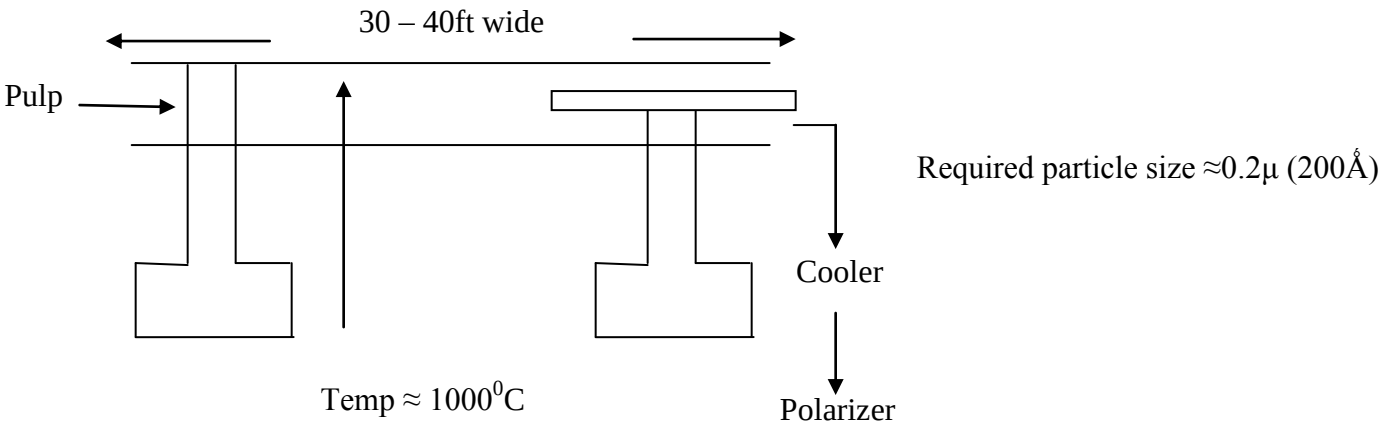


The composition of the entering pulp is

| | |
|---|---|
| 40% | $TiO_2$ |
| 4% | $H_2SO_4$ |
| 56% | $H_2O$ |

Control during calcination is based on physical testing of the product for example, colour, undertone and tint–reducing power.

vii Discharging the calcined material at the end of the kiln after several hours, then cooling and passing to a polarizer to break up any aggregates. Purities of ≈98–99% can be achieved by this process.

**2.5.1.2 The Chloride process**

In this chloride process, rutile titanium dioxide ore is initially treated with chlorine in the presence of carbon as a reducing agent at 800—1000°C to form titanium tetrachloride (Nkeonye, 2012). After purification by distillation, the tetrachloride is subjected to gas-phase oxidation at 1500°C with air or oxygen to yield a high purity, fine particle size rutile titanium dioxide pigment. Chlorine is generated at this stage and may be recycled. The two manufacturing processes are of roughly comparable importance on a worldwide basis. However, the chloride process offers certain inherent advantages over the sulfate route.

These include suitability for continuous operation, excellent control of pigment properties and fewer by-products, which in the case of the sulphate process can lead to waste disposal problems.

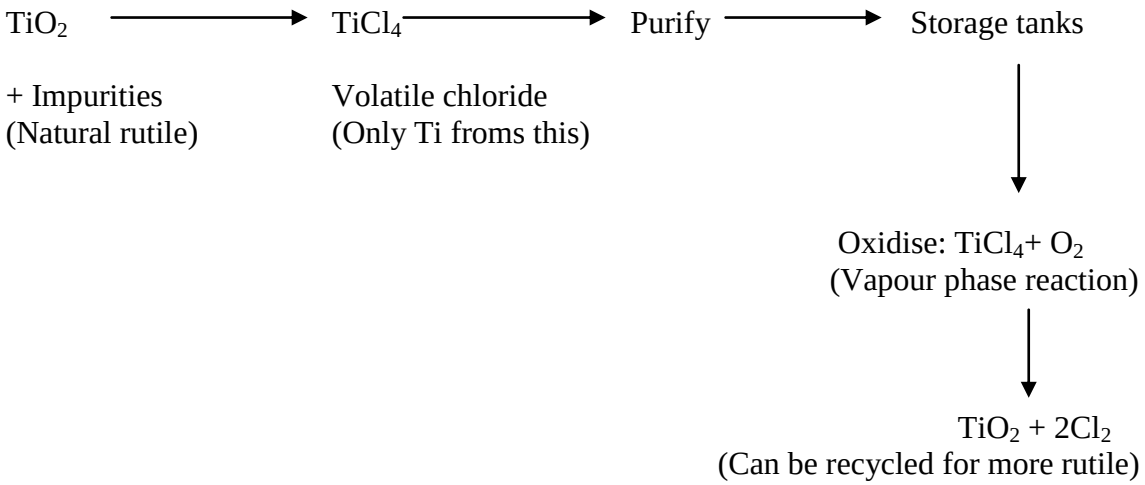


By strict control of the reaction, pure rutile of the required particle size can be obtained.

**2.5.2 Applications of Titanium Dioxide**

Titanium dioxide has seen many applications for its unique photocatalytic properties. Sunlight and near-UV light photoactivates the $TiO_2$. In the presence of water, the catalyst produces hydroxyl radicals that are capable of oxidizing organic compounds to carbon dioxide and water. Because of this important quality, $TiO_2$ has seen many uses in water treatment and purification (Tang and Huren, 1995; Pizarro *et al*., 2005). $TiO_2$ is a great material to work with because of its stability, low cost, and nontoxicity. There are two common forms of titanium dioxide, anatase and rutile, with anatase being the stronger oxidizer. However, most $TiO_2$ powders contain both types since performance is enhanced with the presence of rutile (Thiruvenkatachari *et al*., 2008). The fascination with titanium dioxide has continued to grow and products incorporating the material have reached market (Staff, 2009). Because of the knowledge, familiarity and wide acceptance in the scientific

community, $TiO_2$ is an ideal material to use in studies. Moreover, it is one of the most efficient photocatalysts (Reutergådh and Iangphasuk, 1997). Extensive studies have been carried out using $TiO_2$ for the degradation of organic compounds in attempts to understand the oxidation process (Tang and Huren, 1995; Pizarro *et al*., 2005; Liu *et al*., 2006b).

Titanium dioxide has been used as pigment, sunscreen, UV absorber and photocatalyst. These are further elaborated in the subsequent subsections.

#### 2.5.2.1 Pigment

Titanium dioxide is the most widely used white pigment because of its brightness and very high refractive index ($n$ = 2.7) in which it is surpassed only by a few other materials (Nkeonye, 2012). Approximately, 4 million tons of pigmentary $TiO_2$ are consumed annually worldwide (Winkler, 2003). When deposited as a thin film, its refractive index and colour makes it an excellent reflective optical coating for dielectric mirrors and some gemstones like "mystic fire topaz". $TiO_2$ is also an effective opacifier in powder form, where it is employed as a pigment to provide whiteness and opacity to products such as paints, coatings, plastics, papers, inks, foods, medicines (that is pills and tablets) as well as most toothpastes (Koleske, 1995). In paint, it is often referred to off handedly as "the perfect white", "the whitest white", or other similar terms. Opacity is improved by optimal sizing of the titanium dioxide particles. In ceramic glazes, titanium dioxide acts as an opacifier and seeds crystal formation.

Titanium dioxide is also used to whiten skimmed milk; this has been shown statistically to increase skimmed milk's palatability (Lance and Barbano, 1997).

#### 2.5.2.2 Sunscreen and UV absorber

In cosmetic and skin care products, titanium dioxide is used as a pigment, sunscreen and a

In cosmetic and skin care products, titanium dioxide is used as a pigment, sunscreen and a thickener. It is also used as a tattoo pigment and in styptic pencils (Marchand *et al*., 1980). Titanium dioxide is produced in varying particle sizes, oil and water dispersible, and with varying coatings for the cosmetic industry. This pigment is used extensively in plastics and other applications for its UV resistant properties where it acts as a UV absorber, efficiently transforming destructive UV light energy into heat (Winkler, 2003). Titanium dioxide is found in almost every sunscreen with a physical blocker because of its high refractive index, its strong UV light absorbing capabilities and its resistance to discoloration under ultraviolet light. This advantage enhances its stability and ability to protect the skin from ultraviolet light. Sunscreens designed for infants or people with sensitive skin are often based on titanium dioxide and/or zinc oxide, as these mineral UV blockers are believed to cause less skin irritation than other UV absorbing chemicals (Shaw *et al*., 2010). The titanium dioxide particles used in sunscreens have to be coated with silica or alumina, because titanium dioxide creates radicals in the photocatalytic reaction. These radicals are carcinogenic, and could damage the skin (Shaw *et al*., 2010).

**2.5.2.3 Photocatalyst**

Titanium dioxide, particularly in the anatase form, is a photocatalyst under ultraviolet (UV) light. Recently it has been found that titanium dioxide, when spiked with nitrogen ions or doped with metal oxide like tungsten trioxide, is also a photocatalyst under either visible or UV light. The strong oxidative potential of the positive holes oxidizes water to create hydroxyl radicals (Kurtoglu *et al*., 2011). It can also oxidize oxygen or organic materials directly. Titanium dioxide is thus added to paints, cements, windows, tiles, or other products for its sterilizing, deodorizing and anti-fouling properties and is used as a

hydrolysis catalyst. It is also used in dye-sensitized solar cells, which are a type of chemical solar cell (also known as a Graetzel cell).

Titanium dioxide has potential for use in energy production: as a photocatalyst, it can carry out hydrolysis; i.e., break water into hydrogen and oxygen. Were the hydrogen collected, it could be used as a fuel (Science daily, 2011). The efficiency of this process can be greatly improved by doping the oxide with carbón. Further efficiency and durability has been obtained by introducing disorder to the lattice structure of the surface layer of titanium dioxide nanocrystals, permitting infrared absorption. It can also produce electricity when in nanoparticle form. Research suggests that by using these nanoparticles to form the pixels of a screen, they generate electricity when transparent and under the influence of light (Earle, 1942). If subjected to electricity on the other hand, the nanoparticles blacken, forming the basic characteristics of a LCD screen. According to creator Zoran Radivojevic, Nokia has already built a functional 200-by-200-pixel monochromatic screen which is energetically self-sufficient.

In 1995, Fujishima and his group discovered the superhydrophilicity phenomenon for titanium dioxide coated glass exposed to sun light (Japan Nanonet Bulletin, 2005). This resulted in the development of self-cleaning glass and anti-fogging coatings. $TiO_2$ incorporated into outdoor building materials, such as paving stones in noxer blocks or paints, can substantially reduce concentrations of airborne pollutants such as volatile organic compounds and nitrogen oxides.

**2.5.2.4 Other applications of titanium dioxide**

i. Titanium dioxide in solution or suspension can be used to cleave protein that contains the amino acid proline at the site where proline is present.

ii. Titanium dioxide is also used as a material in the memristor, a new electronic circuit element. It can be employed for solar energy conversion based on dye, polymer, or quantum dot sensitized nanocrystalline $TiO_2$ solar cells using conjugated polymers as solid electrolytes.

iii. Synthetic single crystals and films of $TiO_2$ are used as a semiconductor and also in Bragg-stack style dielectric mirrors due to the high refractive index (2.5 – 2.9) of $TiO_2$ (Paschotta, 2009).

## 2.6 PIGMENTS/DYES REMOVAL TECHNIQUES FROM WASTE WATER

Several techniques including physical, chemical and biological pre-treatment and post-treatment have been employed over the years for the removal of colour from wastewaters (Nkeonye and Olivera-Campos, 2005; Abbas and Robab, 2010; Rauf, *et al*., 2005; and Ahmad and Pussa, 2007). The physical and chemical techinques include; adsorption, coagulation/flocculation, sedimentation and membrane filtration etc. The biological techniques include; aerobic and anaerobic treatment processes, bacterial and fungi biosorption process. Even though several factors (such as type of dye, the composition of the wastewaters, cost and dose of the chemicals used etc.) determine the efficacy of each of the techniques, they have certain disadvantages associated with them. The aerobic treatment process is associated with production and disposal of large amounts of biological sludge, while wastewater treated by anaerobic treatment method does not bring down the pollution parameters to the satisfactory level and activated charcoal adsorption and air stripping methods simply transfer the pollutants from one medium to another. They either transfer it to the atmosphere, which causes air pollution, or to a solid which is often disposed off in landfills or must be treated in an energy-intensive regeneration process.

Merely transferring toxic materials from one medium to another is not a long term solution to the problem of hazardous waste loading on the environment. The recent developments in water decontamination processes are concerned with the oxidation of these bio-recalcitrant organic compounds. These methods rely on the formation of highly reactive chemical species that degrade more number of recalcitrant molecules into biodegradable compounds and are called advanced oxidation processes (AOP's). Some of these dyes/pigments removal techniques are therefore discussed below.

### 2.6.1 Advanced Oxidation Processes (AOP's)

Advanced oxidation process (AOP) is defined as the oxidation process which generates hydroxyl radicals in sufficient quantity to effect water treatment. AOP uses Fenton's reagent to achieve high performance (Weinberg and Glaze, 1997). Presence of ozone and UV radiation enhances the performance of Fenton's reagent and is sometimes used for AOP (Ara˜na *et al.*, 2001). Hydroxyl radicals have very high oxidizing power of 2.8 eV and is next to fluorine, hence, degrade the organic hazardous dyes to $CO_2$ and $H_2O$ (Rathi *et al*., 2003) as shown in the equations below.

$$\bullet OH + RH \rightarrow R^{\bullet} + H_2O \qquad \text{(Eq. 2.1)}$$

$$R^{\bullet} + O_2 \rightarrow RO_2^{\bullet} \rightarrow \text{Products and } CO_2 \qquad \text{(Eq. 2.2)}$$

In literature, Fenton and Fenton-like reactions are found to be efficient for decolorizing and detoxifying textile effluents (Robinson *et al.*, 2001; Lunar *et al*., 2000; Kitis *et al*., 1999; Andreozzi *et al.*, 1999; Kuo, 1992; Kang *et al*., 2000; P´erez *et al*., 2002 and Meric *et al.*, 2004). Fenton reactions and $O_3$ oxidation are still the most basic and yet practical advanced oxidation processes for the treatment of industrial effluents including textile effluents (Martinez *et al*., 2003; Kaludjerski and Kurol, 2004).

AOPs have common principles in terms of the participation of hydroxyl radicals that are assumed to be operative during the reaction. Due to the instability of OH* radical, it must be generated continuously insitu through chemical or photochemical reactions (Yoon *et al.*, 2001). Hydroxyl radicals are generated by the reaction between $H_2O_2$ and ferrous ions. The slow reduction of $Fe^{3+}$ to $Fe^{2+}$ is the rate-determining step of the overall reaction. Thus, in AOP, rate of dye degradation is fast in the beginning due to high initial concentration of $Fe^{2+}$. However, subsequently the rate drastically reduces due to the drop in the concentration of $Fe^{2+}$ and poor rate of its regeneration (Neyens and Baeyens, 2003).

Several other combinations of homogenous and heterogeneous methods which involve the generation of free radicals are; (i) Photochemical irradiation with ultraviolet light (coupled with powerful oxidizing agents like ozone, hydrogen peroxide and /or a semiconductor), (ii) Fenton and Photo-Fenton catalytic processes (iii) Electron Beam irradiation technique and (iv) Sonolysis.

The advanced oxidative processes can be classified into two which include; homogeneous photocatalysis and heterogeneous photocatalysis.

**2.6.1.1 Homogeneous Photocatalysis**

Photocatalysis may be defined as a photoinduced reaction which is accelerated by the presence of a catalyst (Mills and Hunte, 1997). These types of reactions are activated by absorption of a photon with sufficient energy (equals or higher than the band-gap energy ($E_{bg}$) of the catalyst) (Carp *et al.*, 2004). The absorption leads to a charge separation due to promotion of an electron ($e^-$) from the valence band of the semiconductor catalyst to the conduction band, thus generating a hole ($h^+$) in the valence band (the schematic diagram of the process is presented in Figure 2.7.

The resulting hole is an oxidizing agent while the electron is a reducing agent. In the generally accepted mechanism for the photocatalytic process, the hole can react with water to generate the hydroxyl radical and the electron can reduce molecular oxygen, hydrogen peroxide or some other oxidizing agent in the solution. This creates the reactive radicals responsible for the removal of hazardous components from the water.

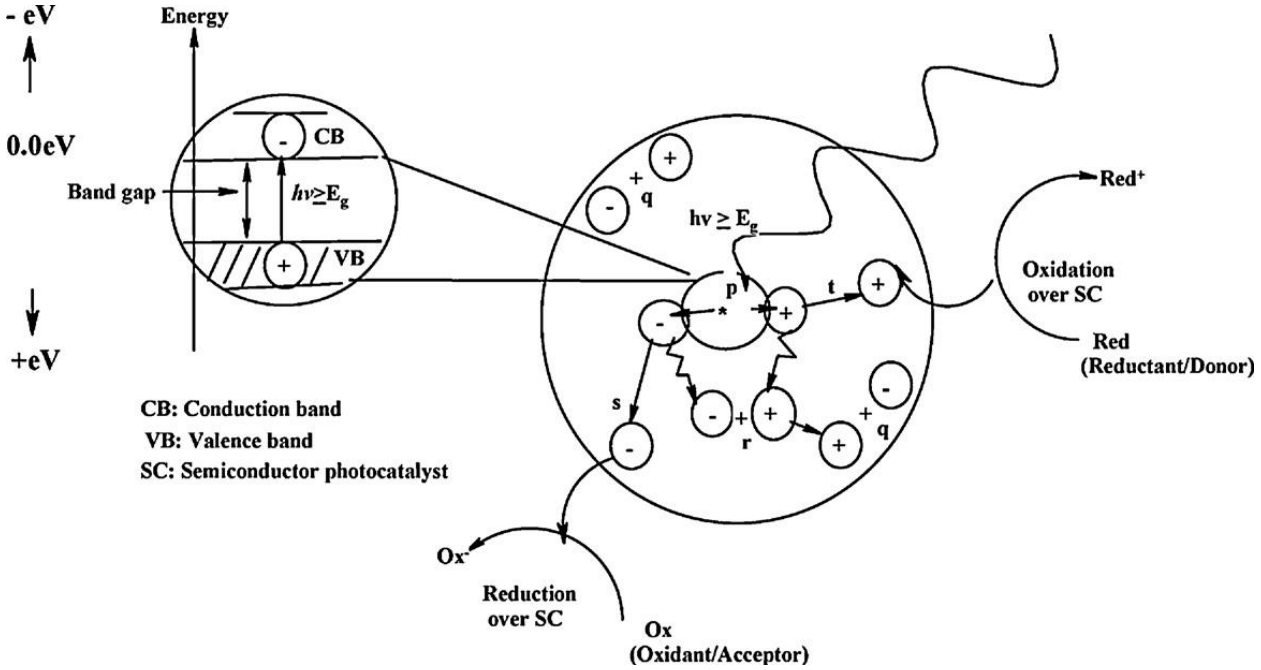


Fig. 2.7: Schematic diagram of photocatalytic process initiated by photon acting on the semiconductor (Gaya and Abdullahi, 2008).

The applications of homogeneous photodegradation (single-phase system) to treat contaminated water, involves the use of an oxidant to generate radicals which attack the organic pollutants to initiate oxidation. The major oxidants used are:

Hydrogen peroxide (UV /$H_2O_2$)

Ozone (UV /$O_3$)

Hydrogen peroxide and Ozone (UV /$O_3$/$H_2O_2$)

Photo-Fenton system ($Fe^{+3}$ /$H_2O_2$)

### 2.6.1.2 Heterogeneous photocatalysis.

This entails using the near UV radiation to photo-excite a semiconductor catalyst in the presence of oxygen. Under these circumstances oxidizing species, either bound hydroxyl radicals or free holes are generated.

Using photocatalysis, organic pollutants can be completely mineralized by reacting with the oxidizers to form $CO_2$, water and dilute concentration of simple mineral acid (Akpan and Hameed, 2013). Due to the efficacy of the advance oxidation processes, the environmental protection agency has approved it inclusion as the best available technology to meet the standard with specification that provide safe and sufficient pollution control of industrial processes and remediation of contaminated sites (Rashidi *et al*., 2014). The process is heterogeneous because there are two active phases, solid and liquid. This process can also be carried out utilizing the near part of solar spectrum ($\lambda$ < 380nm) which transforms it into a good option to be used (Malato *et al*., 2002).

The semiconductor may be in the form of a powder suspended in the water or fixed on a support. The most active photocatalyst for this application is the anatase form of $TiO_2$ because of its high stability, good performance and low cost (Andreozzi *et al*., 1999). The primary photocatalytic mechanism is believed to proceed as follows (Kaur, 2007):

$$TiO_2 + h\nu \longrightarrow e^-_{CB} + h^+_{VB} \quad \text{(Eq. 2.3)}$$

$$h^+_{VB} + H_2O \longrightarrow {}^{\cdot}OH + H^+ \quad \text{(Eq. 2.4)}$$

$$e^-_{CB} + O_2 \longrightarrow O_2^{\cdot -} \quad \text{(Eq.2.5)}$$

$$2O_2^{\cdot -} + 2H_2O \longrightarrow H_2O_2 + 2OH^- + O_2 \quad \text{(Eq.2.6)}$$

$$H_2O_2 + e^-_{CB} \longrightarrow OH^- + \cdot OH \quad \text{(Eq.2.7)}$$

In solids, the electrons occupy energy bands as a consequence of the extended bonding network. In a semiconductor, the highest occupied and lowest unoccupied energy bands are separated by a bandgap, a region devoid of energy levels.

### 2.6.1.3 Advantages of Advanced Oxidation Processes (AOP's) over other methods

AOP's hold several advantages that are unparalleled in the field of wastewater treatment and they include;

i. It could effectively eliminate organic compounds in aqueous phase, rather than collecting or transferring pollutants into another phase.
ii. Due to the remarkable reactivity of ·OH, it virtually reacts with almost every aqueous pollutants without much discrimination. AOPs could therefore be applicable in many, if not all, scenarios where many organic contaminants are expected to be removed at the same time.
iii. Some heavy metals could also be removed in forms of precipitated $M(OH)_x$ (Munter, 2001).
iv. In some AOP's designs, disinfection could also be achieved, leading AOP's to an integrated solution to some of the water quality problems.
v. Since the complete reduction product of ·OH is $H_2O$, AOP's theoretically do not introduce any new hazardous substances into the water.

### 2.6.2 Decolorization by fungi

Ligninolytic fungi are able to degrade numerous aromatic organic pollutants via oxidative mechanisms (Adosinda *et al*., 2001; Bogan and Lamar, 1995). A range of acid, reactive, and mordant azo dyes have been shown to be decolorized by this ligninolytic fungus (Knapp *et al*., 1995; Chagas and Durrant, 2001; Moreira *et al*., 2000), hence there exist a

correlation between dye decolorization and the production of ligninolytic enzymes as implied by the work of Wesenberg and co-workers (Wesenberg *et al*., 2003). The ligninolytic enzymes are extracellularly excreted by the fungi to initiate the oxidation of substrates in the extracellular environment of the fungal cells (Mester and Tien, 2000). Essential extracellular enzymes involved in the degradation of lignin in wood and recalcitrant pollutants (that is azo dyes/pigments) in the environment are laccase, lignin peroxidase (LiP), and manganese peroxidase (MnP). All of these enzymes are generally believed to form during secondary metabolism of white rot fungi (Hou *et al*, 2003; Zapanta and Tien, 1997).

### 2.6.3 Membrane Filtration

Membrane filtration can as well be used to remove dyes and pigments molecules. The classification of membranes is conducted on the basis of their pore size to retain solutes with different molecular weights. The membrane parameter is called molecular weight cut off (MWCO). In the case of dye and pigment separation, reverse osmosis (MWCO < 1000), nanofiltration (500 < MWCO < 15000) and ultrafiltration (1000 < MWCO < 100000) membranes can be used according to the dye or pigment characteristics. In addition to the dye or pigment solution separation, membranes can be used also for the separation of particles after the adsorption or coagulation/precipitation instead of the sedimentation (Hao *et al*, 2000). Ultrafiltration and microfiltration are not suitable since they have large pore sized membranes through which particles of dyes, pigments and other substances can pass (Cooper, 1993). The major problem here is the reduction in flux and smells generated by the membranes thus requiring incessant cleaning and perhaps replacement of the modules.

### 2.6.4 Coagulation/Flocculation

Coagulation can be induced by an electrolytic reaction at electrode surface or by changing pH or adding coagulants (Shakir *et al*., 2010). It is therefore employed in the treatment of textile wastewater effluent to remove colour (Lin and Peng, 1996).

The process involves addition of coagulant followed by reaction between the coagulant and the pollutants which results in the formation of coagulates/flocculates. The resulting coagulates/flocculates formed then precipitate and removed from the water.

### 2.6.5 Adsorption

This method has gained a favourable interest due to the efficient pollutant removal, quality product and economical feasibility. It is influenced by many physico-chemical factors, e.g. dye-sorbent interaction, adsorbent surface area and particle size, temperature, pH and contact time. Materials like activated carbon, peat, wood chips, fly

ash and coal, silica gel, microbial biomass, and other inexpensive materials (e.g. natural clay, corn cobs, rice hulls), are used, since they do not require regeneration.

### 2.6.6 Sedimentation

Sedimentation is a solid-liquid separation method. In the case of dye and pigments solutions, it is used in combination with chemical or biological methods producing particles containing dye or dye degradation products with coagulation/precipitation or with some other chemical methods, or adsorption on various materials. The rate of sedimentation of particles suspended in a fluid can be described with Stoke's law and is influenced by many physico-chemical factors. The disadvantage here is a high sludge production.

# CHAPTER THREE

## 3.0 MATERIALS AND METHODS

## 3.1 MATERIALS

The studies covered two commercial vat pigments and two synthesized azo pigments. The commercial vat pigments which were used without further purification were purchased from Sigma Aldrich Chemical Company, Germany. The following chemicals and reagents were used for the synthesis of the azo pigments and degradation studies.

p-Nitroaniline (Fluka)

Hydrochloric Acid (HCl)

N, N-dimethylaniline (Sigma Aldrich)

2-hydroxy-3-naphthnilide (Sigma Aldrich)

Sodium hydroxide (NaOH)

Distilled water ($H_2O$)

Sodium nitrite ($NaNO_2$)

Ice blocks

Sodium chloride (NaCl)

Acetone (Sigma Aldrich)

Dimethyl formamide (DMF) (Sigma Aldrich)

Sodium acetate ($CH_3COONa$)

Titanium dioxide ($TiO_2$), P25 (Fluka)

## 3.2 EQUIPMENT AND APPARATUS

Gallenkamp melting point apparatus (Model: Sanyo MPD350.BM3.5)

Digital pH meter (model: Jenway 3505, 78HW)

Top Loading balance (model: 7/SS618)

Mercury bulb (300 W)

Magnetic stirrer

UV/Visible Spectrophotometer (model: Jenway 6305)

GC-MS SHIMADZU Machine (model: GC-MS-QP2010)

FTIR SHIMADZU Machine (model: FTIR-8400S)

Buchner funnel

Filter paper

Photoreactor equipped with a suction fan (model: 361oKL – 04W – B69)

## 3.3 THE COMMERCIAL VAT AND SYNTHESIZED AZO PIGMENTS

### 3.3.1 The Commercial Vat Pigments

Two commercial vat pigments Caledon Khaki 2G (C.I Vat Green 8) and Caledon Green 2G (C.I Vat Green 2) were purchased from Sigma Aldrich Chemical Company, Germany and used in the studies alongside titanium dioxide, $TiO_2$ (Fluka). The structures of these quinone based pigments are shown in Figures. 3.1 and 3.2

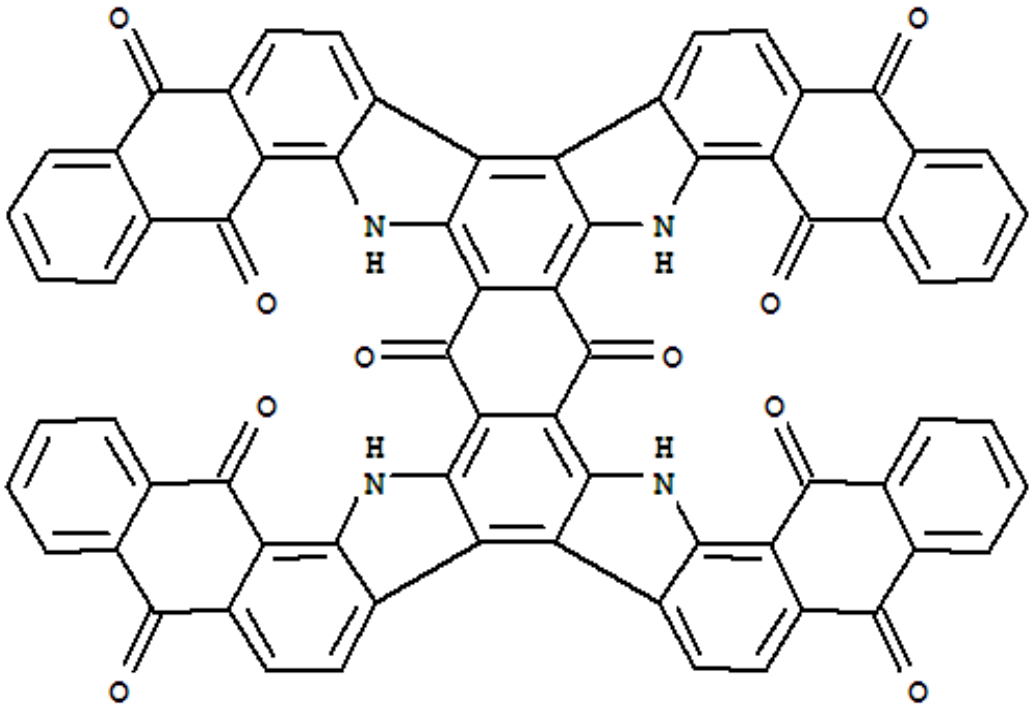

Figure 3.1: The Structure of Caledon Khaki 2G (C.I Vat Green 8) VP1

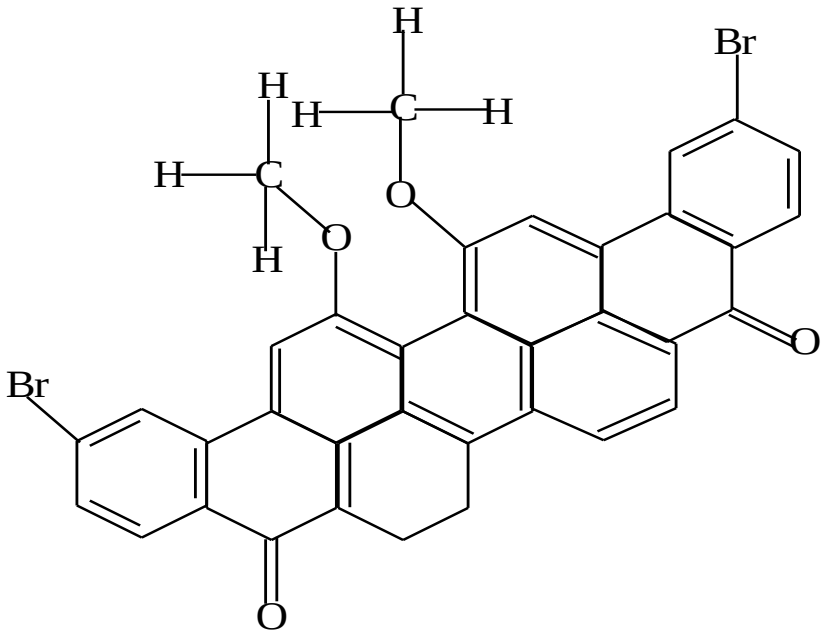

Figure 3.2: The Structure of Caledon Green 2G (C.I Vat Green 2) VP2

### 3.3.2 SYNTHESIS OF THE AZO PIGMENTS

The two azo pigments were obtained by the process of diazotizatioan and coupling.

#### 3.3.2.1 General procedure for diazotization of p-nitroaniline

Hydrochloric acid was used for the diazotization. A (0.17 g, 0.001 mol) of p-nitroaniline (Fluka) was dissolved in 50 ml distilled water. 20 ml of 1M hydrochloric was added and the solution was heated to 70-75°C over 15 minutes and this temperature maintained for 30 minutes to ensure complete dissolution of the diazo component. The reaction mixture was then cooled to 0-5°C in an ice bath and 8.65 ml of 1% $NaNO_2$ was added and the mixture stirred vigorously for 2 hours at the same low temperature of 0-5°C. The completion of diazotization yields diazonium salt which was confirmed by checking for the presence of excess nitrous acid using starch iodide paper.

#### 3.3.2.2 General method for coupling diazotized p-nitroaniline to N, N-dimethylaniline and Naphthol AS

##### 3.3.2.2.1 Azo Pigment 1 (AP1)

A solution of the coupling component N, N-dimethylaniline (2.42 g, 0.02 mol) was dissolved in a mixture of 1.5 ml of 35% HCl inside a beaker equipped with a mechanical stirrer and a pH meter at room temperature. The earlier prepared diazonium salt liquor and a meshed ice (40 ml) was added to the corresponding coupling component solution and the temperature maintained between 0-5°C. The solution was then stirred for 2-3 hours. A solution of 1M sodium acetate was added to adjust the pH between 4 and 5. After, saturated salt solution of sodium chloride was added until precipitation was obtained. The precipitate was then filtered and recrystallized from glacial acetic acid, washed with methanol to eliminate the acetic acid and then dried in an oven at 31°C.

#### 3.3.2.2.2 Azo Pigment 2 (AP2)

The second coupling component was prepared by dissolving the coupling component Naphthol AS (1.84 g, 0.007 mol) in 60 ml of 2.0 M sodium hydroxide with vigorous stirring for over 15 minutes. This solution was then added dropwise to the diazonium salt liquor with vigorous stirring at 0-5$^0$C for 2-3 hours. The resulting precipitate was filtered, recrytallized from glacial acetic acid and then washed with methanol to remove the acetic acid after which it was dried in an oven at 31□C.

### 3.3.3 SPECTRAL ANALYSIS OF THE SYNTHESIZED AZO PIGMENTS

#### 3.3.3.1 Infrared Spectral Characteristics of the Pigments Solution

The infrared spectral of the synthesized azo pigments were measured in KBr pellets on a FTIR-8400S Fourier Transform Infrared Spectrophotometer. The results are shown in Table 4.2.

#### 3.3.3.2 Gas Chromatography-Mass Spectroscopy (GC/MS) of synthesized pigments

The structural elucidations of the synthesized azo pigments were determined using the GC-MS-QP2010 machine. The results obtained are displayed on Table 4.3

#### 3.3.3.3 Visible Absorption Spectral of the synthesized azo pigments

The visible absorption spectroscopic properties of the synthesized azo pigments were recorded in DMF using JENWAY 6305 UV/Vis Spectrophotometer. Absorption maximum wavelength ($\lambda$max) and molar extinction coefficients were calculated and recorded in Table 4.4.

## 3.4 DETERMINATION OF MOLAR EXTINCTION COEFFICIENT OF THE SYNTHESIZED AZO PIGMENTS

The molar extinction coefficients (ε ) of the pigments were calculated using the formula in equation 3.1.

$$\varepsilon = \frac{A}{Cl} \quad \text{----------3.1}$$

Where ε = molar extinction coefficient

A = Absorption at $\lambda_{max}$

C = pigment concentration in mol/litre

$l$ = path length of the cell (1 cm)

## 3.5 PHOTODEGRADATION STUDIES OF SYNTHESIZED AZO PIGMENT AND COMMERCIAL VAT PIGMENTS

The photodegradation of the pigments were carried out in a laboratory scale photoreactor equipped with ultraviolet light bulb of 300 W, a cooling fan to maintain steady temperature inside the reactor and a magnetic stirrer to enable swirling of the magnetic rotor placed inside the beaker containing the pigment solution which stirs the solution (the schematic diagram of the reactor is shown in Figure 3.3). Using a Box Beckhen Design of Experiment (DOE) as generated by Minitab 16 software, the photodegradation parameters such as pigment concentration, catalyst loading, pH of the pigment and the irradiation time for each pigment samples were fed into the system and thus, generated the experimental design for each of the pigment samples. The pigments were then grounded into fine powder out of which 0.1 g of each powdered sample was dissolved in 100 ml of Dimethylformamide (DMF) in separate volumetric flask to form a stock solution. The requisite concentrations (5 mg/L, 12.5 mg/L and 20 mg/L) for each run as generated by the design was then

prepared from the stock solution and other parameters such as catalyst dose, pH and irradiation time were varied as stipulated by the design. Prior to irradiation, the pigment solution was equilibriated for 30 minutes in the dark to establish equilibrium between adsorption and desorption. The pigment solution was then irradiated inside a laboratory scale photoreactor containing a UV light bulb and a magnetic stirrer. At the expiration of the exposure time for each run, the sample was brought out of the reactor after which it was filtered. While the filtrate was discarded, the small particles left on the filter paper were filtered again by addition of 10ml of DMF to dissolve the undegraded pigment particles on the surface of the filter paper. The absorbance was then taken in DMF using UV-Vis spectrophotometer at the maximum absorption wavelength for each sample. This procedure was repeated for each run of the pigment samples by varying the operational parameters earlier mentioned.

The degradation performance of the process was then assessed in terms of decolorization efficiencies defined by equation 3.2.

$$\text{Decolourization (\%)} = \frac{A_0 - A_t}{A_0} \quad \text{----------3.2}$$

Where Ao and $A_t$ are the initial and final absorbance at a given time‘t’.

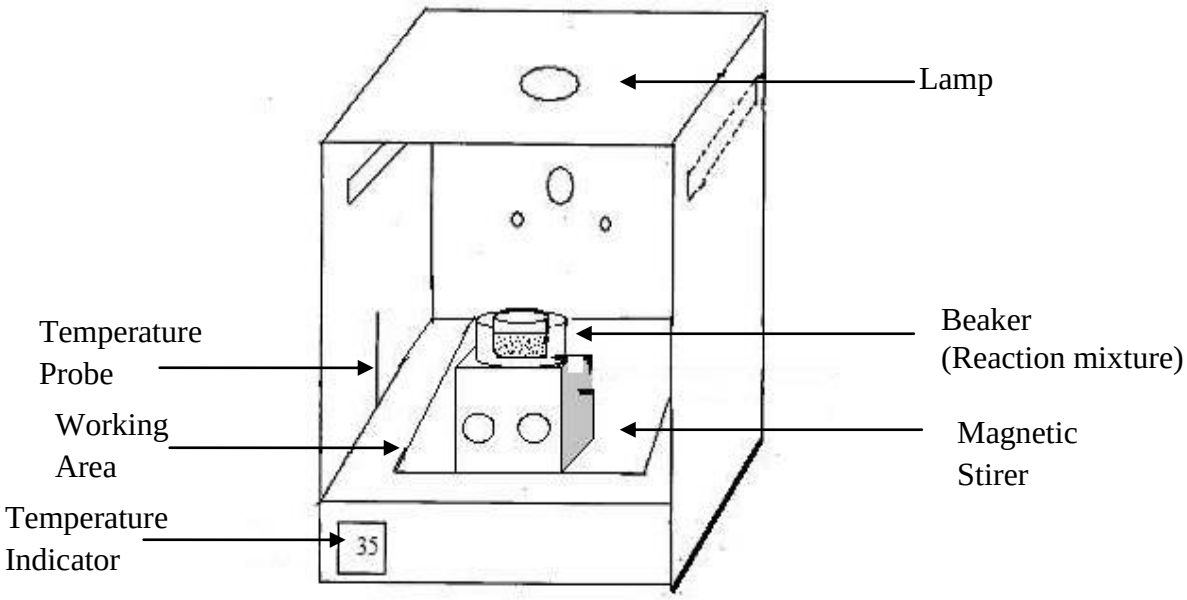


Figure 3.3: Schematic diagram of the laboratory scale photoreactor.

The summary of the experimental design for the commercial vat and synthesized azo pigments are shown in Table 3.1 and 3.2 respectively. The tables display the high and low values of the operational parameters which were fed into the system to generate the design of the experiment, DOE.

Table 3.1: Summary of Experimental Design for Caledon Khaki 2G and Caledon Green 2G

Factors: 4
Runs: 27

| Factor Name Low | Low | High |
|---|---|---|
| **Pigment concentration (mg/L)** | 5 | 20 |
| **Catalyst loading (g/L)** | 0 | 2 |
| **pH** | 7 | 9 |
| **Time (min.)** | 0 | 90 |

Table 3.2: Summary of Experimental Design for AP 1 and AP2

Factors: 4
Runs: 27

| Factor Name Low | Low | High |
|---|---|---|
| **Pigment concentration (mg/L)** | 5 | 20 |
| **Catalyst loading (g/L)** | 0 | 2 |
| **pH** | 8 | 10 |
| **Time (min.)** | 0 | 90 |

The design of experiment generated when the high and low values of the operational parameters for each pigment samples were fed into the system are shown in Tables 3.3 – 3.6.

Table 3.3 Design of Experiment for Caledon Khaki 2G (VP1)

| Run Order | Pigment Concentration (mg/L) | Catalyst Loading (g/L) | pH | Time (min.) | Degradation % |
|---|---|---|---|---|---|
| 1 | 20.0 | 2 | 8 | 45 | |
| 2 | 5.0 | 1 | 7 | 45 | |
| 3 | 5.0 | 2 | 8 | 45 | |
| 4 | 5.0 | 0 | 8 | 45 | |
| 5 | 20.0 | 1 | 8 | 0 | |
| 6 | 5.0 | 1 | 8 | 90 | |
| 7 | 12.5 | 2 | 7 | 45 | |
| 8 | 12.5 | 1 | 8 | 45 | |
| 9 | 20.0 | 1 | 9 | 45 | |
| 10 | 12.5 | 2 | 9 | 45 | |
| 11 | 12.5 | 1 | 8 | 45 | |
| 12 | 12.5 | 0 | 8 | 0 | |
| 13 | 5.0 | 1 | 8 | 0 | |
| 14 | 12.5 | 1 | 8 | 45 | |
| 15 | 12.5 | 2 | 8 | 0 | |
| 16 | 12.5 | 1 | 9 | 0 | |
| 17 | 12.5 | 0 | 8 | 90 | |
| 18 | 20.0 | 1 | 8 | 90 | |
| 19 | 20.0 | 1 | 7 | 45 | |
| 20 | 12.5 | 1 | 7 | 90 | |
| 21 | 5.0 | 1 | 9 | 45 | |
| 22 | 12.5 | 1 | 7 | 0 | |
| 23 | 5.0 | 0 | 8 | 90 | |
| 24 | 12.5 | 2 | 8 | 90 | |
| 25 | 12.5 | 0 | 9 | 45 | |
| 26 | 12.5 | 0 | 7 | 45 | |
| 27 | 12.5 | 1 | 9 | 90 | |

Table 3.4 Design of Experiment for Caledon Green 2G (VP2)

| Run Order | Pigment Concentration (mg/L) | Catalyst Loading (g/L) | pH | Time (min.) | Degradation % |
|---|---|---|---|---|---|
| 1 | 12.5 | 1 | 7 | 0 | |
| 2 | 20.0 | 1 | 8 | 90 | |
| 3 | 20.0 | 1 | 8 | 0 | |
| 4 | 5.0 | 1 | 8 | 90 | |
| 5 | 12.5 | 0 | 8 | 0 | |
| 6 | 12.5 | 1 | 8 | 45 | |
| 7 | 12.5 | 2 | 9 | 90 | |
| 8 | 12.5 | 1 | 7 | 90 | |
| 9 | 12.5 | 1 | 8 | 45 | |
| 10 | 12.5 | 1 | 8 | 45 | |
| 11 | 12.5 | 1 | 9 | 0 | |
| 12 | 12.5 | 2 | 8 | 90 | |
| 13 | 20.0 | 2 | 8 | 45 | |
| 14 | 12.5 | 0 | 7 | 45 | |
| 15 | 5.0 | 0 | 8 | 90 | |
| 16 | 12.5 | 2 | 9 | 45 | |
| 17 | 5.0 | 1 | 8 | 0 | |
| 18 | 12.5 | 0 | 8 | 90 | |
| 19 | 12.5 | 0 | 9 | 45 | |
| 20 | 20.0 | 1 | 7 | 45 | |
| 21 | 20.0 | 1 | 9 | 45 | |
| 22 | 5.0 | 1 | 7 | 45 | |
| 23 | 12.5 | 2 | 8 | 0 | |
| 24 | 5.0 | 0 | 8 | 45 | |
| 25 | 5.0 | 2 | 8 | 45 | |
| 26 | 12.5 | 2 | 7 | 45 | |
| 27 | 5.0 | 1 | 7 | 45 | |

Table 3.5 Design of Experiment for AP 1

| Run Order | Pigment Concentration (mg/L) | Catalyst Loading (g/L) | pH | Time (min.) | Degradation % |
|---|---|---|---|---|---|
| 1 | 5.0 | 0 | 9 | 45 | |
| 2 | 12.5 | 2 | 9 | 90 | |
| 3 | 20.0 | 1 | 9 | 0 | |
| 4 | 12.5 | 1 | 10 | 90 | |
| 5 | 5.0 | 0 | 8 | 45 | |
| 6 | 12.5 | 0 | 8 | 45 | |
| 7 | 12.5 | 0 | 9 | 90 | |
| 8 | 12.5 | 0 | 9 | 0 | |
| 9 | 12.5 | 2 | 9 | 0 | |
| 10 | 12.5 | 1 | 9 | 45 | |
| 11 | 5.0 | 1 | 9 | 90 | |
| 12 | 12.5 | 0 | 10 | 45 | |
| 13 | 5.0 | 1 | 9 | 0 | |
| 14 | 20.0 | 1 | 10 | 45 | |
| 15 | 12.5 | 1 | 8 | 0 | |
| 16 | 5.0 | 1 | 10 | 45 | |
| 17 | 12.5 | 1 | 9 | 45 | |
| 18 | 20.0 | 1 | 9 | 90 | |
| 19 | 5.0 | 1 | 8 | 45 | |
| 20 | 20.0 | 1 | 8 | 45 | |
| 21 | 5.0 | 2 | 9 | 45 | |
| 22 | 12.5 | 2 | 10 | 45 | |
| 23 | 12.5 | 1 | 10 | 0 | |
| 24 | 20.0 | 2 | 9 | 45 | |
| 25 | 12.5 | 1 | 8 | 90 | |
| 26 | 12.5 | 1 | 9 | 45 | |
| 27 | 12.5 | 2 | 8 | 45 | |

Table 3.6 Design of Experiment for AP2

| Run Order | Pigment Concentration (mg/L) | Catalyst Loading (g/L) | pH | Time (min.) | Degradation % |
|---|---|---|---|---|---|
| 1 | 5.0 | 2 | 9 | 45 | |
| 2 | 12.5 | 1 | 8 | 0 | |
| 3 | 12.5 | 0 | 9 | 0 | |
| 4 | 20.0 | 1 | 8 | 45 | |
| 5 | 12.5 | 2 | 9 | 90 | |
| 6 | 5.0 | 1 | 8 | 45 | |
| 7 | 12.5 | 1 | 9 | 45 | |
| 8 | 20.0 | 1 | 9 | 0 | |
| 9 | 12.5 | 2 | 9 | 0 | |
| 10 | 12.5 | 2 | 8 | 45 | |
| 11 | 12.5 | 1 | 9 | 45 | |
| 12 | 5.0 | 1 | 9 | 0 | |
| 13 | 12.5 | 0 | 8 | 45 | |
| 14 | 5.0 | 0 | 9 | 45 | |
| 15 | 12.5 | 2 | 10 | 45 | |
| 16 | 5.0 | 0 | 8 | 45 | |
| 17 | 5.0 | 1 | 9 | 90 | |
| 18 | 12.5 | 1 | 10 | 90 | |
| 19 | 12.5 | 0 | 9 | 90 | |
| 20 | 12.5 | 1 | 9 | 45 | |
| 21 | 12.5 | 0 | 10 | 45 | |
| 22 | 20.0 | 1 | 10 | 45 | |
| 23 | 20.0 | 2 | 9 | 45 | |
| 24 | 12.5 | 1 | 8 | 90 | |
| 25 | 12.5 | 1 | 10 | 0 | |
| 26 | 20.0 | 1 | 9 | 90 | |
| 27 | 5.0 | 1 | 10 | 45 | |

# CHAPTER FOUR

## 4.0 RESULTS

### 4.1 Structures and Physical Characteristics of the Pigments

The structures and the physical properties of both the commercial and synthesized azo pigments are presented in Table 4.1.

Table 4.1 Physical Characteristics of the Pigments

| PIGMENT SAMPLES | PIGMENT STRUCTURES | MOLECULAR FORMULA | MOLECULAR WEIGTH (g/mol) | MELTING POINT ($^0$C) | %YIELD |
|---|---|---|---|---|---|
| **VP1** | 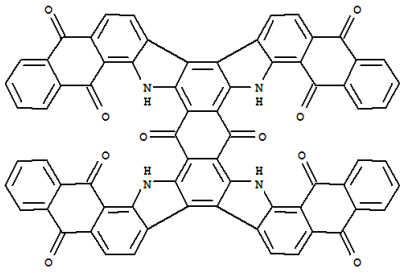 | $C_{17}H_{28}N_4O_{10}$ | 1084.99 | >320 | - |
| **VP2** | 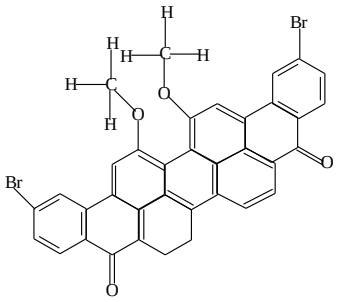 | $C_{36}H_{18}Br_2O_4$ | 674.33 | >320 | - |
| **AP1** | 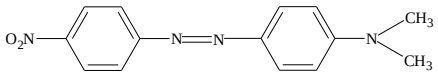 | $C_{14}H_{14}N_4O_4$ | 270 | 176-179 | 64 |
| **AP2** | 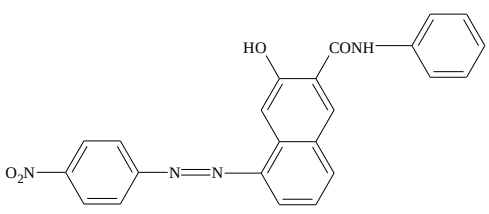 | $C_{23}H_{16}N_4O_4$ | 412 | 216-220 | 72 |

### 4.2 Infra-red Spectra of Synthesized Azo Pigments

The analyses of the infra red spectral of the synthesized azo pigments are presented in Table 4.2.

Table 4.2 Infrared spectra analysis of the synthesized azo pigments

| Pigment Sample | ArC-H | C-H | N-H | O-H | N=N | C=C | C≡C | C-O | -NO2 |
|---|---|---|---|---|---|---|---|---|---|
| | $^{+}$B | $^{++}$S | $^{++}$S | $^{++}$S | $^{++}$S | $^{++}$S | $^{++}$S | $^{++}$S | $^{++}$S |
| **AP1** | 701.15 | 2917.43 | 3455.59 | - | 1500.67 | 1597.11 | 2278.97 | 1121.64 | 1329.00 |
| | 839.06 | - | - | - | - | - | - | - | - |
| **AP2** | 727.19 | 3302.24 | 3460.41 | 3762.28 | 1463.06 | 1617.37 | 2275.11 | 1183.37 | 1346.36 |
| | 864.14 | 3046.67 | - | - | - | - | - | 1059.92 | - |

$^{+}$B – Bending, $^{++}$S - Stretching

### 4.3. Gas Chromatography–Mass Spectroscopy (GC-MS) of Synthesized pigments

The GC-MS of the pigment (AP1) gives a complete elucidation of the structure with the parent analyte ($M^{+}$) occurring at 270 and different fragmentation patterns as shown below. Table 4.3 shows the values found in comparison with those calculated.

Table 4.3: GC-MS analysis of AP1.

| Found | Calculated |
|---|---|
| N, $C_2H_6$: 43 | 44 |
| $C_6H_4$: 74 | 74 |
| $C_6H_4$, $NO_2$: 129 | 122 |
| $C_6H_4$, N=N: 101 | 104 |
| $C_6H_4$, $NC_2H_6$: 115 | 120 |
| N=N, $C_6H_4$, $NC_2H_6$: 142 | 148 |
| $NC_2H_6$, $C_6H_4$, N=N, $C_6H_4$: 227 | 224 |
| $NO_2$, $C_6H_4$, N=N, $C_6H_4$, $NC_2H_6$: 270 | 270 |

**4.4 Visible Absorption Spectra of Synthesized Azo Pigment.**

The analyses of the visible absorption spectra of the synthesized azo pigments are presented in Table 4.4.

Table 4.4: Visible Absorption Spectra of Synthesized Azo Pigment

| **Pigment Sample** | **λmax**<br>**DMF** | **Molar Extinction Coefficient ($LMol^{-1}cm^{-1}$) x $10^4$** |
|---|---|---|
| **AP1** | 515 | 5.54 |
| **AP2** | 510 | 4.98 |

Table 4.5 – 4.8 is the design of experiment containing the degradation results of the pigments samples.

Table 4.5: Design of Experiment for Caledon Khaki 2G (VP1)

| Run Order | Pigment Concentration (mg/L) | Catalyst Loading (g/L) | pH | Time (min.) | Degradation % |
|---|---|---|---|---|---|
| 1 | 20.0 | 2 | 8 | 45 | 98.40 |
| 2 | 5.0 | 1 | 7 | 45 | 94.33 |
| 3 | 5.0 | 2 | 8 | 45 | 93.60 |
| 4 | 5.0 | 0 | 8 | 45 | 32.11 |
| 5 | 20.0 | 1 | 8 | 0 | 0 |
| 6 | 5.0 | 1 | 8 | 90 | 95.30 |
| 7 | 12.5 | 2 | 7 | 45 | 97.00 |
| 8 | 12.5 | 1 | 8 | 45 | 97.96 |
| 9 | 20.0 | 1 | 9 | 45 | 98.66 |
| 10 | 12.5 | 2 | 9 | 45 | 96.65 |
| 11 | 12.5 | 1 | 8 | 45 | 97.95 |
| 12 | 12.5 | 0 | 8 | 0 | 0 |
| 13 | 5.0 | 1 | 8 | 0 | 0 |
| 14 | 12.5 | 1 | 8 | 45 | 97.96 |
| 15 | 12.5 | 2 | 8 | 0 | 0 |
| 16 | 12.5 | 1 | 9 | 0 | 0 |
| 17 | 12.5 | 0 | 8 | 90 | 38.32 |
| 18 | 20.0 | 1 | 8 | 90 | 99.31 |
| 19 | 20.0 | 1 | 7 | 45 | 98.11 |
| 20 | 12.5 | 1 | 7 | 90 | 97.28 |
| 21 | 5.0 | 1 | 9 | 45 | 95.47 |
| 22 | 12.5 | 1 | 7 | 0 | 0 |
| 23 | 5.0 | 0 | 8 | 90 | 35.13 |
| 24 | 12.5 | 2 | 8 | 90 | 97.42 |
| 25 | 12.5 | 0 | 9 | 45 | 36.89 |
| 26 | 12.5 | 0 | 7 | 45 | 28.43 |
| 27 | 12.5 | 1 | 9 | 90 | 98.49 |

Table 4.6: Design of Experiment for Caledon Green 2G (VP2)

| Run Order | Pigment Concentration (mg/L) | Catalyst Loading (g/L) | pH | Time (min.) | Degradation % |
|---|---|---|---|---|---|
| 1 | 12.5 | 1 | 7 | 0 | 0 |
| 2 | 20.0 | 1 | 8 | 90 | 99.24 |
| 3 | 20.0 | 1 | 8 | 0 | 0 |
| 4 | 5.0 | 1 | 8 | 90 | 95.59 |
| 5 | 12.5 | 0 | 8 | 0 | 0 |
| 6 | 12.5 | 1 | 8 | 45 | 98.90 |
| 7 | 12.5 | 2 | 9 | 90 | 97.98 |
| 8 | 12.5 | 1 | 7 | 90 | 97.42 |
| 9 | 12.5 | 1 | 8 | 45 | 98.90 |
| 10 | 12.5 | 1 | 8 | 45 | 98.92 |
| 11 | 12.5 | 1 | 9 | 0 | 0 |
| 12 | 12.5 | 2 | 8 | 90 | 98.81 |
| 13 | 20.0 | 2 | 8 | 45 | 98.61 |
| 14 | 12.5 | 0 | 7 | 45 | 28.04 |
| 15 | 5.0 | 0 | 8 | 90 | 25.68 |
| 16 | 12.5 | 2 | 9 | 45 | 98.35 |
| 17 | 5.0 | 1 | 8 | 0 | 0 |
| 18 | 12.5 | 0 | 8 | 90 | 32.41 |
| 19 | 12.5 | 0 | 9 | 45 | 30.73 |
| 20 | 20.0 | 1 | 7 | 45 | 96.15 |
| 21 | 20.0 | 1 | 9 | 45 | 98.89 |
| 22 | 5.0 | 1 | 7 | 45 | 95.28 |
| 23 | 12.5 | 2 | 8 | 0 | 0 |
| 24 | 5.0 | 0 | 8 | 45 | 23.21 |
| 25 | 5.0 | 2 | 8 | 45 | 93.46 |
| 26 | 12.5 | 2 | 7 | 45 | 96.09 |
| 27 | 5.0 | 1 | 7 | 45 | 90.68 |

Table 4.7: Design of Experiment for AP 1

| Run Order | Pigment Concentration (mg/L) | Catalyst Loading (g/L) | pH | Time (min.) | Degradation % |
|---|---|---|---|---|---|
| 1 | 5.0 | 0 | 9 | 45 | 35.51 |
| 2 | 12.5 | 2 | 9 | 90 | 96.96 |
| 3 | 20.0 | 1 | 9 | 0 | 0 |
| 4 | 12.5 | 1 | 10 | 90 | 98.78 |
| 5 | 5.0 | 0 | 8 | 45 | 32.31 |
| 6 | 12.5 | 0 | 8 | 45 | 36.34 |
| 7 | 12.5 | 0 | 9 | 90 | 41.22 |
| 8 | 12.5 | 0 | 9 | 0 | 0 |
| 9 | 12.5 | 2 | 9 | 0 | 0 |
| 10 | 12.5 | 1 | 9 | 45 | 96.92 |
| 11 | 5.0 | 1 | 9 | 90 | 93.57 |
| 12 | 12.5 | 0 | 10 | 45 | 38.72 |
| 13 | 5.0 | 1 | 9 | 0 | 0 |
| 14 | 20.0 | 1 | 10 | 45 | 99.37 |
| 15 | 12.5 | 1 | 8 | 0 | 0 |
| 16 | 5.0 | 1 | 10 | 45 | 94.86 |
| 17 | 12.5 | 1 | 9 | 45 | 97.24 |
| 18 | 20.0 | 1 | 9 | 90 | 99.52 |
| 19 | 5.0 | 1 | 8 | 45 | 93.47 |
| 20 | 20.0 | 1 | 8 | 45 | 99.20 |
| 21 | 5.0 | 2 | 9 | 45 | 93.85 |
| 22 | 12.5 | 2 | 10 | 45 | 98.52 |
| 23 | 12.5 | 1 | 10 | 0 | 0 |
| 24 | 20.0 | 2 | 9 | 45 | 98.76 |
| 25 | 12.5 | 1 | 8 | 90 | 97.18 |
| 26 | 12.5 | 1 | 9 | 45 | 97.37 |
| 27 | 12.5 | 2 | 8 | 45 | 96.79 |

Table 4.8 Design of Experiment for AP 2

| Run Order | Pigment Concentration (mg/L) | Catalyst Loading (g/L) | pH | Time (min.) | Degradation % |
|---|---|---|---|---|---|
| 1 | 5.0 | 2 | 9 | 45 | 94.42 |
| 2 | 12.5 | 1 | 8 | 0 | 0 |
| 3 | 12.5 | 0 | 9 | 0 | 0 |
| 4 | 20.0 | 1 | 8 | 45 | 98.58 |
| 5 | 12.5 | 2 | 9 | 90 | 96.73 |
| 6 | 5.0 | 1 | 8 | 45 | 94.92 |
| 7 | 12.5 | 1 | 9 | 45 | 97.38 |
| 8 | 20.0 | 1 | 9 | 0 | 0 |
| 9 | 12.5 | 2 | 9 | 0 | 0 |
| 10 | 12.5 | 2 | 8 | 45 | 96.84 |
| 11 | 12.5 | 1 | 9 | 45 | 97.41 |
| 12 | 5.0 | 1 | 9 | 0 | 0 |
| 13 | 12.5 | 0 | 8 | 45 | 39.23 |
| 14 | 5.0 | 0 | 9 | 45 | 34.36 |
| 15 | 12.5 | 2 | 10 | 45 | 96.72 |
| 16 | 5.0 | 0 | 8 | 45 | 32.13 |
| 17 | 5.0 | 1 | 9 | 90 | 95.04 |
| 18 | 12.5 | 1 | 10 | 90 | 97.58 |
| 19 | 12.5 | 0 | 9 | 90 | 41.22 |
| 20 | 12.5 | 1 | 9 | 45 | 97.40 |
| 21 | 12.5 | 0 | 10 | 45 | 37.48 |
| 22 | 20.0 | 1 | 10 | 45 | 99.06 |
| 23 | 20.0 | 2 | 9 | 45 | 98.16 |
| 24 | 12.5 | 1 | 8 | 90 | 97.45 |
| 25 | 12.5 | 1 | 10 | 0 | 0 |
| 26 | 20.0 | 1 | 9 | 90 | 99.12 |
| 27 | 5.0 | 1 | 10 | 45 | 94.63 |

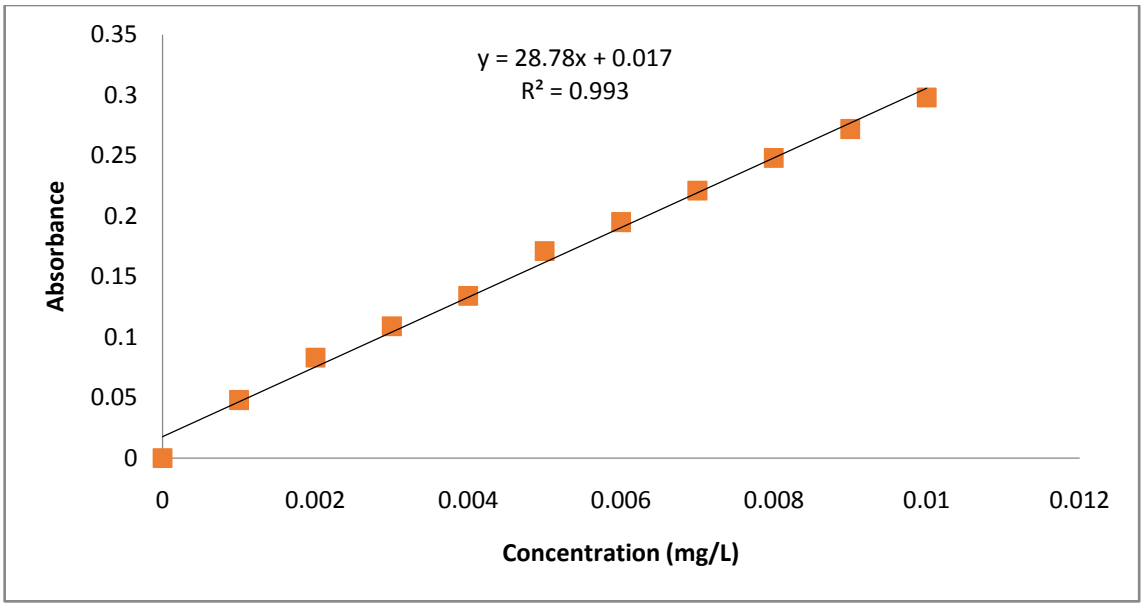


Figure 4.1: Calibration Curve for VP1

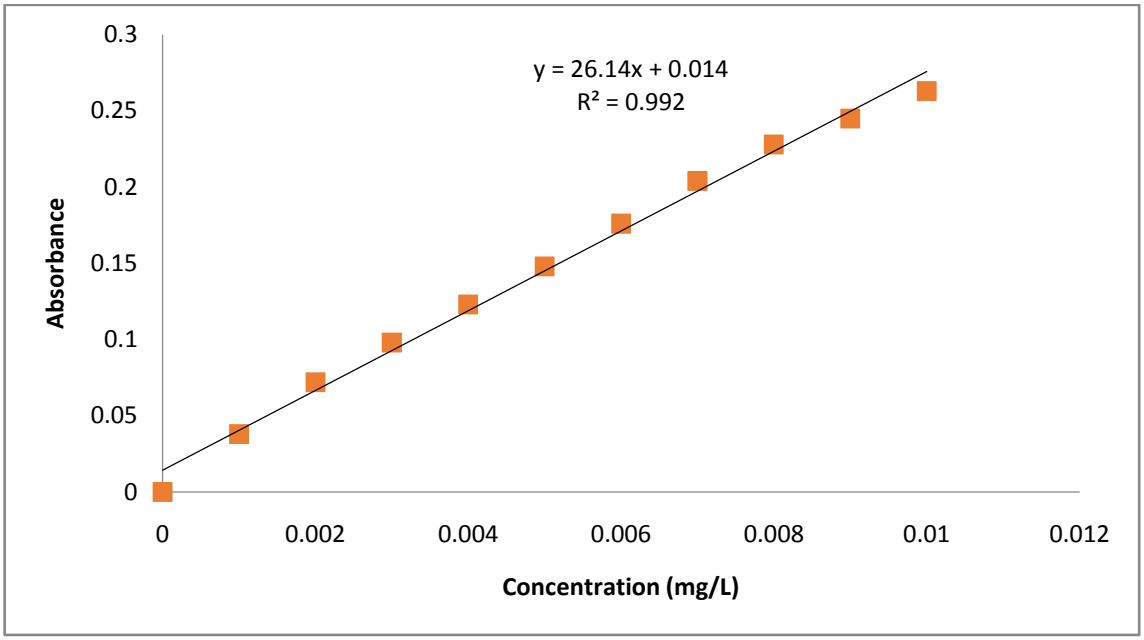


Figure 4.2: Calibration Curve for VP2

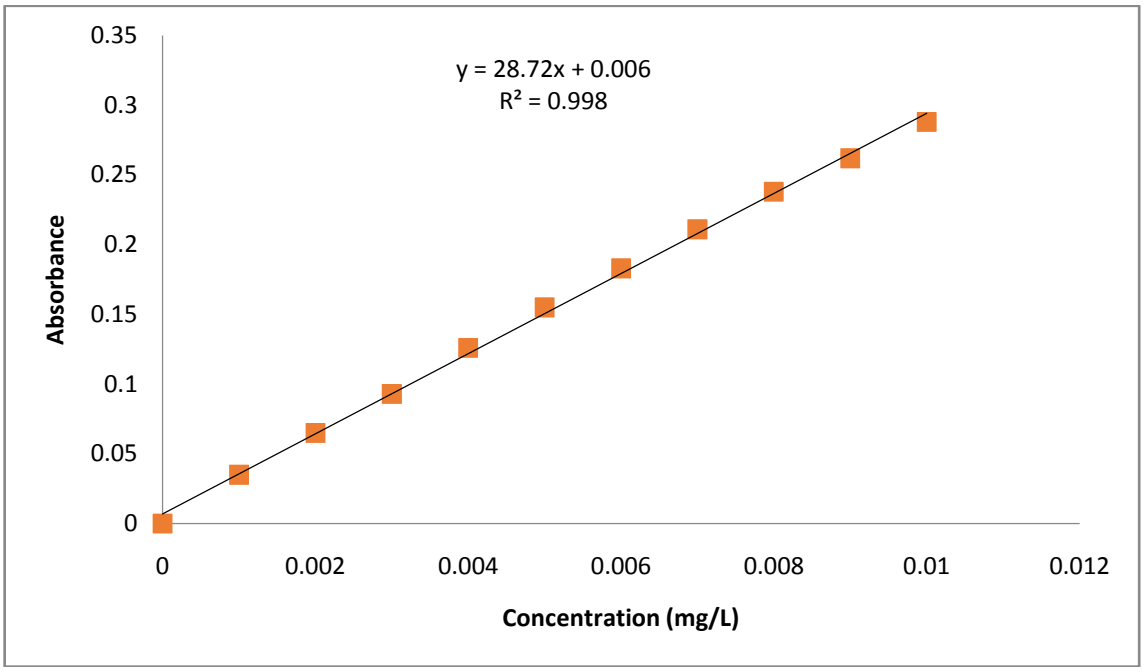


Figure 4.3: Calibration Curve for AP1

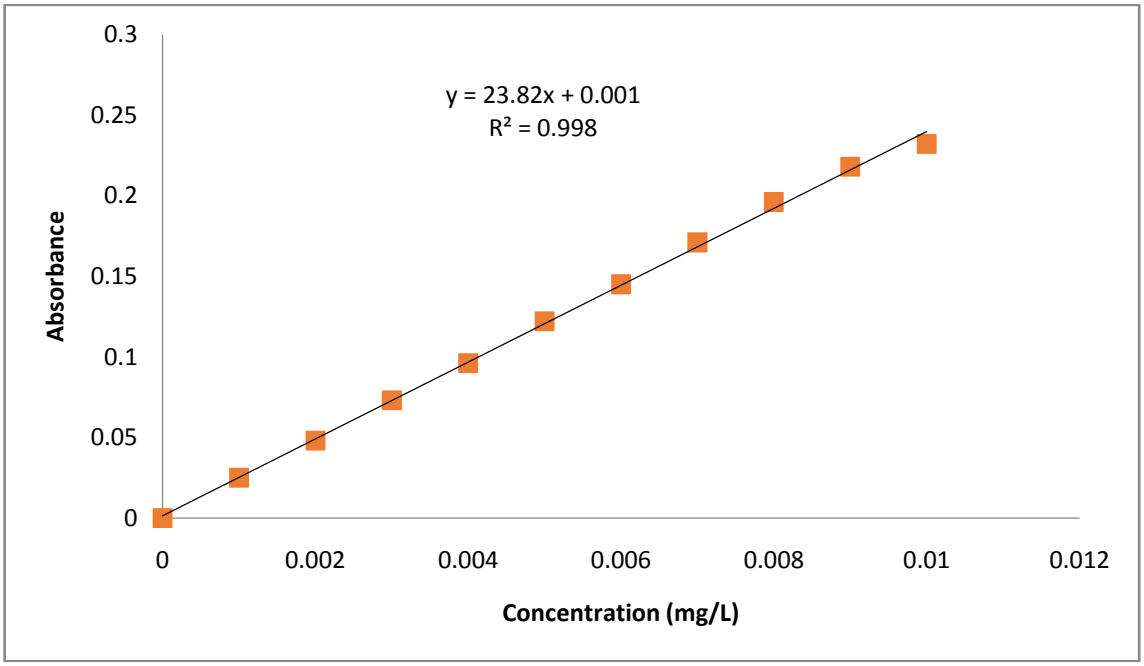


Figure 4.4: Calibration Curve for AP2

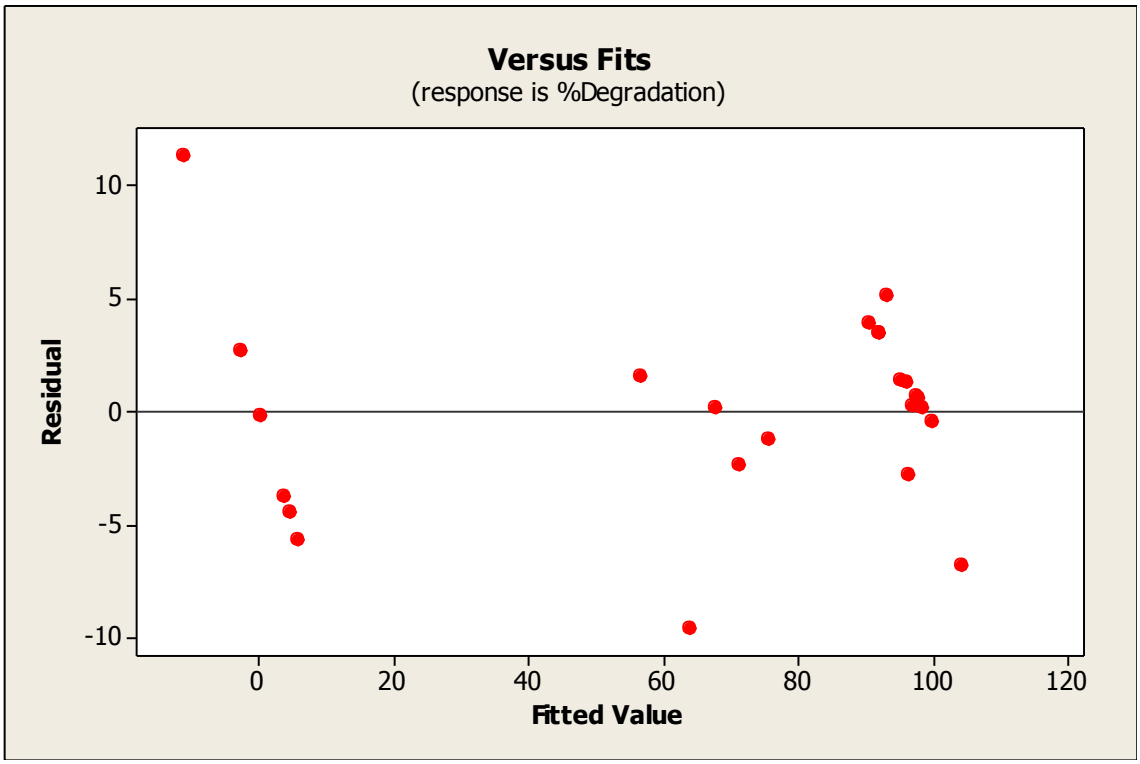


Figure 4.1a: Standard residual vs Fitted value (VP1)

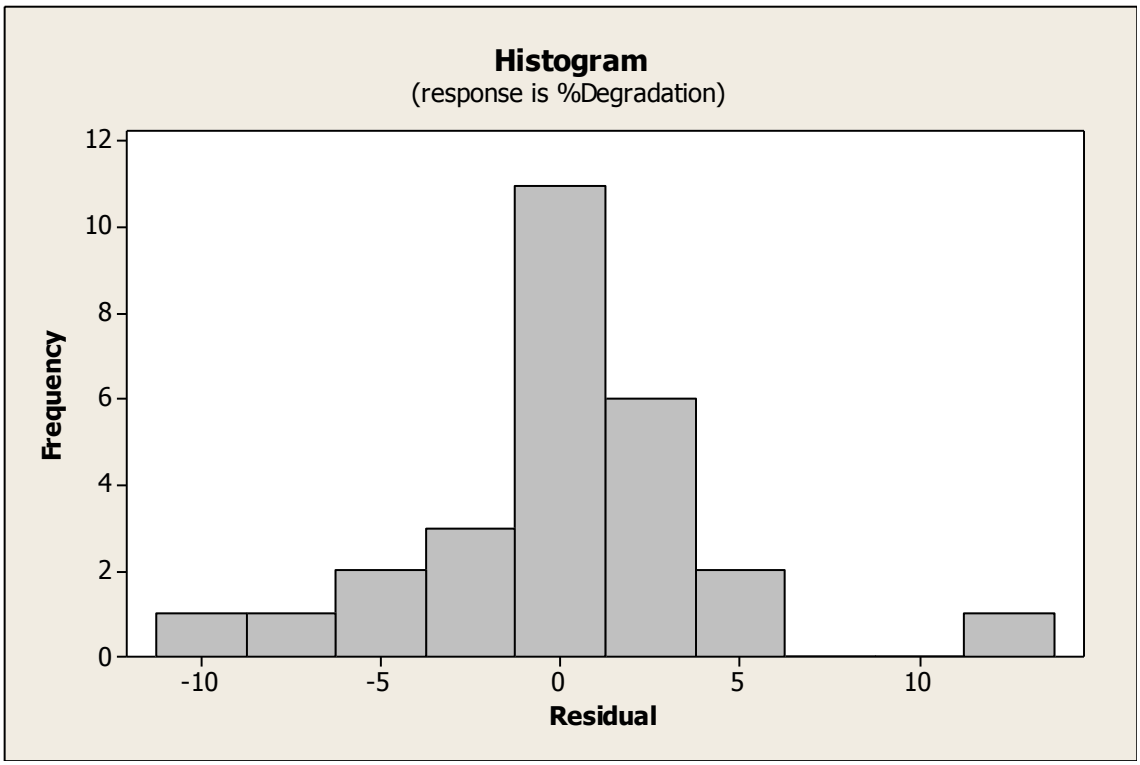


Figure 4.1b: Histogram of frequency vs Standardized residuals (VP1)

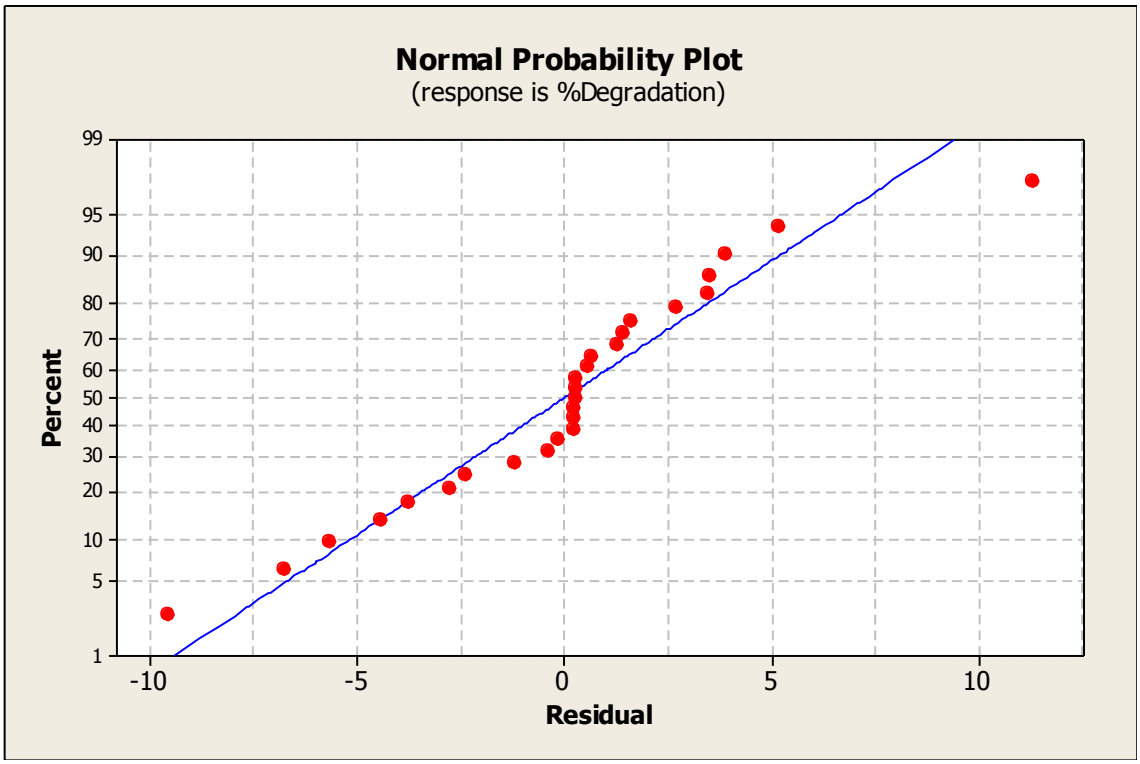


Figure 4.1c: Normal Probability Plot of Residual (VP1)

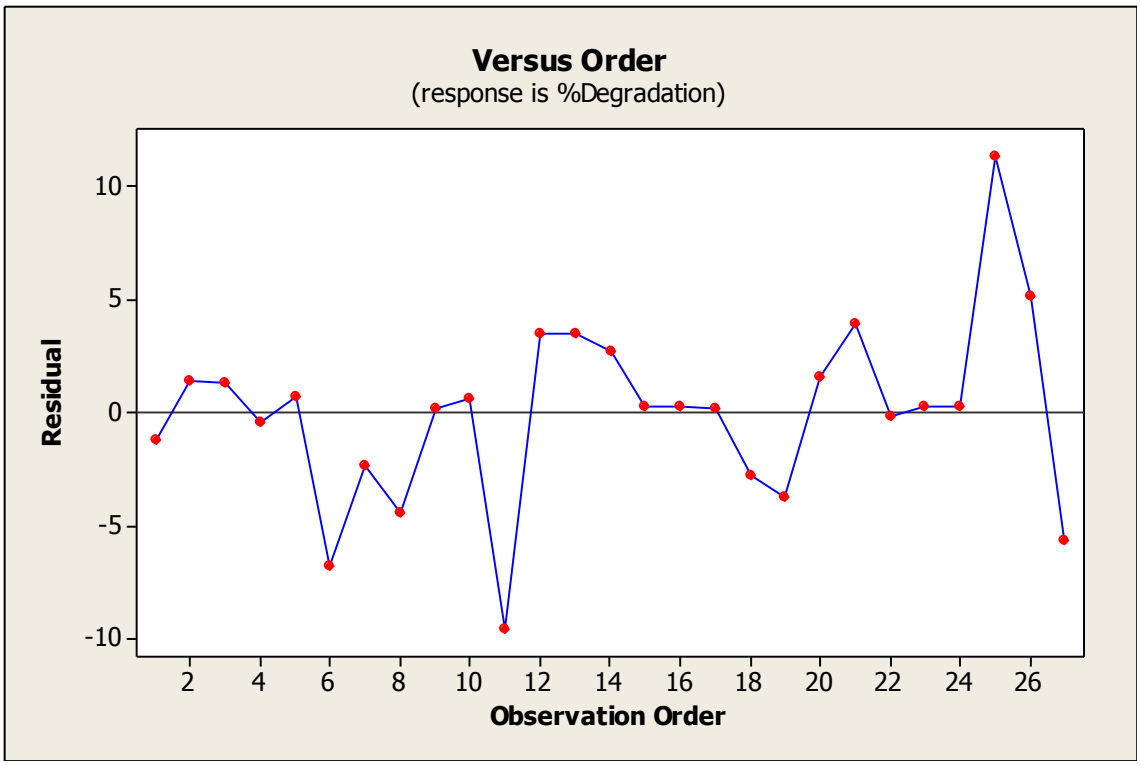


Figure 4.1d: Standardized Residual vs Observation Order (VP1)

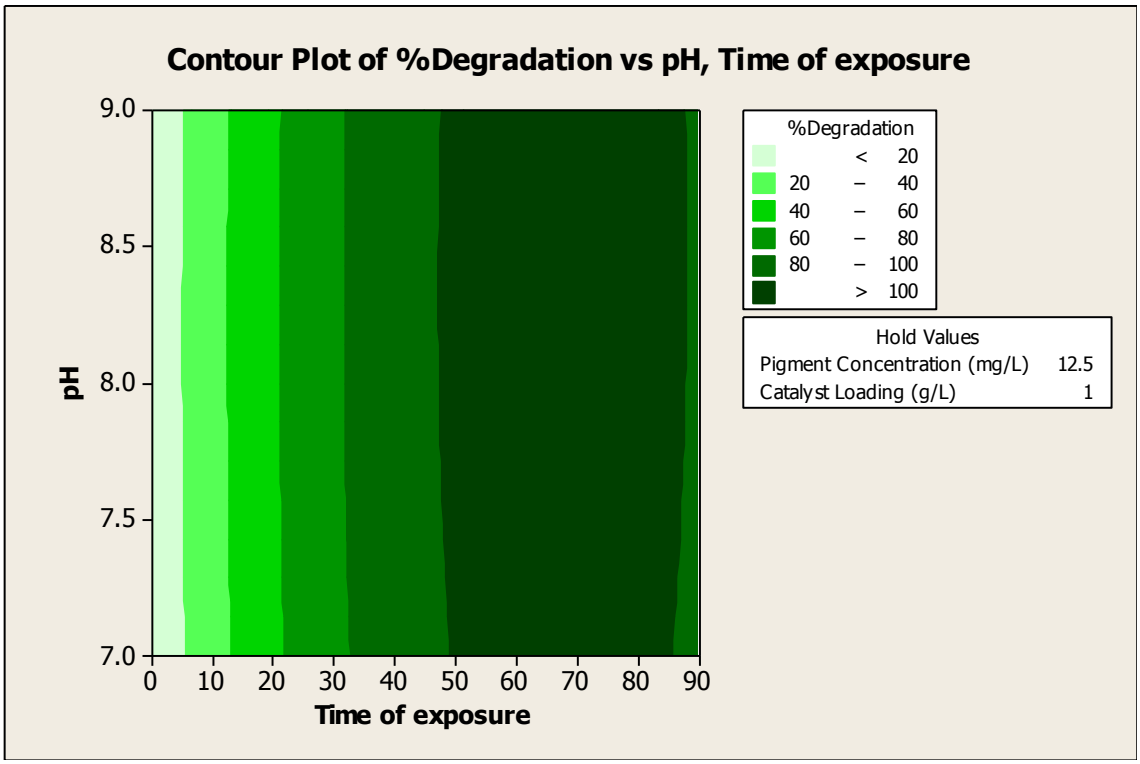


Figure 4.1e: Contour plot of %Degradation Vs pH, Time of exposure (min.) VP1

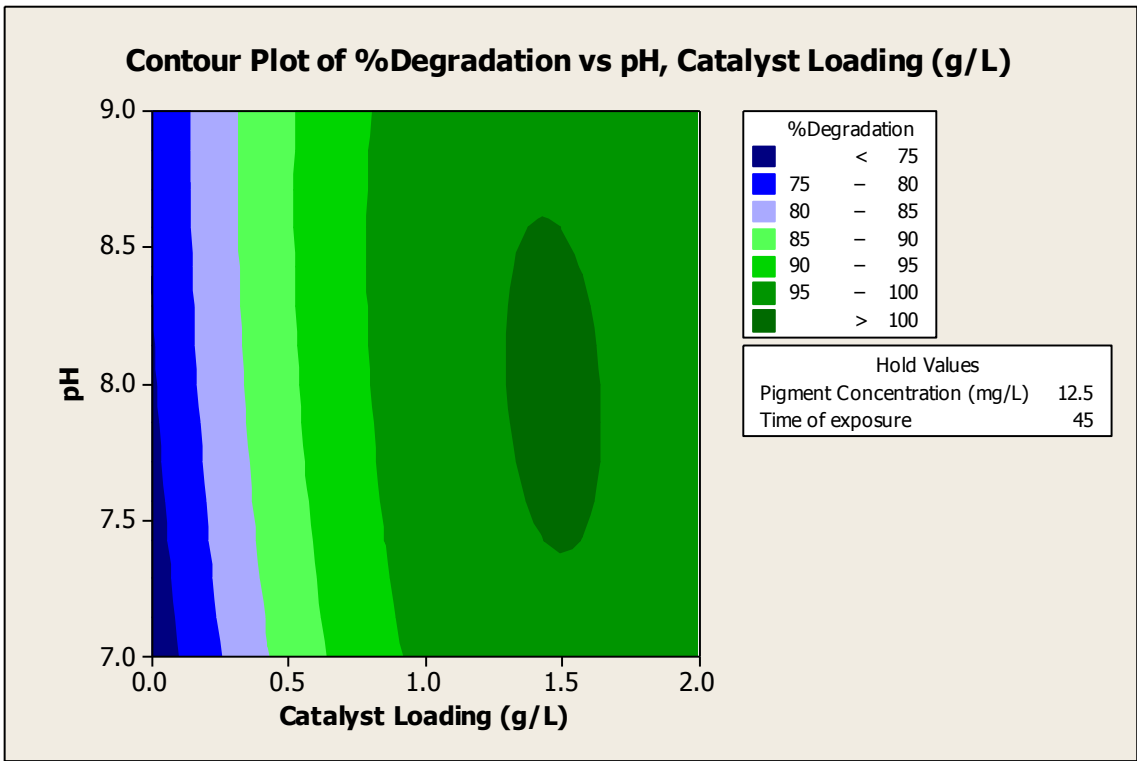


Figure 4.1f: Contour plot of %Degradation vs pH, Catalyst Loading (g/L) (VP1)

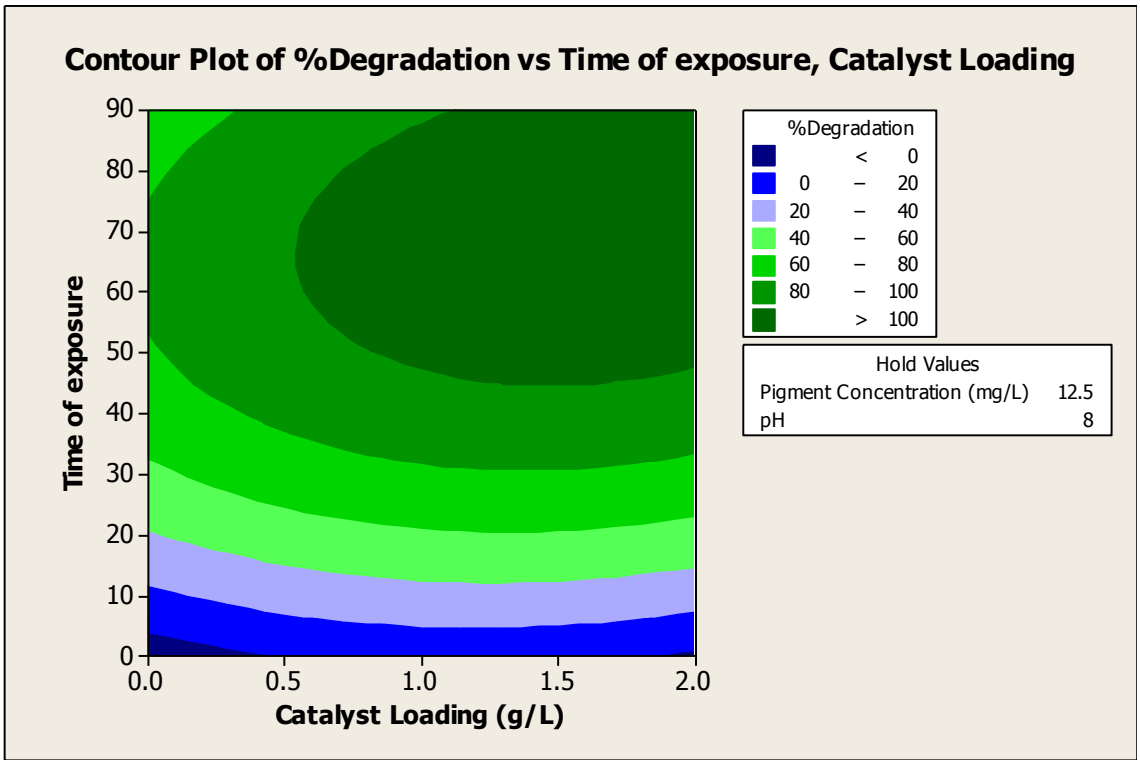


Figure 4.1g: Contour Plot of %Degradation vs time (min.), Catalyst loading (g/L) (VP1)

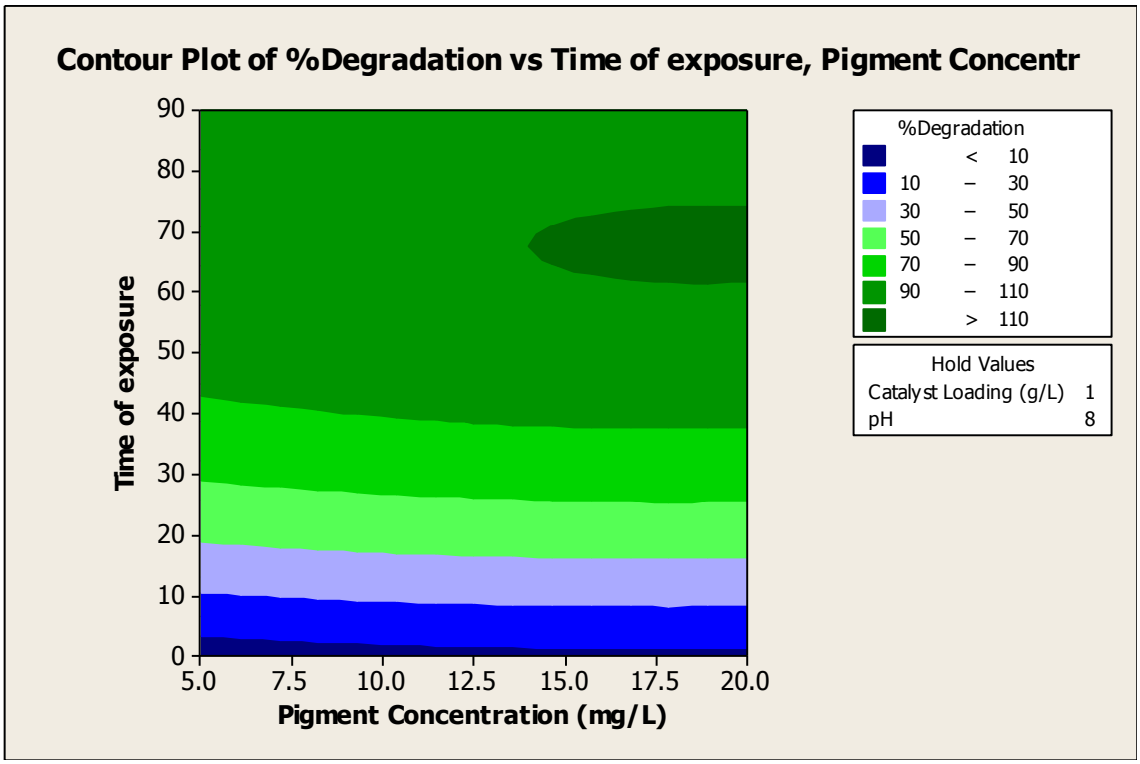


Figure 4.1h: Contour Plot of %Degradation vs Time of exposure (min), Pigment Concentration (mg/L) (VP1)

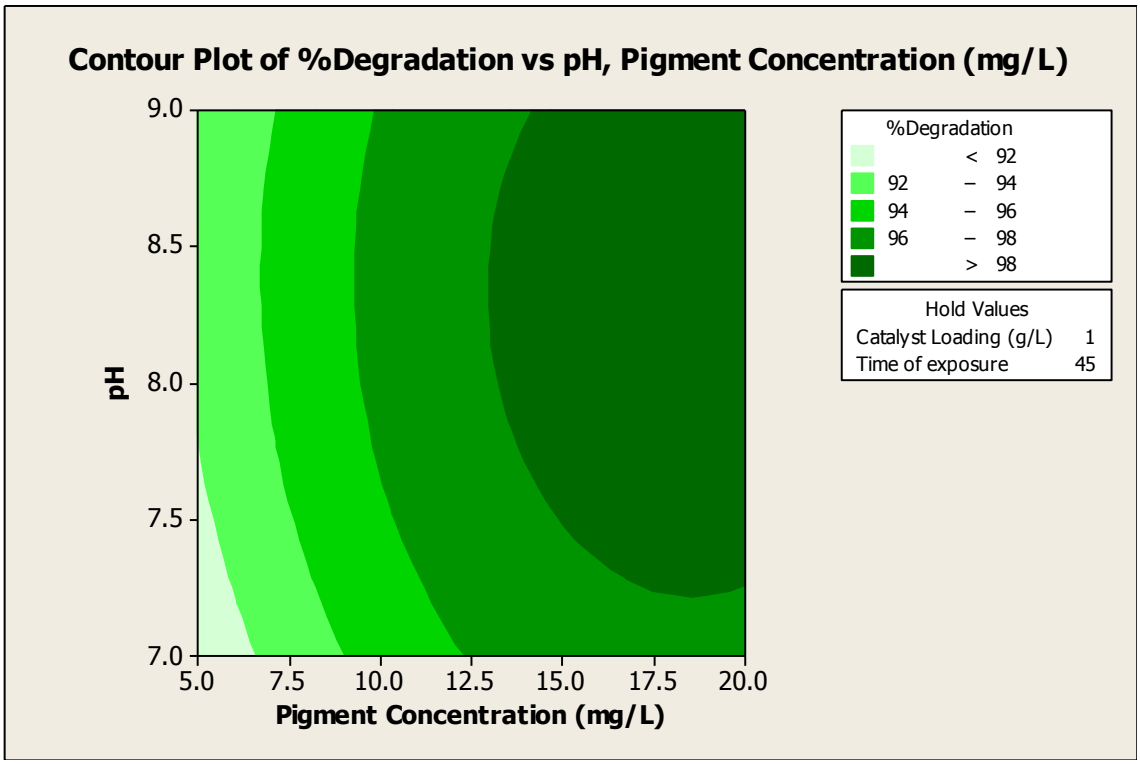


Figure 4.1i: Contour Plot of %Degradation vs pH, Pigment Concentration (mg/L) (VP1)

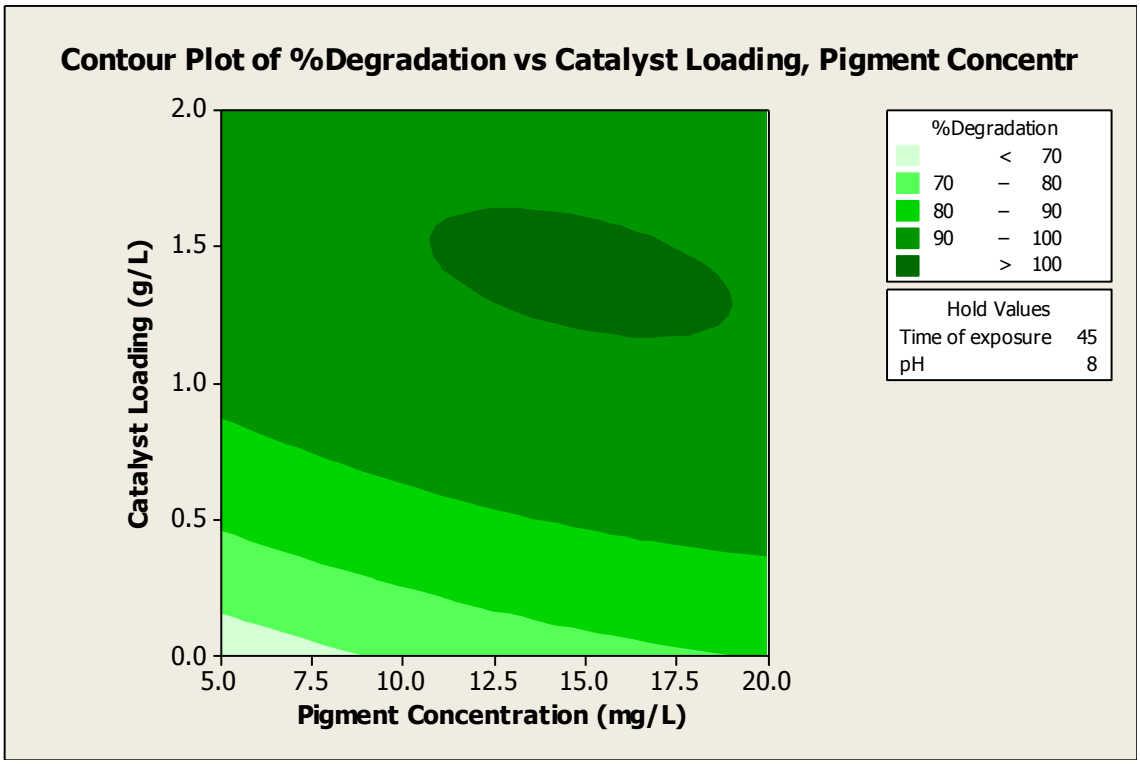


Figure 4.1j: Contour Plot of %Degradation vs Catalyst Loading (g/L), Pigment Concentration (mg/L) (VP1)

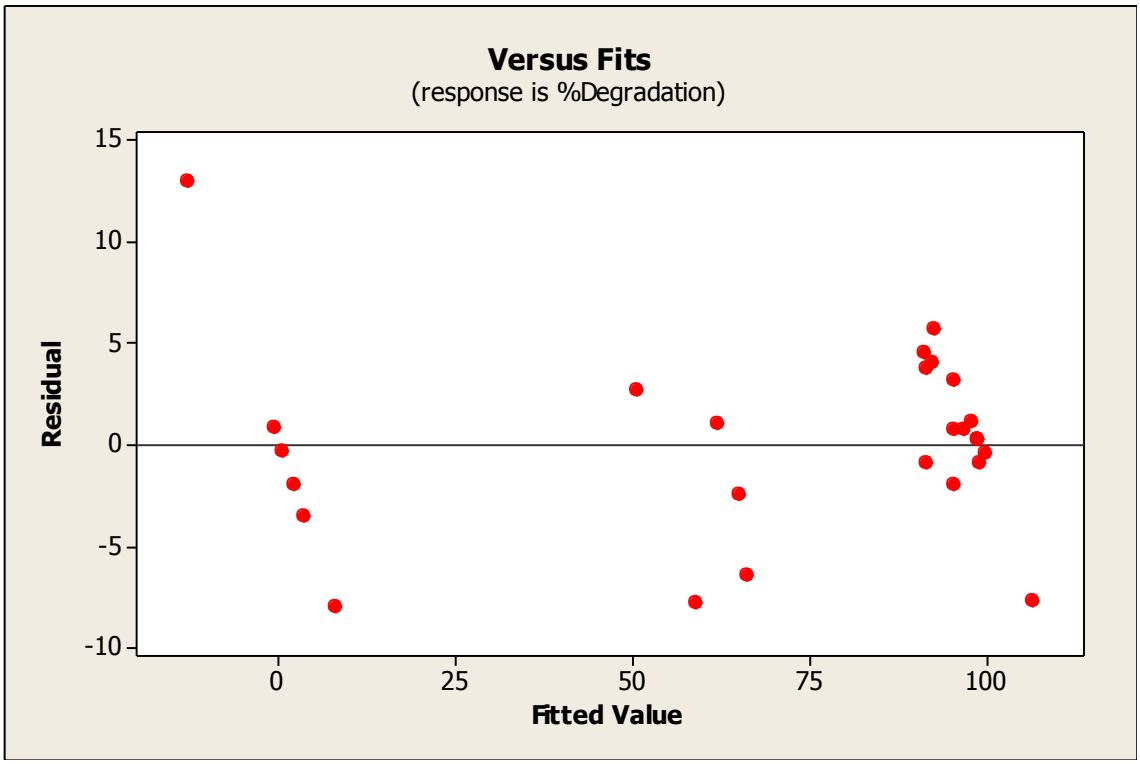


Figure 4.2a: Standard residual vs Fitted value (VP2)

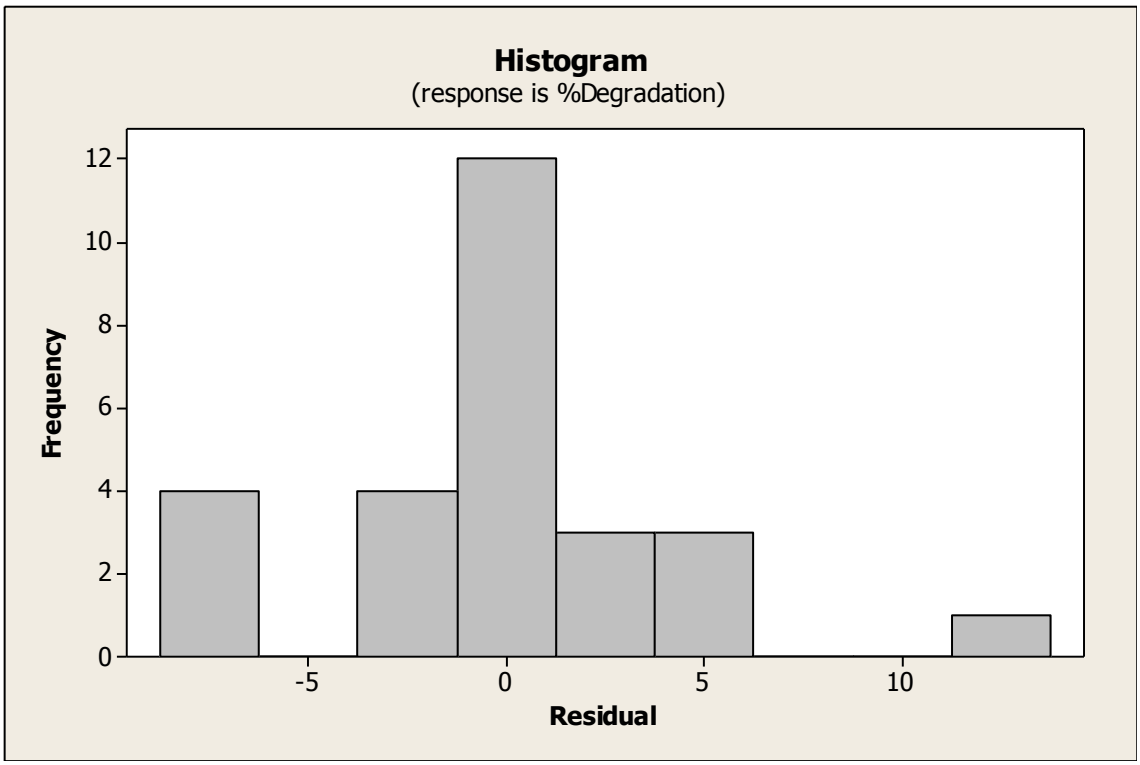


Figure 4.2b: Histogram of Frequency vs Standardized Residual (VP2)

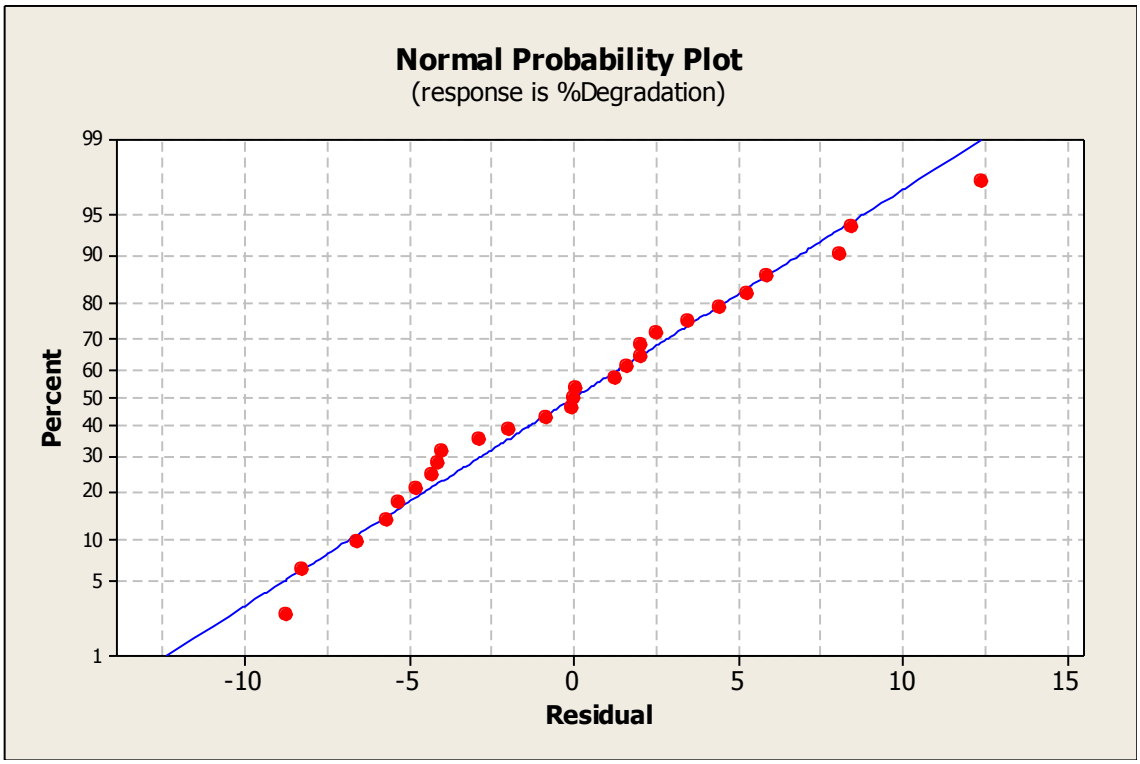


Figure 4.2c: Normal Probability Plot of Residual (VP2)

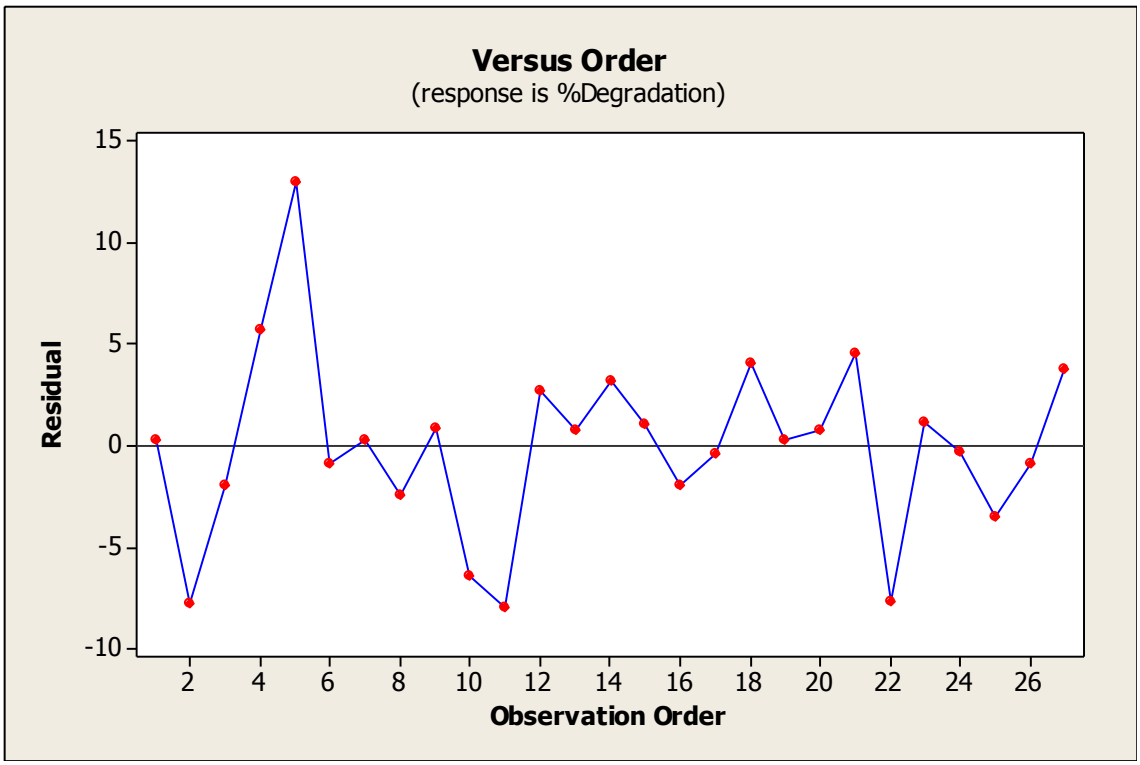


Figure 4.2d: Standardized residual residual versus Observation Order (VP2)

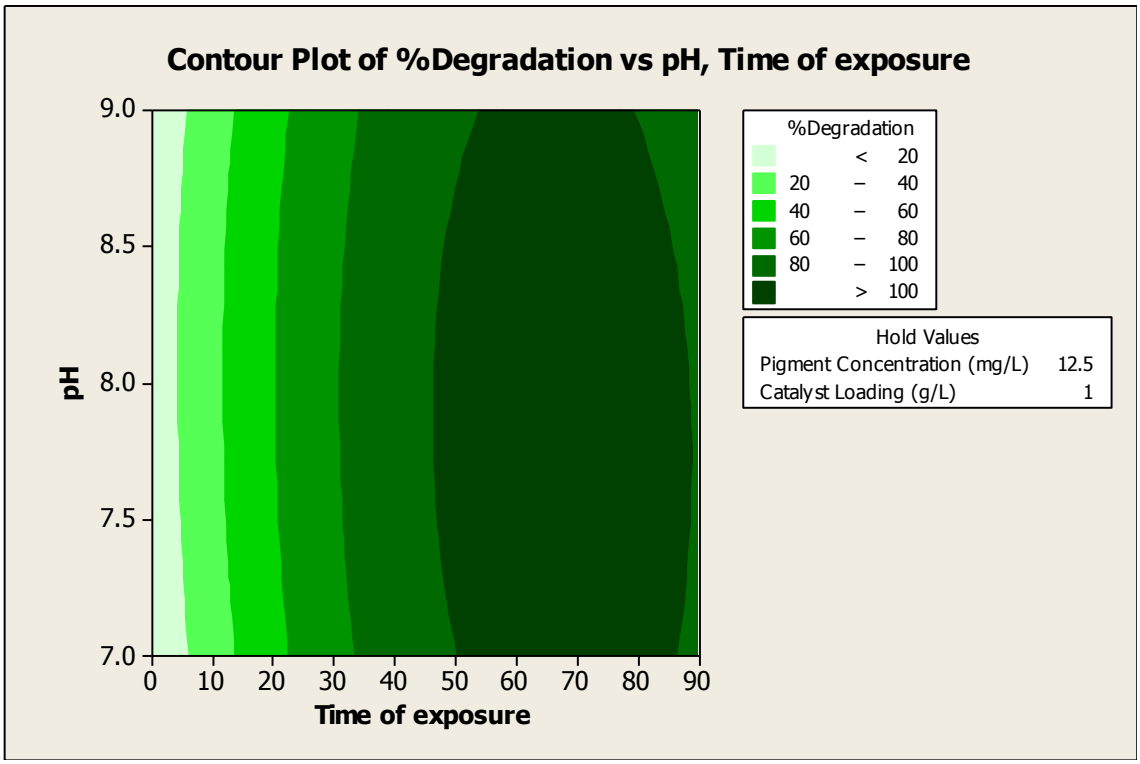


Figure 4.2e: Contour Plot of %Degradation vs pH, Time of exposure (min) (VP2)

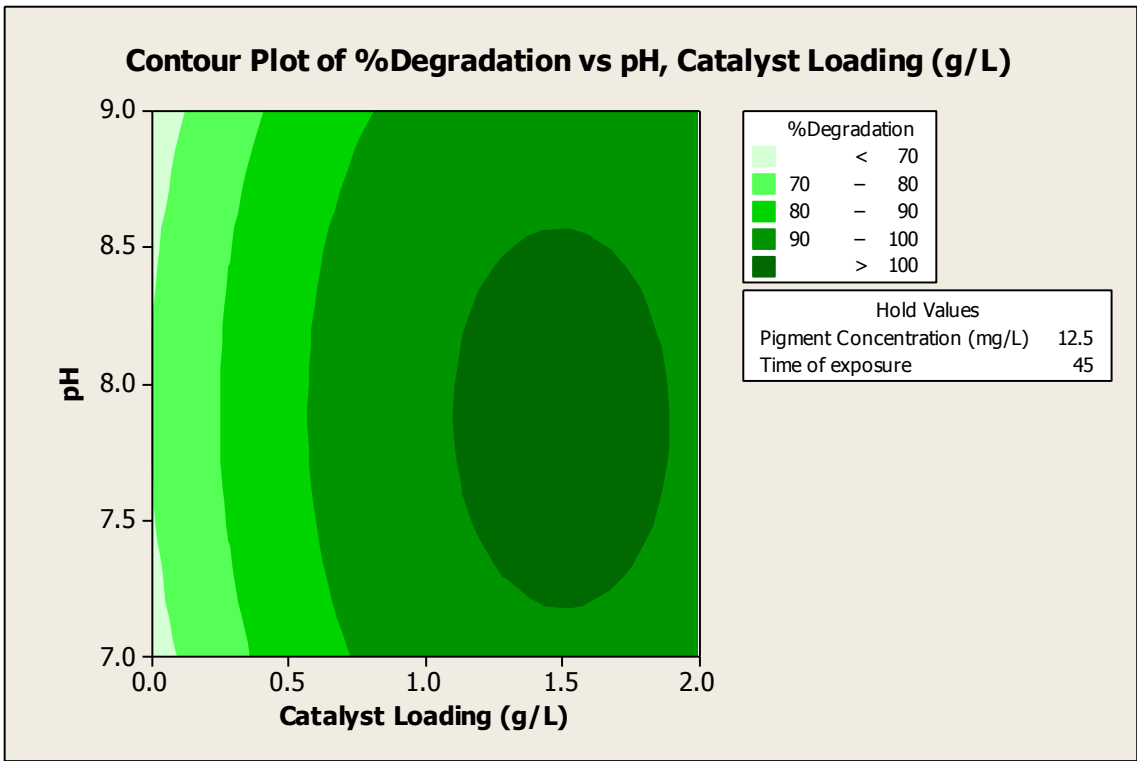


Figure 4.2f: Contour Plot of %Degradation vs pH, Catalyst Loading (g/L) (VP2)

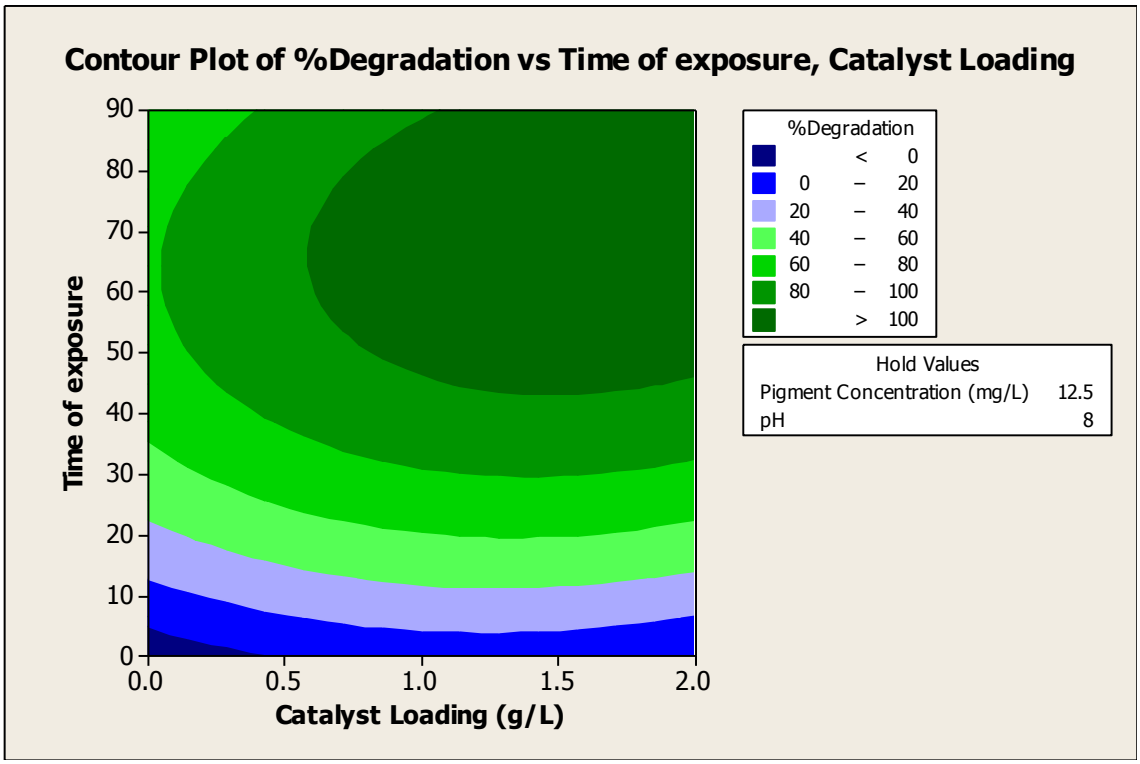


Figure 4.2g: Contour Plot of %Degradation vs Time of exposure (min.), Catalyst Loading (g/L) (VP2)

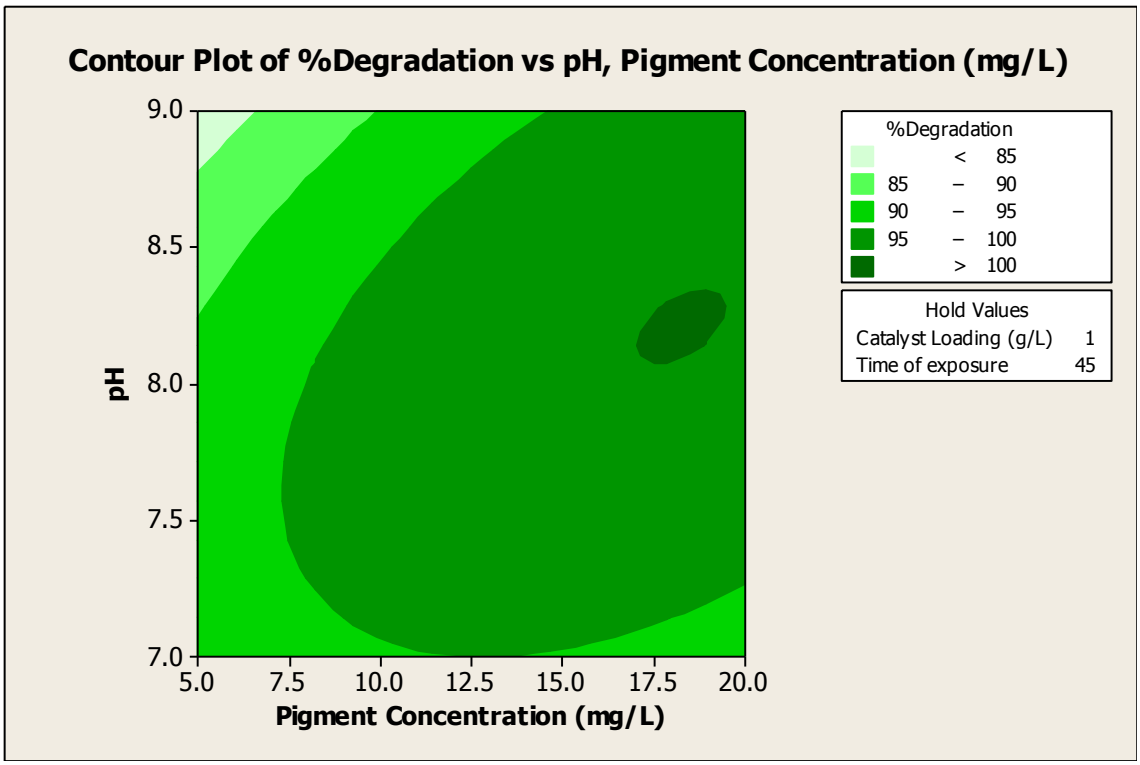


Figure 4.2h: Contour Plot of %Degradation versus pH, Pigment Concentration (mg/L) VP2

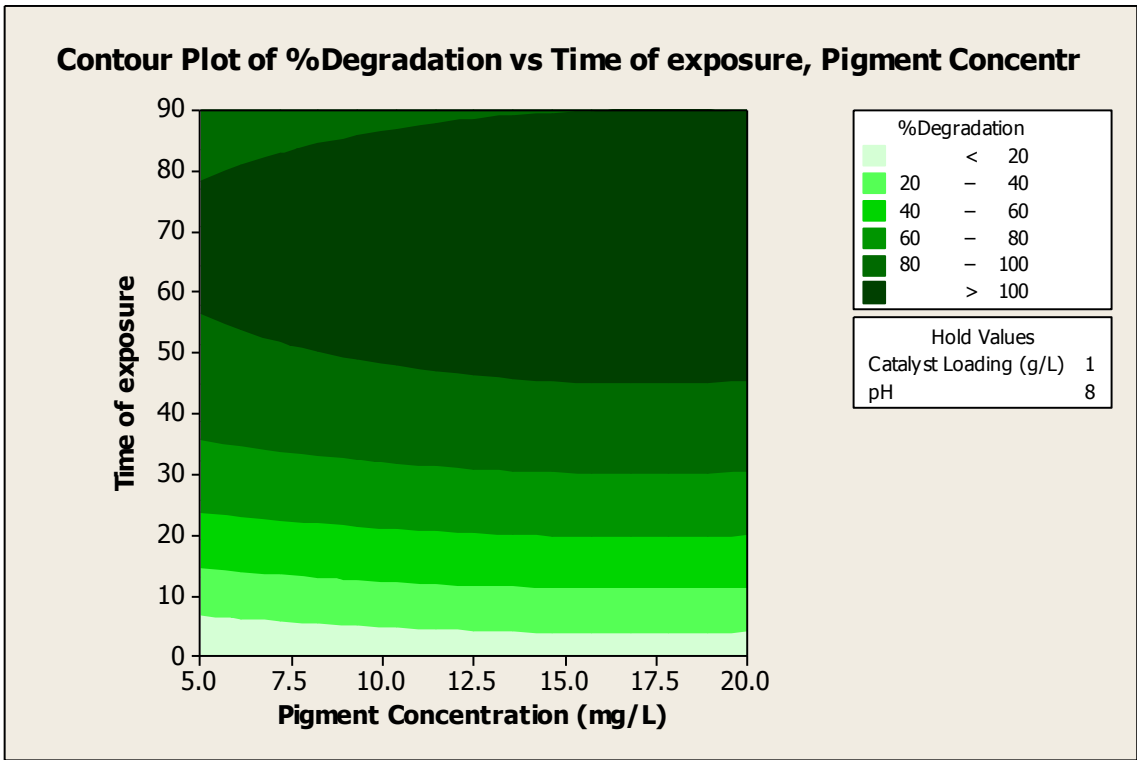


Figure 4.2i: Contour Plot of %Degradation versus Time of exposure (min), Pigment Concentration (mg/L) (VP2)

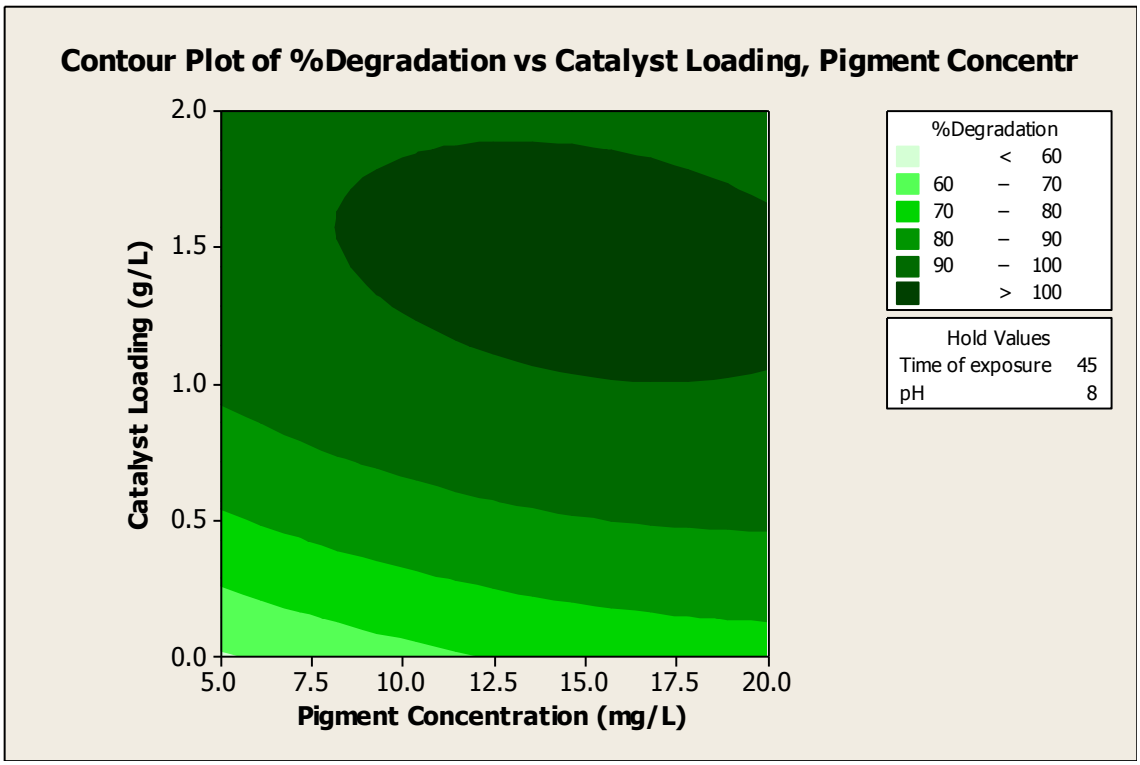


Figure 4.2j: Contour Plot of %Degradation vs Catalyst Loading (g/L), Pigment Concentration (mg/L) (VP2)

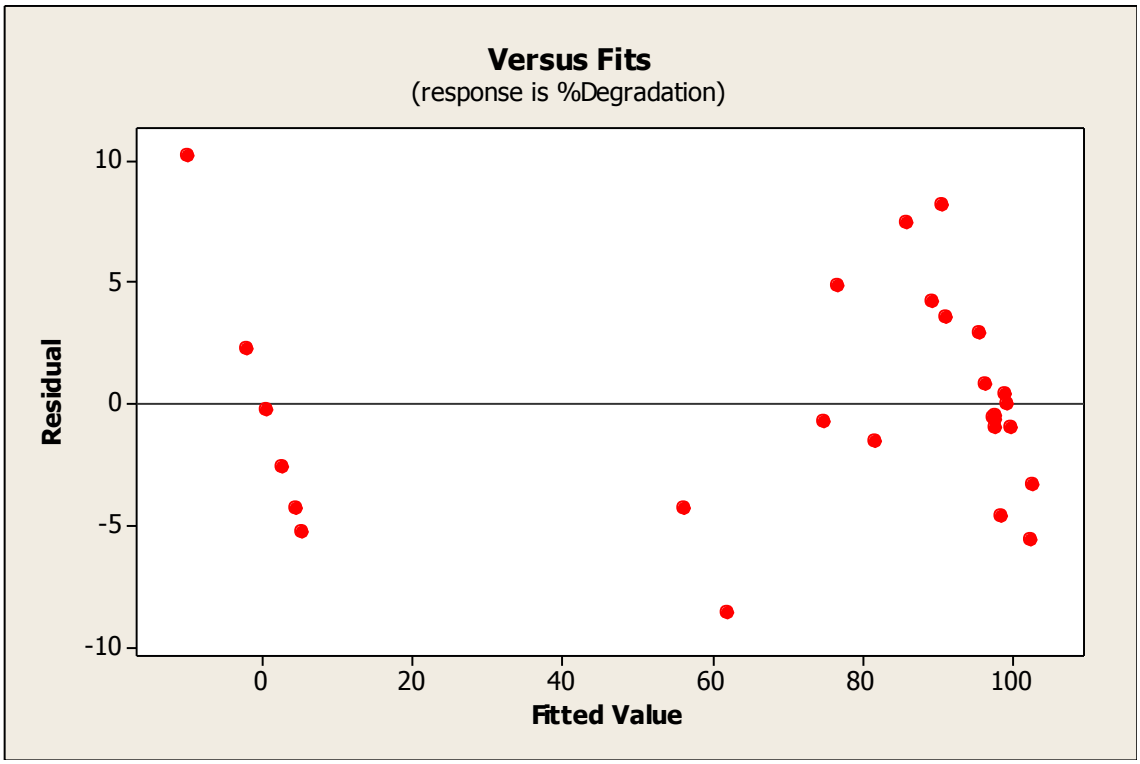


Figure 4.3a: Standardized Residual vs Fitted Value (AP1)

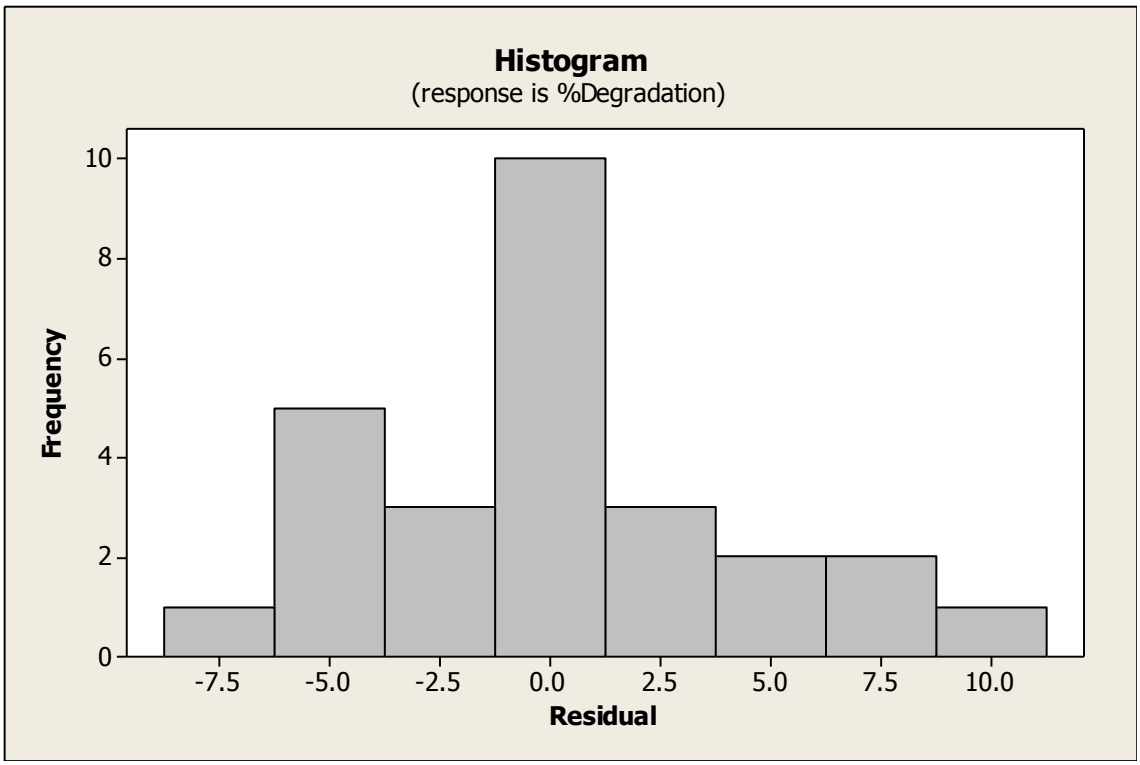


Figure 4.3b: Histogram of Frequency vs Standardized Residual (AP1)

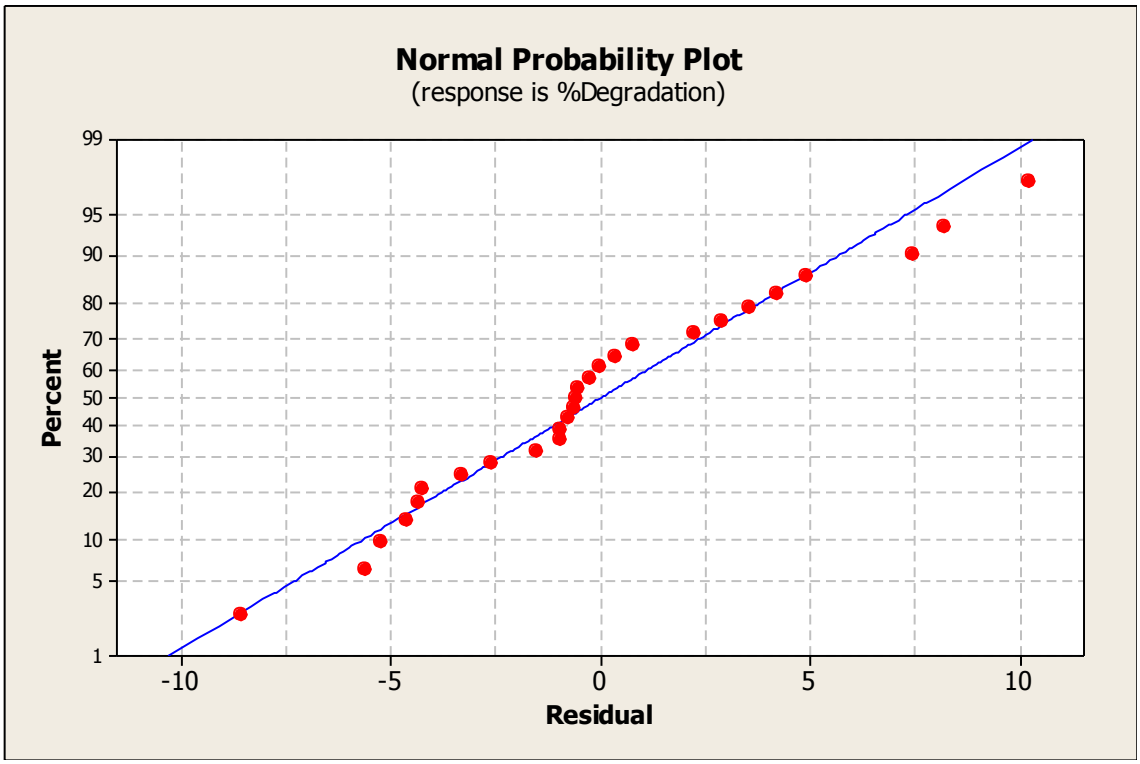


Figure 4.3c: Normal Probability Plot of Residual (AP1)

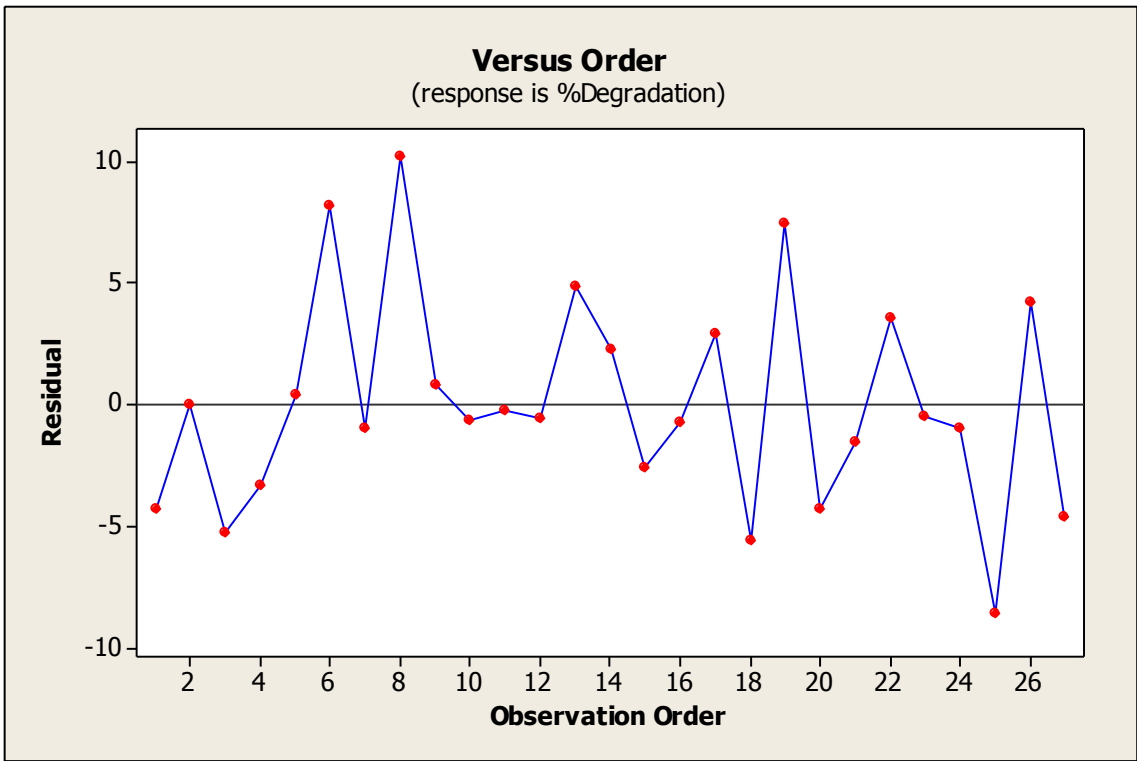


Figure 4.3d: Standardized Residual vs Observation Order (AP1)

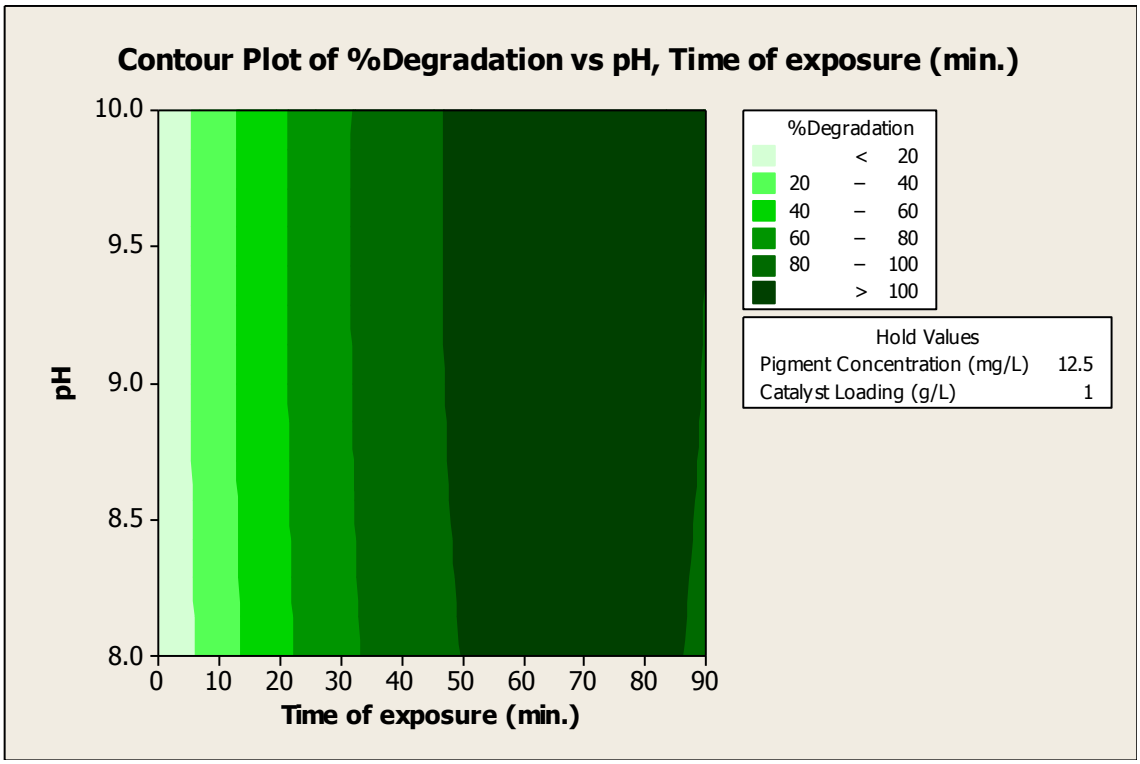


Figure 4.3e: Contour Plot of %Degradation vs pH, Time of exposure (min.) (AP1)

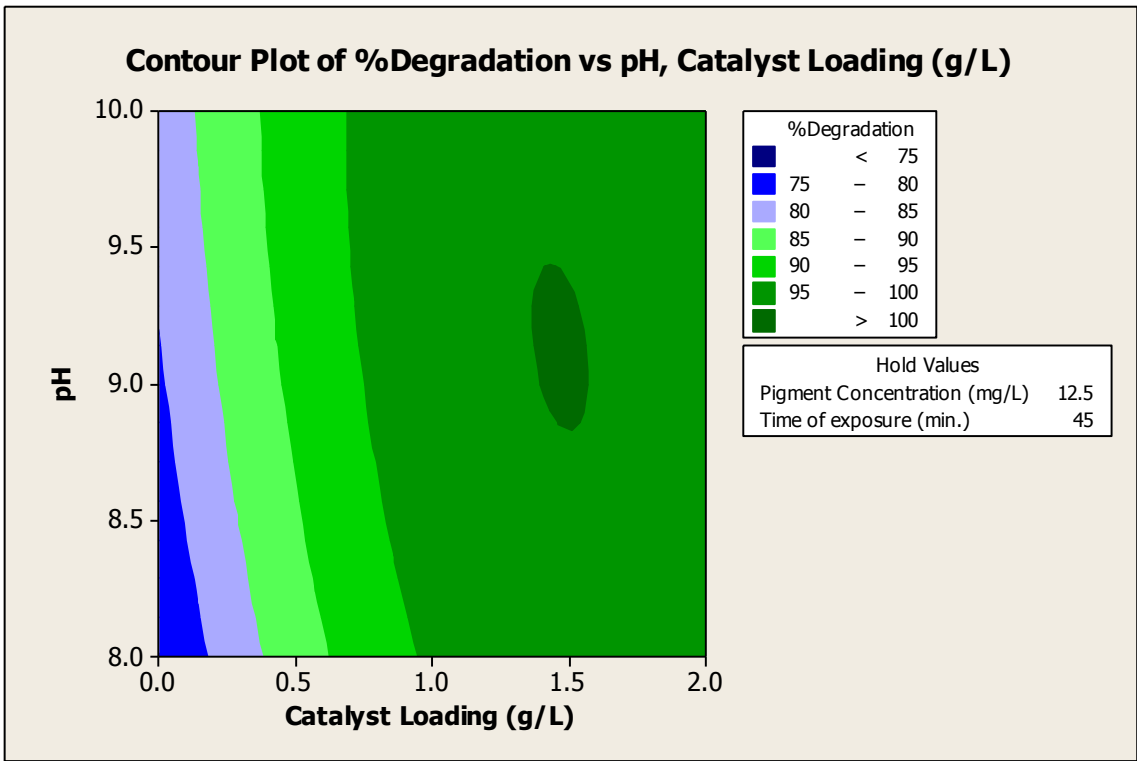


Figure 4.3f: Contour Plot of %Degradation vs pH, Catalyst Loading (g/L) (AP1)

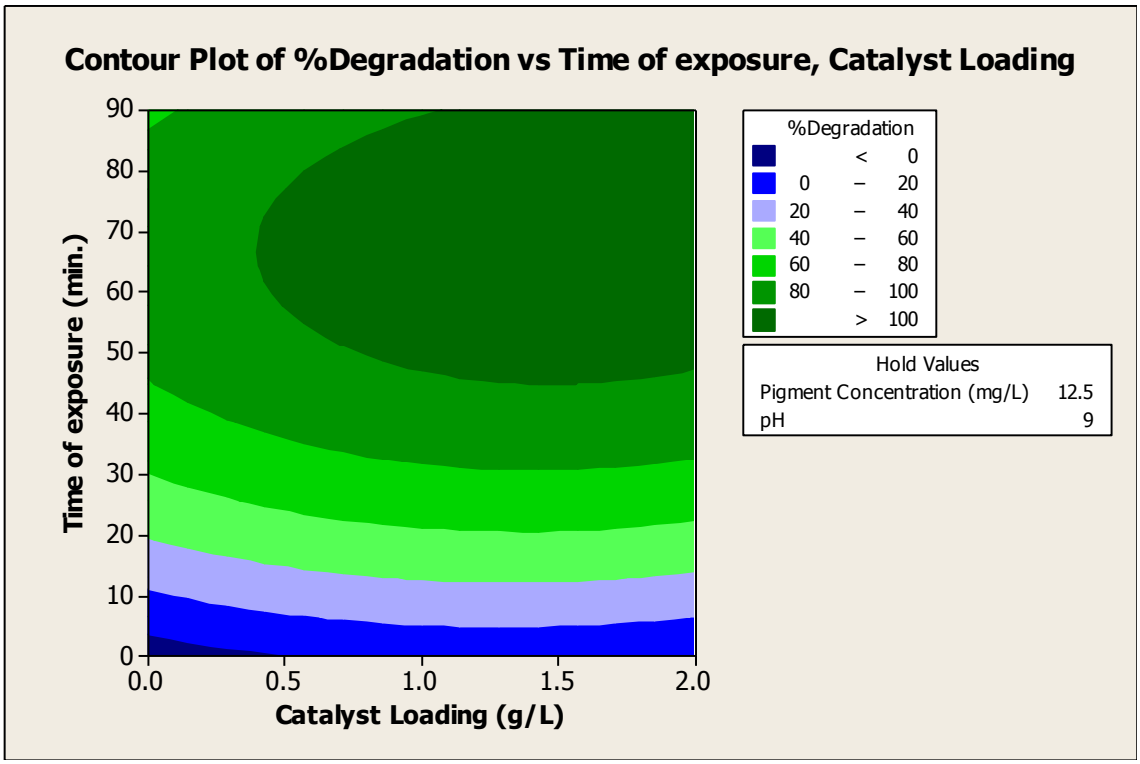


Figure 4.3g: Contour Plot of %Degradation vs Time of exposure (min.), Catalyst Loading (g/L) (AP1)

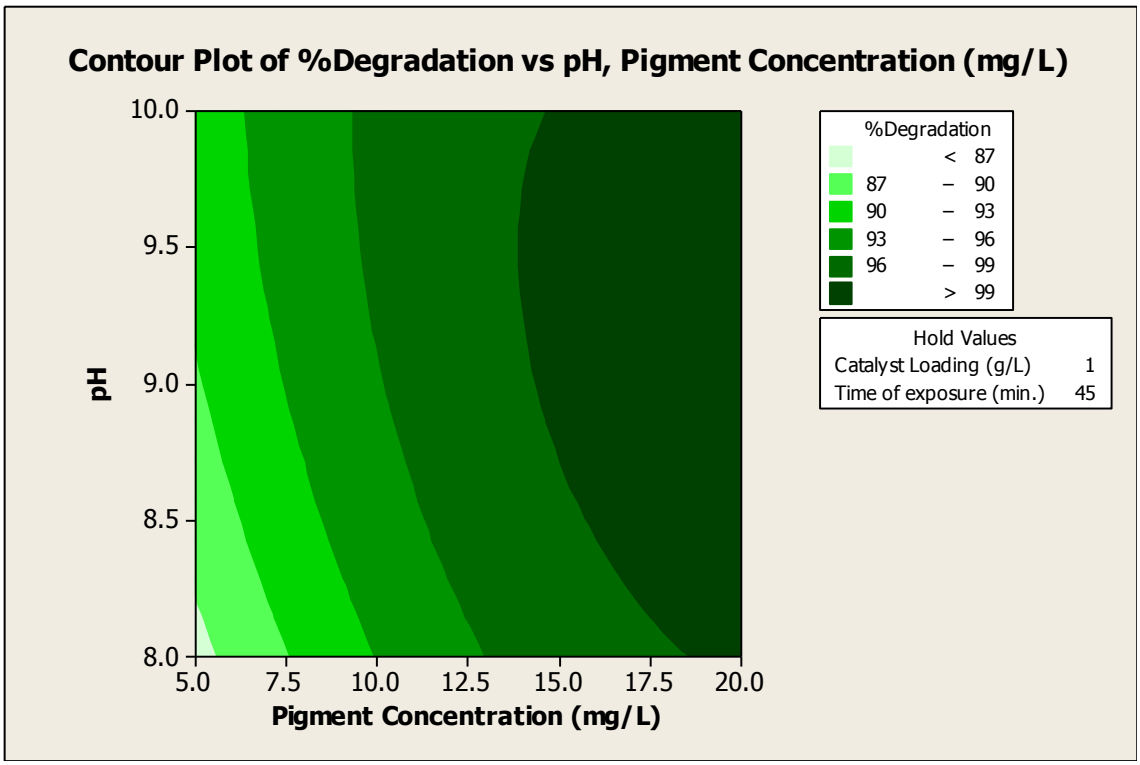


Figure 4.3h: Contour Plot of %Degradation vs pH, Pigment Concentration (mg/L) AP1

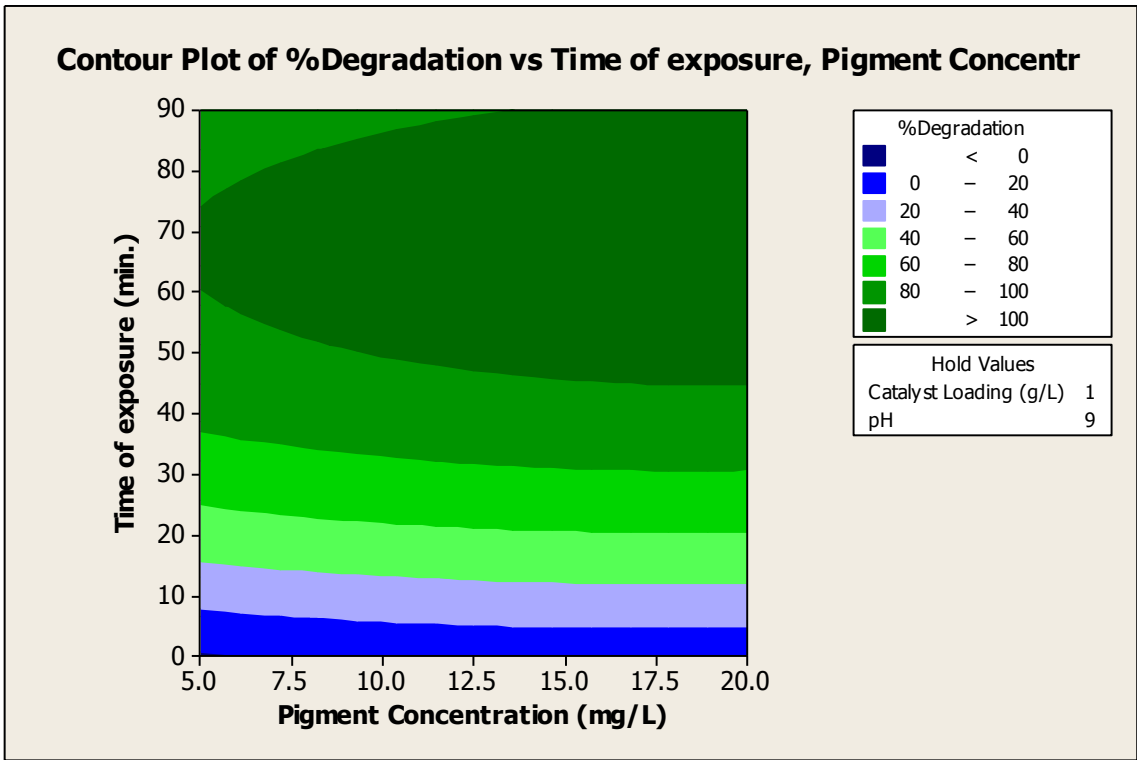


Figure 4.3i: Contour Plot of %Degradation vs Time of exposure (min.), Pigment Concentration (mg/L) (AP1)

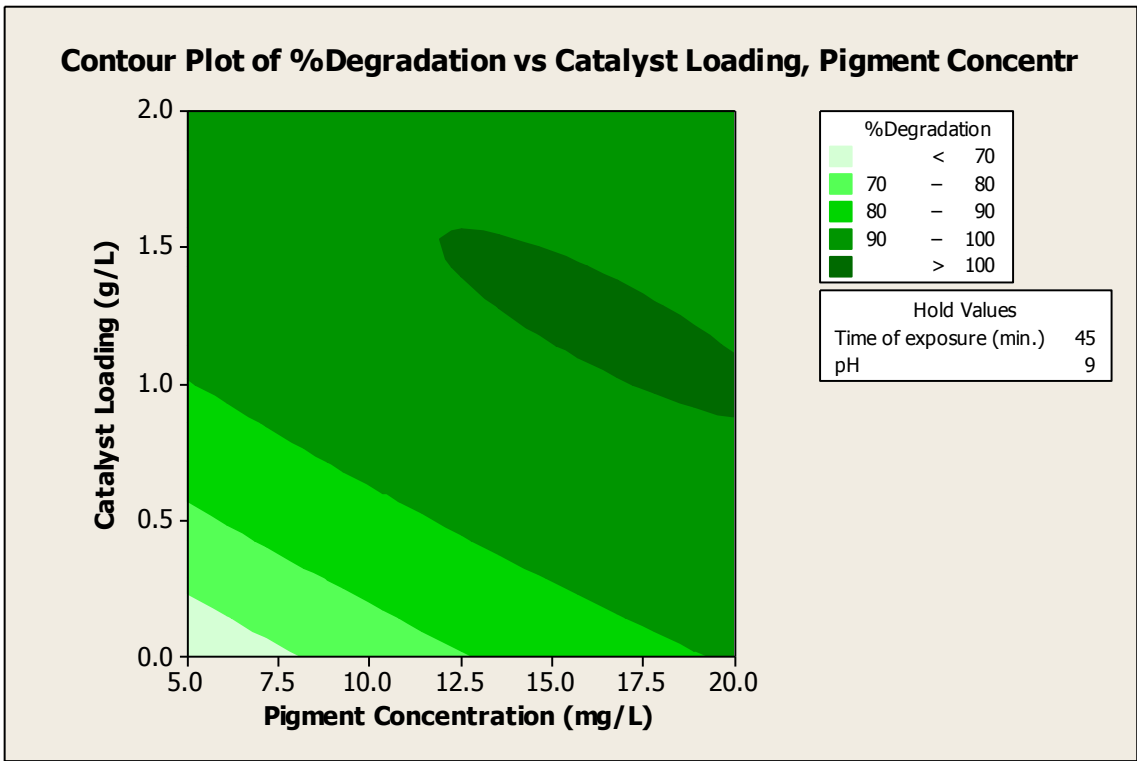


Figure 4.3j: Contour Plot of %Degradation vs. Catalyst Loading (g/L), Pigment Concentration (mg/L) (AP1)

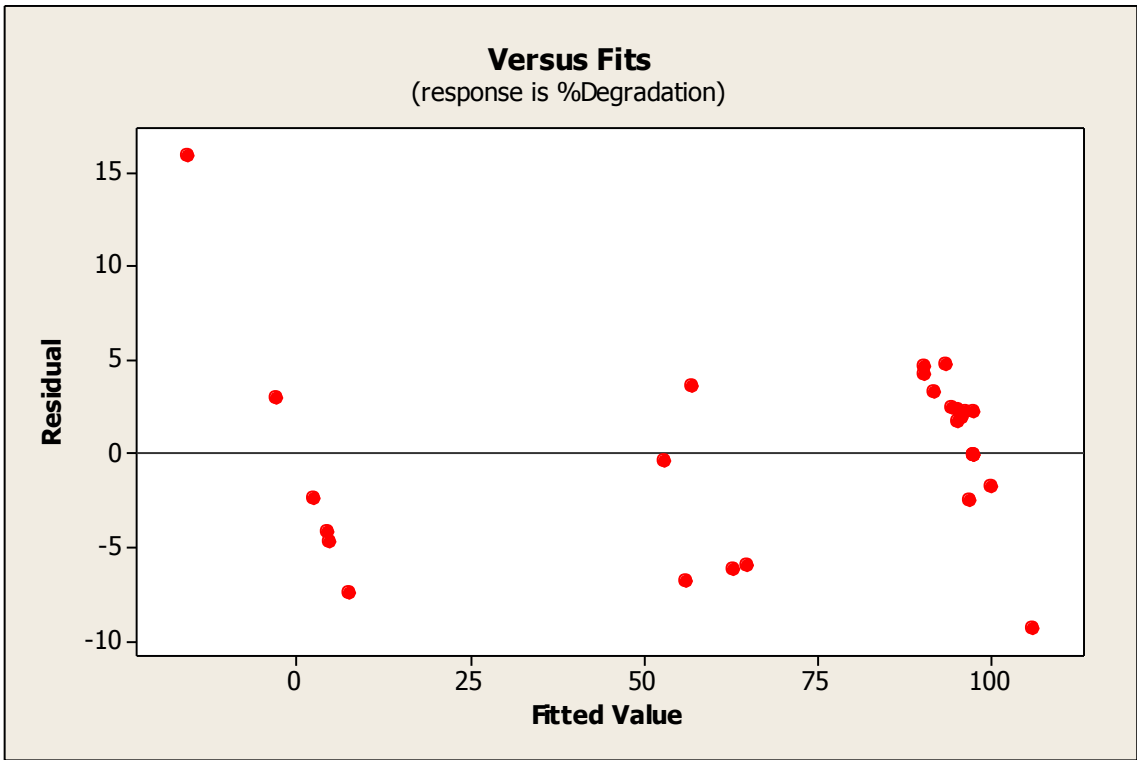


Figure 4.4a: Standardized Residual vs Fitted Value (AP2)

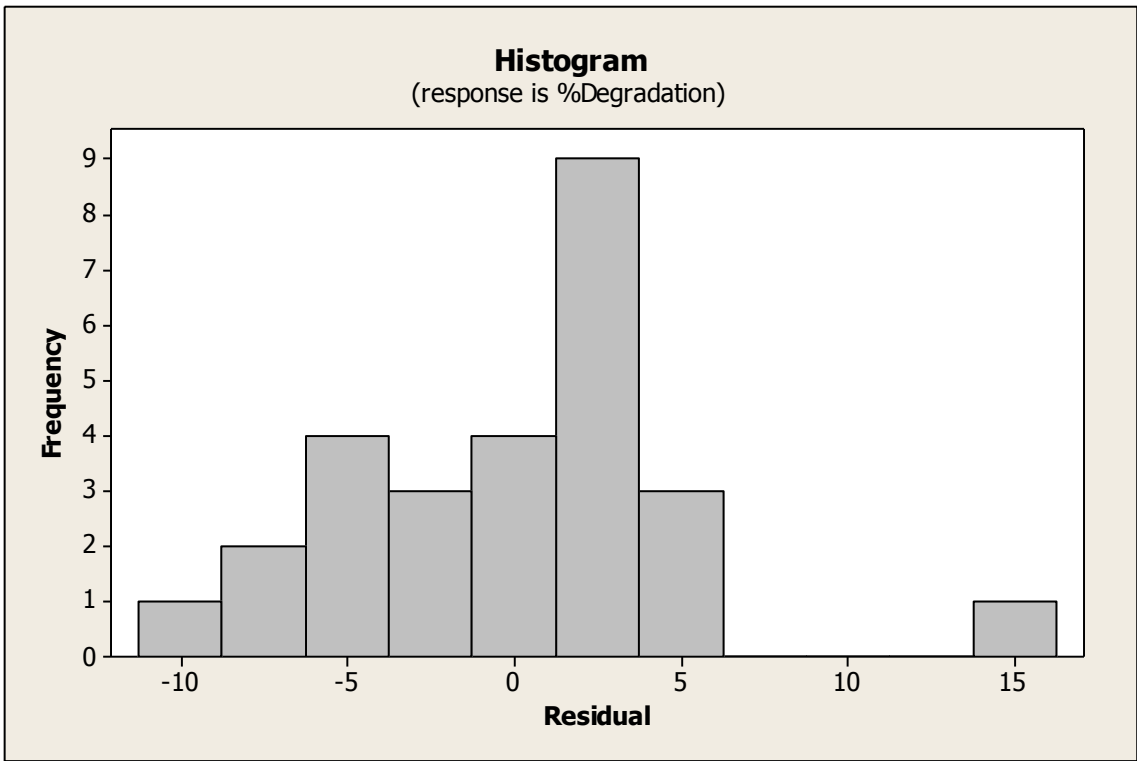


Figure 4.4b: Histogram of Frequency vs Standardized Residuals (AP2)

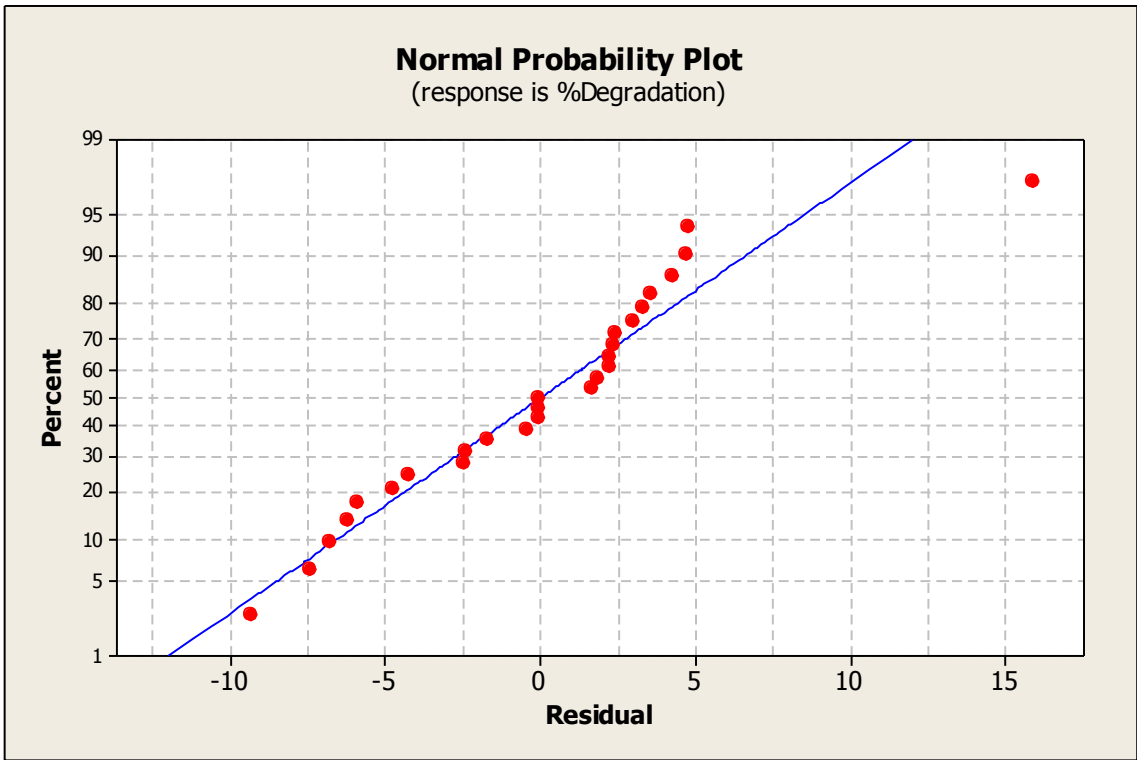


Figure 4.4c: Normal Probability Plot of Residual (AP2)

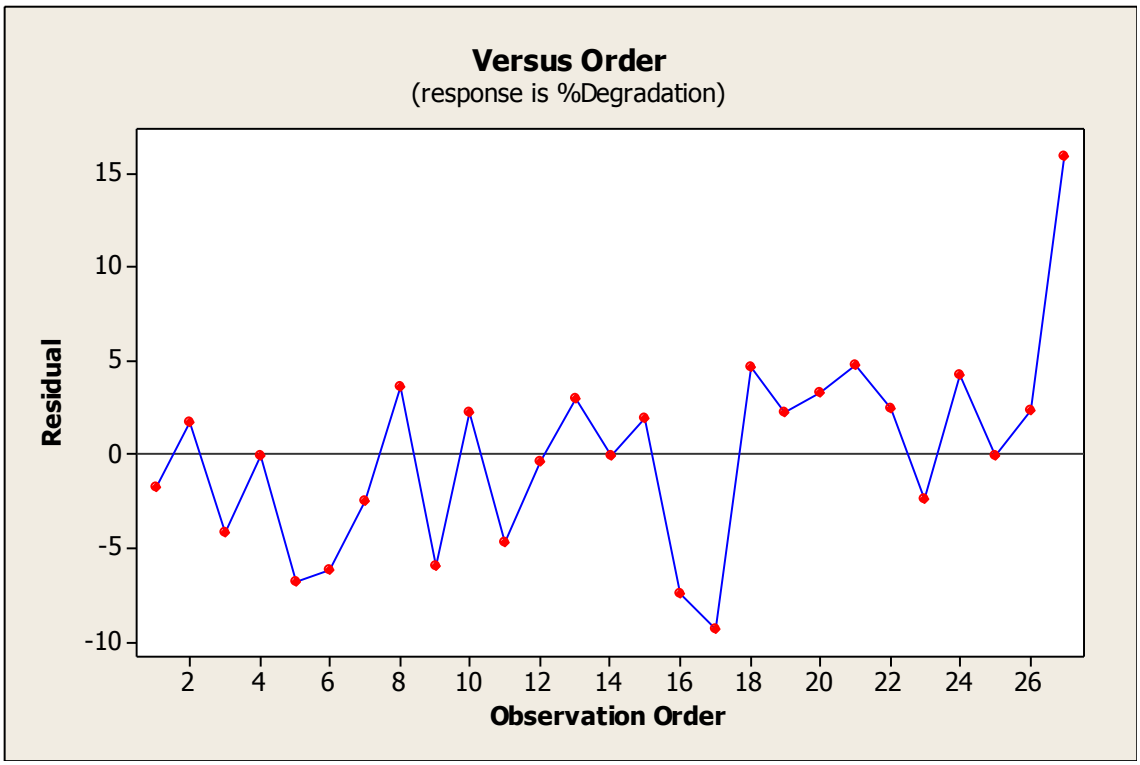


Figure 4.4d: Standardized residual vs Observation Order (AP2)

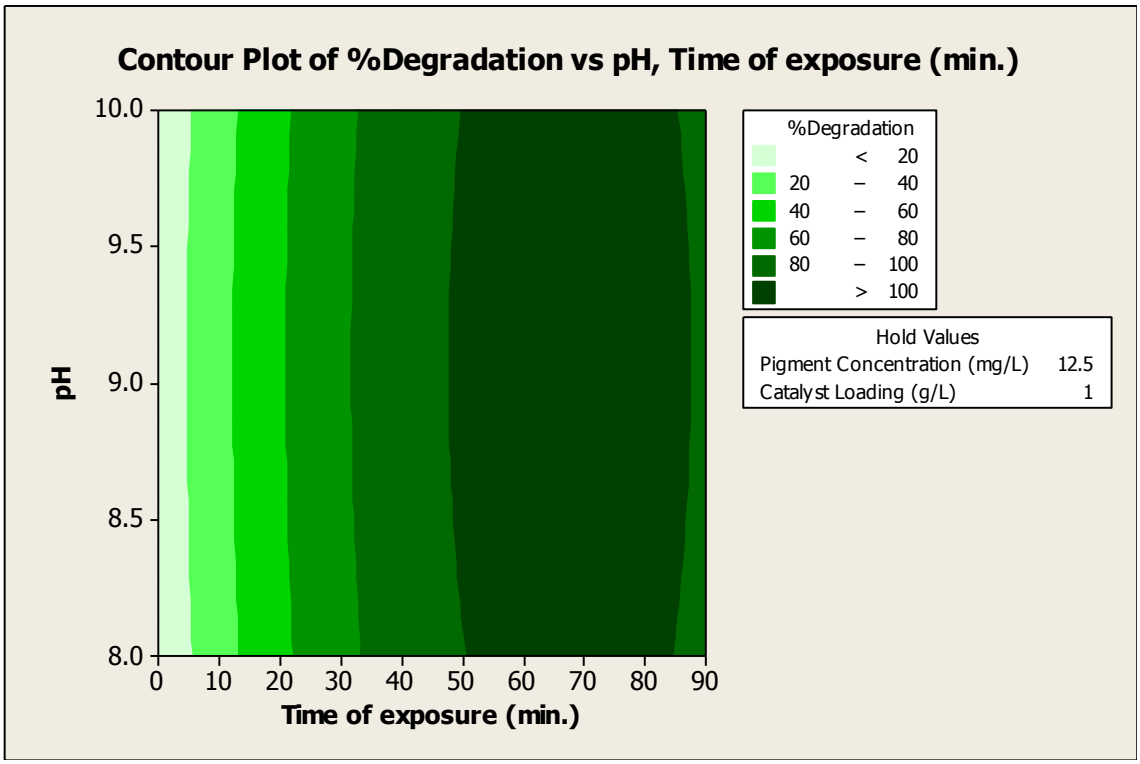


Figure 4.4e: Contour Plot of %Degradation vs pH, Time of exposure (min.) (AP2)

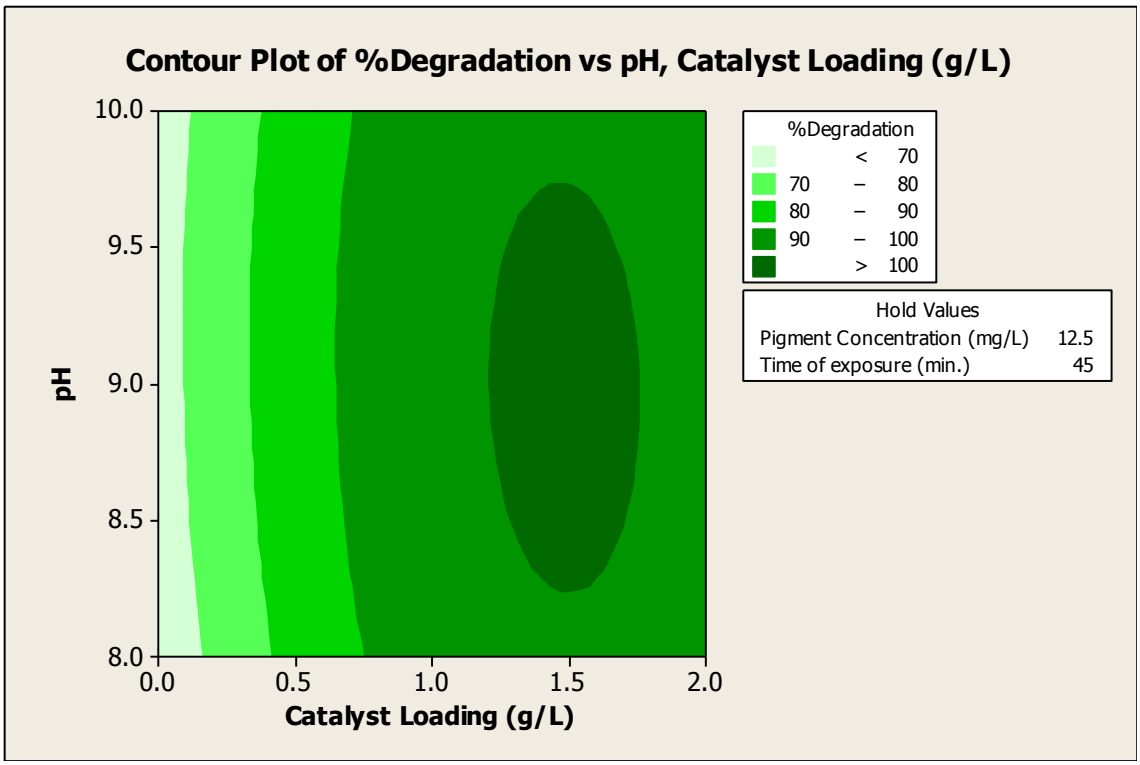


Figure 4.4f: Contour Plot of %Degradation vs pH, Catalyst Loading (g/L) (AP2)

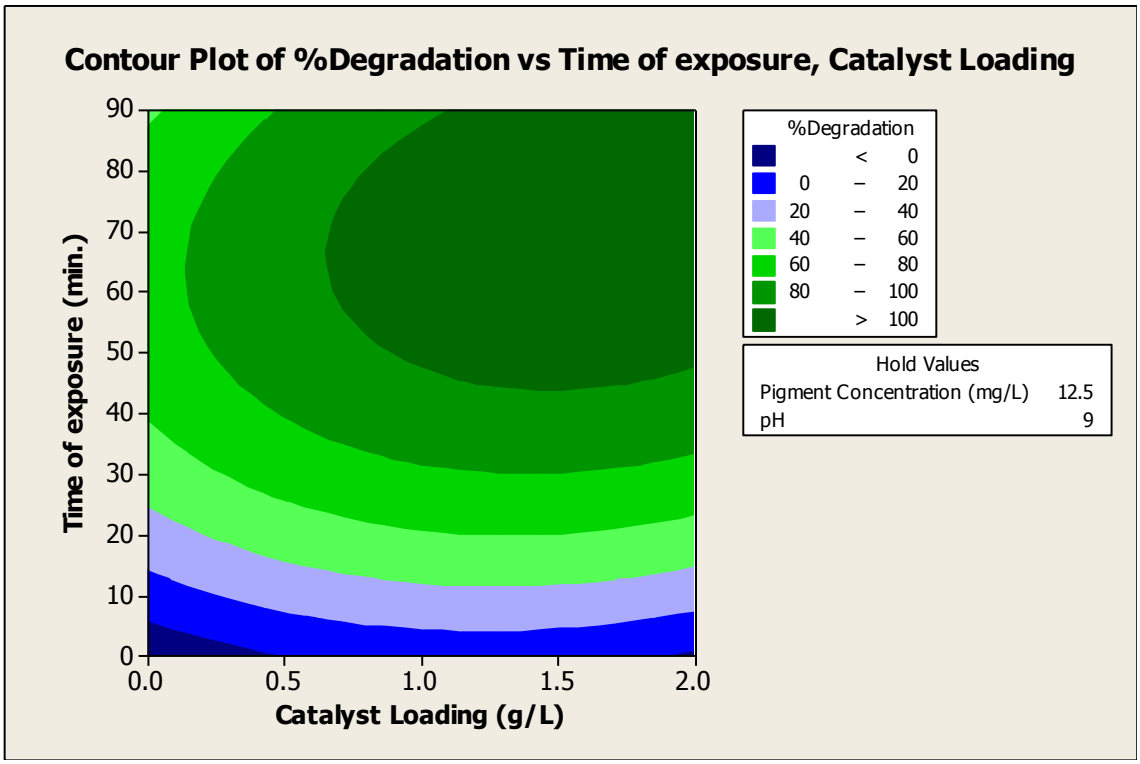


Figure 4.4g: Contour Plot of %Degradation vs Time of exposure (min.), Catalyst Loading (g/L) (AP2)

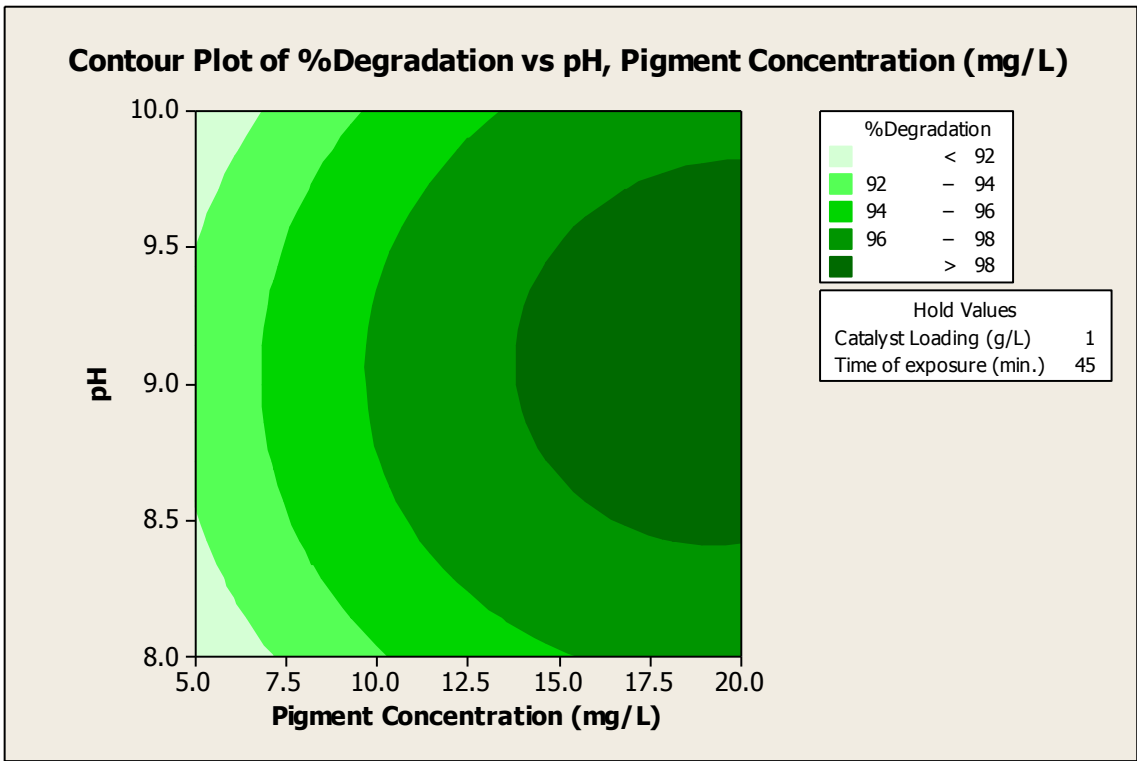


Figure 4.4h: Contour Plot of %Degradation vs pH, Pigment Concentration (mg/L) AP2

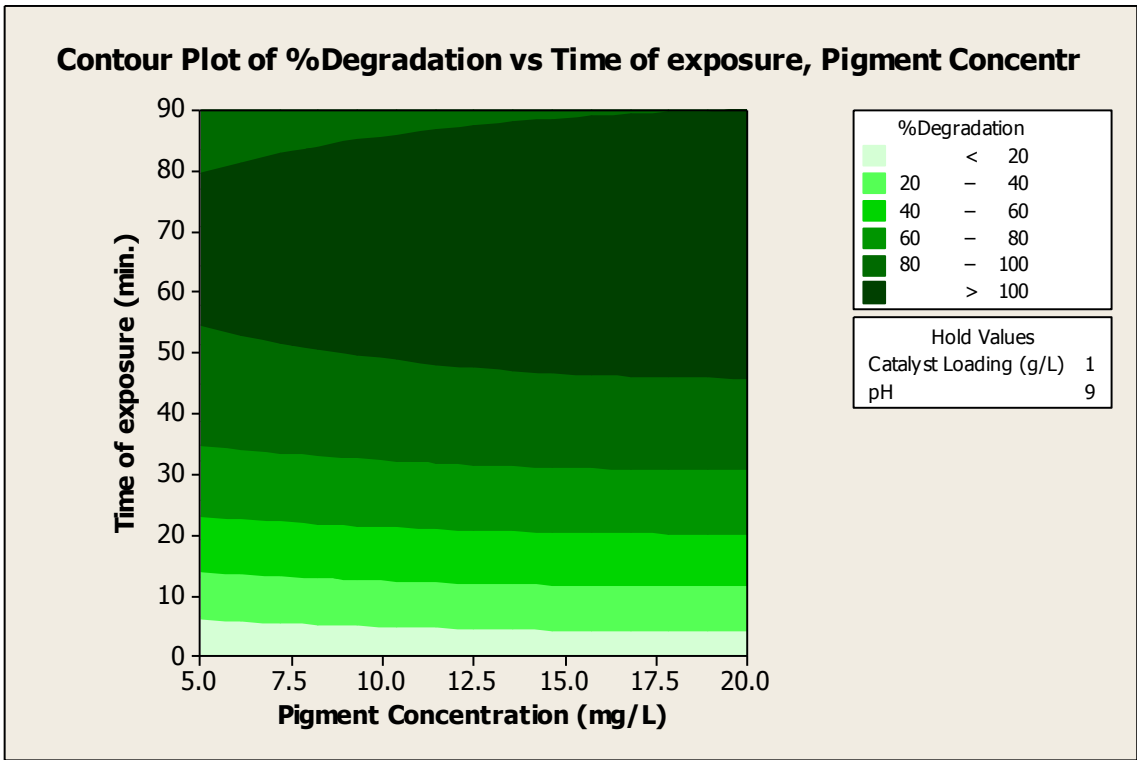


Figure 4.4i: Contour Plot of %Degradation vs Time of exposure (min.), Pigment Concentration (mg/L) (AP2)

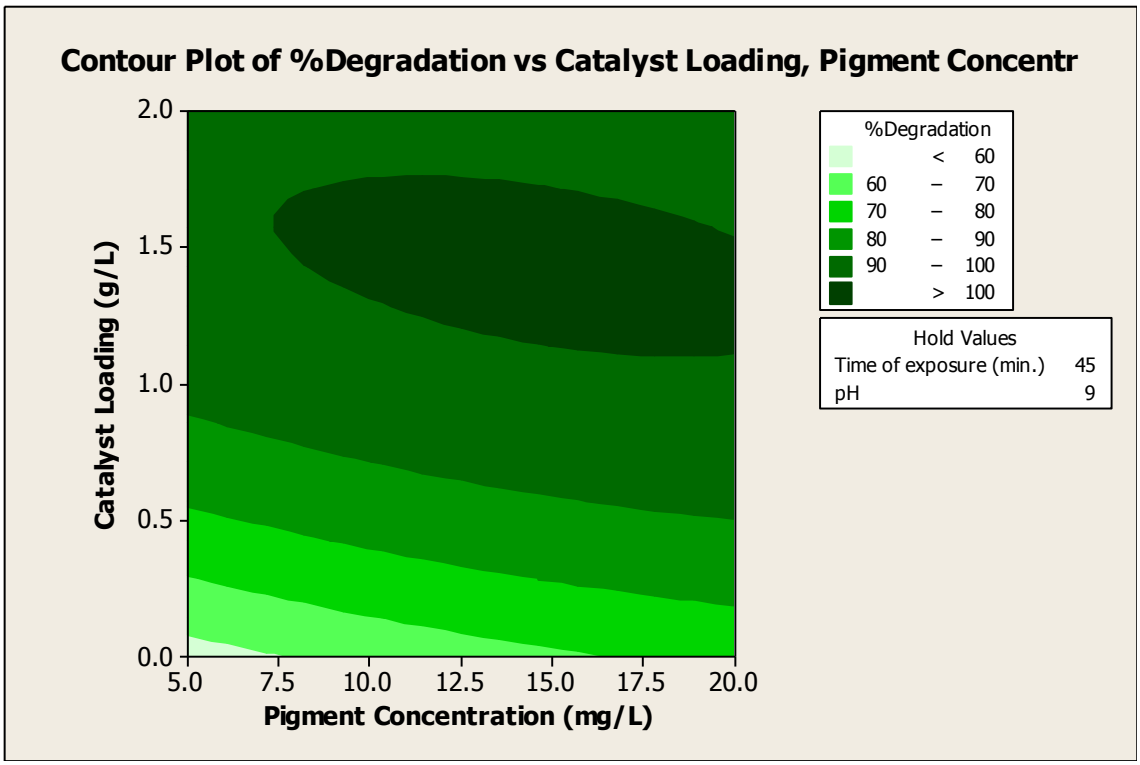


Figure 4.4j: Contour Plot of %Degradation vs Catalyst Loading (g/L), Pigment Concentration (mg/L) (AP2).

# CHAPTER FIVE

## 5.0 DISCUSSION

## 5.1 SYNTHESIS OF THE DIAZONIUM SALT

One diazo component, p-nitro aniline was used in this study. It was diazotized using the indirect method of diazotization as summarized by the reaction scheme below.

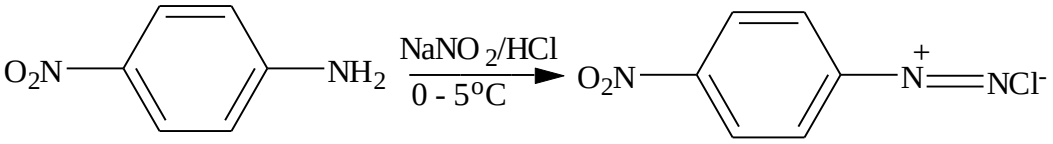


Scheme 5.1: Schematic route for the diazotization of p-nitroaniline

In the above reaction scheme, p-nitro aniline was reacted with a mixture of hydrochloric acid and distilled water. The entire mixture was then heated to about 70$^{o}$C in order to dissolve the aniline. The resulting solution was then cooled to about 0-5$^{o}$C and freshly prepared sodium nitrite was then added dropwise for about 20 minutes and stirred further for 2 hours which generated the diazonium salt.

## 5.2 SYNTHESIS OF THE AZO PIGMENTS

Two different azo pigments were synthesized by coupling the diazotized diazonium salt with N, N-dimethylaniline and Naphtol AS both of which are coupling components. The reaction scheme shown below is an illustration of the summary of the coupling reaction.

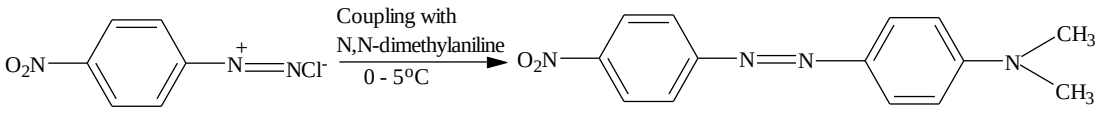


Scheme 5.2: Schematic route for coupling with N, N-dimethylaniline

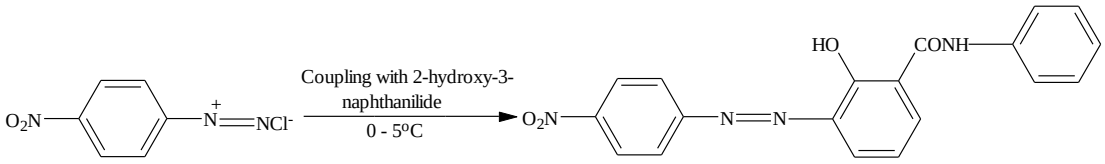

Scheme 5.3: Schematic route for coupling with 2-hydroxy-3-naphthanilide

The coupling components used for the synthesis of the azo pigments are shown in Figure 5.1. They include N,N-dimethylaniline and 2-hydroxy-3-naphthanilide.

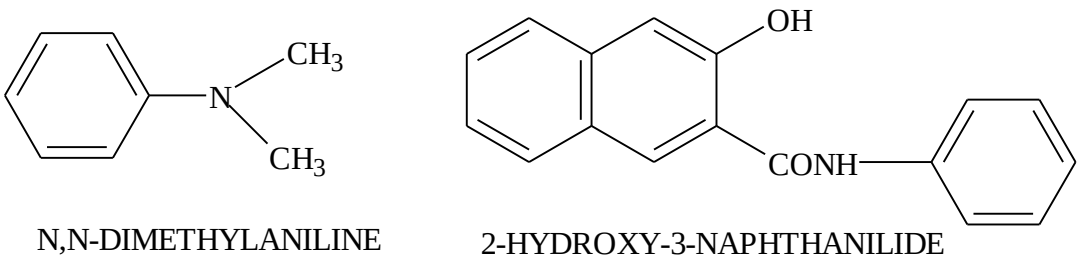


N,N-DIMETHYLANILINE 2-HYDROXY-3-NAPHTHANILIDE

Figure 5.1: Structures of the coupling components used

## 5.3 VISIBLE ABSORPTION SPECTRA OF THE PIGMENTS

The visible absorption spectral of the synthesized azo pigments was measured in DMF and their molar extinction coefficients were calculated. The results obtained are shown in Table 4.4.

## 5.4 MELTING POINT DETERMINATION OF THE PIGMENTS

In the results displayed in Table 4.1, it is obvious that the vat pigments had melting points above 320$^{o}$C. For the synthesized azo pigments, a melting point within the range of 176 – 220$^{o}$C was observed. The azo pigment formed by coupling p-nitroaniline with Naphthol AS had higher melting point than the one coupled with N, N-dimethylaniline and this may be attributed to the higher molecular weight of the Naphthol AS as compared with the N, N-dimethylaniline.

## 5.5 SPECTRA ANALYSIS OF THE PIGMENTS

### 5.5.1 Infrared spectra of the synthesized azo pigments

Table 4.2 gives the infrared spectra of the synthesized azo pigments. It is evident from the table that the aromatic C-H bending vibration occurs at 701.15-839.06 for AP1 and 727.19-

864.14 for AP2. The O-H stretch occurs at 3762.28 for AP2. N-H vibration occurs at 3455.59 for AP1 and 3460.41 for AP2. The vibration due to N=N occurs at 1463.06 and 1500.67 for AP2 and AP1 respectively. Also, the C=C vibration occurs at 1597.11 and 1617.37 for AP1 and AP2 respectively. Stretching vibration due to C≡C, C-O and $–NO_2$ occurs at 2278, 1121, 1329.97 and 2275.11, 1183.37, 1346.36 for AP1 and AP2 respectively.

### 5.5.2 Gas chromatography – Mass Spectroscopy (GC-MS) Spectra of Synthesized Azo Pigments.

The GC-MS of AP1 reveals the various values corresponding to $NC_2H_5$, $C_6H_4$, N=N, $NO_2$. The various fragments occurred at 43, 74, 129, 101, 115, 142, 227, and 270 as shown in Table 4.3. The values were correlated with the fragmentation pattern and compared with calculated values for which no deviation was observed.

## 5.6 CALIBRATION CURVES OF THE PIGMENTS

The calibration curves were constructed by plotting the absorbance values against the concentration of each pigment. The obtained curves are shown in Figures 4.1 - 4.4.

Each of the calibration curves obeys Beer-Lambert's equation as shown below.

$$L_n \frac{I_0}{I_t} = \varepsilon cl \quad \text{----------5.1}$$

Where $I_o$= Intensity of incident light

$I_t$= Intensity of transmitted light

ε = Extinction coefficient

I = Cell path length (cm)

c = Concentration (mg/L)

Hence, the relationship between absorbance and pigment/dye concentration is governed by the Beer-Lambert's equation shown below (Skooge et al., 1992; Golob and Tusek, 1999).

$$A = \text{Log}\left(\frac{I_o}{I_t}\right) = \varepsilon cl \text{ ----------5.2}$$

Where A = absorbance

$I_o$ = Intensity of incident light

$I_t$= Intensity of transmitted light

ε = Extinction coefficient/Absorptivity ($Lmol^{-1}cm^{-1}$)

I = Cell path length (cm)

c = Concentration (mg/L)

The pigments sample where dissolved in DMF so as to improve intermolecular solute-solvent interaction force which enhances the pigment solubility significantly. To ensure validity of Beer-Lambert's law, a set of 10 different calibration solutions were prepared for each sample. These pigment concentration were chosen since the solution for testing absorbance correlation are best kept in the absorbance range of 0.2 – 1.5. This procedure is similar to the one used in the studies of Do and Chen, (1994) and Szpyrkowicz et al., (2000).

**5.7 PHOTODEGRADATION EFFECTS ON THE PIGMENTS SOLUTIONS**

Figure 4.1a, 4.2a, 4.3a and 4.4a shows a plot of residual against fitted values. It helped to show whether the fit is uniformly good or different for lower or higher values of the residual. Residual plots are the best single check for violation of assumptions, such as:

(i). Variance not being constant across the explanatory variables.

(ii). Fitted relationships being non-linear.

(iii). Random variation not having a normal distribution

Residuals are random variables and are functions of data. Examining residuals is a key part of all statistical modeling including Design of Experiments (DOE's). Residual tell us

how well or otherwise the model fits the data. One problem with using residuals is that their values depend on the scale and units used. Since the residuals are in units of the dependent variable Y there are no cut-off points for defining what a "large" residual is. The problem is overcome by using standardised residuals. They are calculated by residual divided by standard error of the residual. The standard error of each residual is different, and using standardised residuals helps one to get round the problem.

Plotting residuals on the Y axis against fitted values on the X axis is a useful diagnostic procedure. If the model is appropriate for the data, the plot should show an even scatter. The plots can be used to check the drift of the variance during the experimental process, when data are time-ordered. If the residuals are randomly distributed around zero as obtained above, it means that there is no drift in the process.

Figure 4.1b, 4.2b, 4.3b and 4.4b above are histograms which illustrates a plot of frequency against residuals. The histogram is a frequency plot obtained by placing the data in regularly spaced cells and plotting each cell frequency versus the center of the cell. These histograms are illustrations of an approximately normal distribution of residuals produced by a model for a calibration process. It also provides a view of the overall distribution of the residuals; hence, it will help to check the assumption about normal distribution (Box *et al*., 1987). Sample sizes of residuals are generally small (<50) because experiments have limited treatment combinations, hence a histogram is not the best choice for judging the distribution of residuals. A more sensitive graph is the normal probability plot as shown in Figue 4.1c, 4.2c, 4.3c and 4.4c.

Figure 4.1c, 4.2c, 4.3c and 4.4c illustrates the normal probability plot. The normal probability plot often produces an approximately straight line which is an indication that

the points come from a normal distribution (Roger and Donald, 2002). Small departures from the straight line in the normal probability plot are common, but a clearly "S" shaped curve on this graph suggests a bimodal distribution of residuals. This technique is better to use than the histogram since the linearity pattern can easily be seen than a bell-shaped pattern of an histogram. The histogram, however, is also a useful plot since it helps to pick up other abnormalities (Box *et al*., 1987).

Figure 4.1d, 4.2d, 4.3d and 4.4d is a plot of residual vs observation order. The sequence of positive and negative residual in this plot shows that the observations are not independent. This may mean that the run order was more important or that variables that change over time were more important.

Figure 4.1e, 4.2e, and 4.4e is the plot showing the variation of %degradation with respect to pH and irradiation time. It is evident from the plot that as the irradiation time increases, there is a steady increase in degradation. Also, as the pH increases, the degradation also increases. This increase in percentage degradation as a result of increasing pH in alkaline region is attributed to the fact that more hydroxyl radicals were generated as a result of the reaction between the hydroxide ions and the positive holes of the photocatalyst thereby increasing the rate of photodegradation. This is in agreement with the findings of (Akpan and Hameed, 2009; Tang and An, 1995; Goncalves *et al*., 1991).

It is worthy of mention that in an alkaline solution there exist a Coulombic repulsion between the negatively charged surface of the photocatalyst and the hydroxide anions at higher pH and this could prevent the formation of •OH in higher alkaline solution thus decreasing the rate of photocatalytic degradation of the pigments (Akpan and Hameed, 2009). This shows that degradation does not increase at all time in an alkaline solution.

Figure 4.1f, 4.2f, 4.3f and 4.4f are contour plots which show the effect of pH and catalyst loading at a pigment concentration of 12.5 mg/L and irradiation time of 45 minutes. Changes in pH can influence the adsorption of the pigments on the surface of $TiO_2$ which is an important step for photocatalytic oxidation to take place (Fox and Dulay, 1993). The % degradation therefore increases as the pH moves towards the alkaline region. This is because in an acidic media, the $TiO_2$ particles agglomerate thereby reducing the surface available for pigment or dye adsorption and photon adsorption (Fox and Dulay, 1993) while the alkaline media favours the generation of more hydroxyl radicals by oxidizing more hydroxide ions available on the surface of the photocatalyst thereby enhancing the efficiency of the photocatalysis (Goncalves *et al.,* 1991). It then implies that % degradation greater than 95% is achievable at a pH of 7-10 and catalyst loading of 2.0 g/L.

Figure 4.1 g, 4.2 g, 4.3 g and 4.4 g are illustrations of % degradation with respect to irradiation time and the catalyst loadings. An increament in irradiation time increases the rate of degradation as seen from the contour plots of Figure 4.1 g, 4.2 g, and 4.4 g but beyond certain time, the rate of degradation could be affected negatively as a result of the short life span of the photocatalyst by active sites deactivation due to strong by-product deposition. The catalyst loading also has an influence on the degradation rate. As the catalyst loading increases from 1 to 2, there was a progressive increase in the rate of degradation as shown in the aforementioned figures. This increment is attributed to the fact that increase in the amount of the photocatalyst increases the number of active sites on the photocatalyst surface which in turn increases the number of hydroxyl and superoxide radicals both of which are predominant species of degradation of the pigments (Konstantinou and Albanis, 2004; Saquiba *et al.,* 2008; Chen *et al.,* 2007; Huang *et al.,*

2008; Sun *et al.*, 2008; Liu *et al.*, 2006a). This is true for a pigment concentration of 12.5 mg/L and a pH of 8 for Figure 4.1 g and 4.2 g while it is 12.5 and pH 9 at an irradiation time of 90 minutes for Figure 4.4 g.

Figure 4.1h illustrates the effect of irradiation time and pigment concentration at a catalyst loading of 1 g/L and a pH of 8. It is evident from Figure 4.1h that as the irradiation time increases there is a corresponding increase in the % degradation. Photocatalytic degradation also increases with increase in the concentration of pigment and this may be attributed to the fact that as the concentration of the pigments increased, more pigments molecules became available for excitation and energy transfer, resulting in an increase in the rate of reaction. But beyond a concentration of 19 mg/L, an increase in concentration of pigment may adversely affect the reaction rate. This is because at higher concentration, pigment or dye molecules starts acting as a blanket or cover and will not permit the desired light intensity to reach the semiconductor surface, thus decreasing the rate of photocatalysis (Davis *et al.*, 1994, Lea and Adesina, 1998;).

Figure 4.1i is an illustration of the effects of pH and pigment concentration for a catalyst loading of 1 g/L and irradiation time of 45 minutes. The % degradation increases as the pH increases from neutral to alkaline region and this can be as a result of the availability of more hydroxide ions in pH range of 7.5 to 9 which combines with holes formed due to electron excitation of the catalyst. This is in agreement with the findings of (Akpan and Hameed, 2009 and Konstantinou and Albanis, 2004) that the rate of degradation is higher at alkaline pH because alkaline pH favours the generation of hydroxyl radicals which enhances the rate of photodegradation (Borker and Salker, 2006; Sun *et al*., 2006; Baran *et*

*al*. 2008; Xiao *et al*., 2007). As the concentration also increases, the rate of degradation also increases as seen from the plot.

Figure 4.1j is an illustration of the effect of catalyst loading and pigment concentration on the rate of degradation. The amount of the photocatalyst is one of the most important parameter that affects the rate of photocatalytic degradation of organic colorants. The effects of variation in the amount of photocatalyst from 0.5 to 2.0 mg/L and concentration of pigment at pH of 8 and irradiation time of 45 minutes were measured. On the rate of degradation, it was found that as catalyst loading increases, the rate of degradation also increases. Increase in the rate of degradation with increase in amount of catalyst is due to the availability of more catalyst surface area for absorption of photon of light and interaction of molecules of reaction mixture with catalyst, with resultant increase in the number of holes, hydroxyl radicals and super oxide ions ($O_2^-$). As the pigment concentration is increased from 7.5 mg/L to 20 mg/L, the number of pigment molecules in the solution also increases with corresponding increase in the percentage degradation as shown in Figure 4.1j.

Response Optimization values:

Parameters

Pigment Concentration = 18.34 mg/L

Catalyst Loading = 1.47 g/L

Time of exposure = 88.36 min.

pH = 8.71

Figure 4.2h shows the Contour Plot of % Degradation vs pH, and pigment concentration (mg/L).

The pH and pigment concentration also affects the rate of degradation as shown in Figure 4.2h at a catalyst loading of 1 g/L and irradiation time of 45 minutes. The %degradation increases as the pigment concentration increases and this may be attributed to the fact that as the concentration of the pigments increased; more pigment molecules became available for excitation and energy transfer thus, resulting in an increase in the rate of photodegradation. Also, as the pH increases towards the alkaline level, the rate of degradation also increases since alkaline pH is known to favor the generation of hydroxyl radicals which is the predominant specie in degradation.

Figure 4.2i is a contour plot showing the effect of irradiation time and pigment concentration on the rate of degradation at a pH of 8 and catalyst loading of 1 g/L. As the irradiation time increases, the rate of degradation also increases. The increase in pigment concentration also increases the rate of degradation as seen from the contour plot and this is in agreement with other reports on literature.

Figure 4.2j is an illustration of the variation of catalyst loading against pigment concentration at a pH of 8 and irradiation time of 45 minutes. As the catalyst loading increases, the rate of degradation also increases as a result of increase in the active sites of the photocatalyst. The pigment concentration also has influence on the rate of degradation. As the concentration increases, the rate of degradation also increases as it is evident from the contour plot but beyond a certain concentration, there could be a decrease in the rate of degradation as a result of UV-screening effect of the pigments. At a higher pigment concentration, a significant amount of UV may be absorbed by the pigment molecules rather than the $TiO_2$ particles and this reduces the efficiencyof the catalytic reaction (Mills *et al.*, 1993, Tang and An, 1995).

Another possible cause is the interference from intermediates formed upon photocatalysis of the parental pigments. These intermediates may include aromatics, aldehydes, ketones and organic acids as shown by previous studies with various aromatic compounds (Serpone *et al*., 1993; d'Hennezel *et al*., 1998; Tanaka *et al*., 2000). They may compete with the pigment molecules for the limited adsorption and catalytic sites on the $TiO_2$ particles (Ollis *et al*., 1989) and thus inhibit decolorization. Such suppression would be even more pronounced in the presence of an elevated level of degradation intermediates formed upon an increased initial pigment concentration.

Response Optimization values:

Parameters

Pigment concentration = 19.13 mg/L

Catalyst Loading = 1.17 g/L

Time of exposure = 81.28 min.

pH = 8.40

The figure 4.3e above is an illustration of the effect of pH and irradiation time on the rate of degradation at a dye concentration of 10 mg/L and catalyst loading of 1 g/L. The plot reveals that as the pH increases, the %degradation also increase with the best result being obtained at pH 8.5. This is because in an alkaline medium, there is a greater probability for the formation of hydroxyl radicals (•OH), which can act as an oxidant, thus increasing the rate of photodegradation of the pigment (Zhang *et al*., 2002, Tunesi and Anderson, 1991). For the irradiation time, the %degradation increases as the irradiation time also increase with maximum degradation being obtained at 83 minutes. Beyond this point, by-products

may accumulate on the active sites of nanoparticles thereby resulting in the deactivation of photocatalyst (Li *et al*., 2008, Chakrabarti and Dutta, 2004).

Figure 4.3f shows that at a pigment concentration of 10 mg/L and irradiation time of 45 minutes, pH of 8.5 and catalysts loading of 2.0 g/L have effect on the rate of degradation. Thus, as the pH and catalyst loading increases, the % degradation also increase.

Figure 4.3g above shows the contour plot of % degradation vs time (min.) and catalyst loading (g/L) for a pigment concentration of 12.5 mg/L and pH 9. The irradiation time and catalyst loading have effect on the %degradation of the pigment. The plot revealed that the %degradation increases gradually from 0 to 80% as the irradiation time rises from 10 minutes to about 90 minutes. Beyond an optimum irradiation time, the %degradation will reduce due to accumulation of by-products on the active sites of the photocatalyst (Li *et al*., 2008). For the catalyst loading, %degradation also increases as the photocatalyst amount increases due to the availability of more sites for pigment adsorption. This agrees with other findings in the literature.

Figure 4.3h shows the contour plot of %degradation vs pH and pigment concentration at a catalyst loading of 1 g/L and irradiation time of 45 minutes. It is evident from the plot that degradation increases steadily as the pH rises from 8 to 10. This is because in alkaline solution, hydroxyl radicals (•OH) are easily generated by oxidizing more hydroxide ions available on $TiO_2$ surface, thus, the efficiency of the process is logically enhanced (Shourong *et al*., 1997; Goncalves *et al*., 1999; Sharma *et al.*, 1995; Sakthivel *et al.*, 1999). It is generally noted that the degradation rate increases with the increase in pigment concentration. Further increase in pigment concentration beyond the optimum will lead to

decrease in the degradation rate of the pigment (Saquib and Muneer, 2003; Sakthivel *et al.*, 2003).

The Figure 4.3i above represents the contour plot of % degradation vs time and pigment concentration at a pH of 8 and catalyst loading of 1 g/L. The plot reveals that as the pigment concentration increases, the % degradation also increases. As the initial concentration of the pigment increases, the probability of reaction between the pigment molecules and oxidizing species also increases, leading to an enhancement in the decolorization rate. On the contrary, the degradation efficiency of the pigment decreases as the pigment concentration increases further. The presumed reason is that at high pigment concentrations the generation of •OH radicals on the surface of the catalyst are reduced since the active sites are covered by pigment ions (Poulios and Aetopoulou, 1999; Zhang *et al.*, 1995).

For the irradiation time, the rate of degradation also increases as the irradiation time increases but beyond certain time, say 90 minutes as regard the figure 4.3i, the rate of degradation will decrease with increase in irradiation time. This is because of the slow reaction of short chain aliphatics with •OH radicals and the short life-time of the photocatalyst due to active sites deactivation by strong by-products deposition.

Figure 4.3j shows the effect of catalyst loading and pigment concentration on the % degradation of pigment at a pH of 9 and irradiation time of 45 minutes. The % degradation increases as the catalyst loading increases from 0.5 to 1.5 g/L and beyond this value, a negative result could be obtained i.e decrease in %degradation which may be due to deactivation of activated molecules by collision with ground state molecules thereby causing shielding by $TiO_2$ to take place.

$$TiO_2^* + TiO_2 \rightarrow TiO_2^{\#} + TiO_2$$

Where $TiO_2^*$ is the $TiO_2$ with active species adsorbed on its surface and $TiO_2^{\#}$ is the deactivated form of $TiO_2$ (Neppolian, 2002).

Excess amount of the photocatalyst could also results in the turbidity of the solution thus, reducing the amount of light penetration needed to activate the photocatalyst hence, slowing down the rate of degradation (Akpan and Hameed, 2011). For the pigment concentration, the % degradation also increases as the concentration increases from 7.5 mg/L as revealed by the plot. This is in agreement with the findings of Konstantinou and Albanis, 2003.

Response Optimization values

Parameters

Pigment Concentration = 20.00 mg/L

Catalyst Loading = 1.53 g/L

Time of Exposure = 89.29 min.

pH = 9.38

Figure 4.4h is a contour plot showing the effects of pigment concentration and pH on the rate of degradation at a catalyst loading of 1 g/L and irradiation time of 45 minutes. It is evident from the plot that, at alkaline pH, the rate of degradation increases as a result of generation of more hydroxyl radicals which enhances the rate of degradation but beyond certain pH value e.g. pH 10 for Figure 4.4h, the rate of degradation could be reduce as a result of Coulombic repulsion between the negatively charged surface of photocatalyst and the hydroxide anions (Pehlivan *et al.,* 2008). This fact could prevent the formation of •OH

and thus decrease the photo-oxidation. The pigment concentration also increases the rate of degradation as it increases steadily.

Figure 4.4i is an illustration of the contour plot of %degradation vs time and pigment concentration at a catalyst loading of 1 g/L and pH of 9. The plot revealed that as the pigment concentration and irradiation time increases, the %degradation also increases. % degradation above 80 % is achievable when the irradiation time is raised further at pigment concentration of 20 mg/L. The reason advanced for this, is that at high pigment concentrations the generation of •OH radicals on the surface of the catalyst are reduced since the active sites are covered by pigment ions (Tang and An, 1995; Daneshvar *et al*., 2003).

Figure 4.4j above is a contour plot which shows the effect of catalyst loading and pigment concentration on the rate of degradation at a pH of 9 and irradiation time of 45 minutes. As the catalyst loading increases from 0.5 to 2.0 g/L, the degradation rate also increases. The increase in pigment concentration also increases the rate of degradation as revealed in Figure 4.4j.

Response Optimization values:

Parameters

Pigment Concentration = 17.14 mg/L

Catalyst Loading = 1.50 g/L

Time = 83.36 min.

pH = 9.85

## 5.8 REGRESSION EQUATION OF PERCENTAGE DEGRADATION VERSUS PIGMENT CONCENTRATION, CATALYST LOADING

The following are the regression equation for each of the pigment sample as shown below.

For Caledon Khaki 2G (VP1)

%Degradation = 3.8 + 0.56 Pigment Concentration (mg/L)

+ 16.2 Catalyst Loading (g/L) + 0.967 Time of exposure + 0.65 pH

For Caledon Green 2G (VP2)

%Degradation = 46.9 + 0.73 Pigment Concentration (mg/L)

+ 17.1 Catalyst Loading (g/L) + 0.931 Time of exposure + 3.13 pH

For AP1

%Degradation = 3.5 + 0.362 Pigment Concentration (mg/L)

+ 11.4 Catalyst Loading (g/L) + 1.05 Time of exposure (min.)

+ 1.18 pH

For AP2

%Degradation = 3.2 + 0.175 Pigment Concentration (mg/L)

+ 16.9 Catalyst Loading (g/L) + 1.01 Time of exposure (min.)

+ 0.01 pH

# CHAPTER SIX

## 6.0 SUMMARY, CONCLUSION AND RECOMMENDATION

### 6.1 SUMMARY

In this research work, the photocatalytic degradation of two commercial vat pigments and two synthesized azo pigments were carried out successfully in DMF using $TiO_2$-P25 (Fluka) as photocatalyst in the presence of ultra violet light.

The rates of degradation of the pigment solution were determined on the basis of absorbance measurement using the JENWAY 6305 UV-Vis Spectrophotometer. The effects of operational parameters such as pigment concentration, catalyst loading, irradiation time and pH have been investigated.

The influence of pH on the rate of degradation cannot be over emphasized as changes in pH influenced the adsorption of pigment molecules onto the $TiO_2$ surfaces, an important step for the photocatalytic oxidation to take place. The hydroxyl radicals are considered as the predominant species at neutral or high pH levels. In alkaline solution, •OH are easier to be generated by oxidation of more hydroxide ions available on $TiO_2$ surface, thus enhancing the efficiency of the process.

The pigment concentration was also found to be another important factor in the photocatlytic reaction. The rate of degradation relates to the probability of •OH radicals formation on the catalyst surface and to the probability of •OH radicals reacting with pigment molecules. As the initial concentration of the pigments increased, the probability of reaction between pigment molecules and oxidizing species also increased, leading to an enhancement in the decolorization rate. On the contrary, the degradation efficiency of the pigment decreased as the pigment concentration increased beyond an optimum value. The

presumed reason is that at high pigment concentration the generation of •OH radicals on the surface of the photocatalyst are reduced since the active sites are covered by pigment ions. Another possible cause for such results is the UV-screening effect of the pigment itself. At a high pigment concentration, a significant amount of UV may be absorbed by the pigment molecules rather than the $TiO_2$ particles and this reduces the efficiency of the catalytic reaction.

Pigment degradation is also influenced by the amount of photocatalyst used. The pigment degradation increased with increasing photocatalyst concentration which is a characteristic of heterogenous photocatalysis. The reason generally advanced for this is that increase in the amount of photocatalyst increases the number of active sites on the photocatalyst surface, which in turn increases the number of hydroxyl and superoxide radicals. Again, when the concentration of the photocatalyst increased above the optimum value, the degradation rate decreased due to the interception of the light by the suspension. Furthermore, the increase of photocatalyst concentration beyond the optimum may result in the agglomeration of catalyst particles, hence the part of the catalyst surface becomes unavailable for photon absorption, and degradation rate decreases.

The irradiation time also played a role in the degradation of the pigments. It was evident that the percentage of decolorization and photodegradation increased with increase in irradiation time. The reaction rate decreased with irradiation time since it follows the apparent first-order kinetics and additionally a competition for degradation may occur between the reactant and the intermediate products. The slow kinetics of pigment degradation after certain time limit may be due to: (a) the difficulty in converting the N-atoms of the pigment into oxidized nitrogen compounds. (b) the slow reaction of short

chain aliphatics with •OH radicals. (c) the short life-time of photocatalyst because of active sites deactivation by strong by-products deposition.

The optimum operational parameters for the pigments are as follows. For Caledon Khaki 2G (VP1), the optimum operational conditions are; 18.34 mg/L for pigment concentration, catalyst loading of 1.47 g/L, pH of 8.71 and irradiation time of 88.36 minutes. For the second vat pigment, Caledon Green 2G (VP 2), its optimum operational conditions were: 19.13 mg/L for pigment concentration, catalyst loading of 1.17 g/L, pH of 8.40 and irradiation time of 81.28 minutes. The first azo pigment synthesized, AP1 has its optimum operational conditions as 20 mg/L for pigment concentration, catalyst loading of 1.53 g/L, pH of 9.38 and irradiation time of 89.29 minutes while the second azo pigment synthesized, AP2 has its optimum operational conditions as 18.14 mg/L for pigment concentration, catalyst loading of 1.50 g/L, pH of 9.85 and irradiation time of 83.46 minutes.

## 6.2 CONCLUSION

The photocatalytic degradation of some selected vat and azo pigments using UV light as radiation source and $TiO_2$ as photocatalyst has been achieved using minitab 16 software to carry out the experimental design. Effective destruction of azo pigments belonging to different chemical groups is possible by photocatalysis in the presence of $TiO_2$ suspensions and UV light as revealed by this study.

The observations in these investigations clearly demonstrate the importance of choosing the optimum degradation parameters to obtain a high degradation rate, which is essential for any practical application of photocatalytic oxidation processes. The experiments show that higher photodegradation efficiency can be achieved under the optimized conditions.

Thus, this can be used as an efficient technology for photocatalytic degradation of the coloured wastewater discharged from the textile industry.

The results obtained also show that degradation rate can be influenced by operational parameters such as pH, irradiation time, catalyst loading and pigment concentration apart from the presence of electron acceptors and other additives that can enhance the process.

In light of these, it is therefore concluded that this process is an efficient and environmentally friendly technique for effluent treatment of industrial wastewater containing organic pigments from textile industry since the organic pigments were mineralized into simple and eco-friendly compounds of carbon (IV) and water.

## 6.3 RECOMMENDATIONS

In view of the above findings, the following recommendations are therefore made.

1. Since the used of titanium dioxide has proved to be effective in the degradation of pigments, the technology could be extended to treatment of textile effluents containing pigments of varying chemicals structures.
2. Future research is needed for the development of alternative and efficient catalysts for harnessing solar energy in the Photocatalytic oxidation process.
3. Highly efficient photoreactors and solar pannels should be designed for photocatalytic treatment of textile waste effluents for both small and large scale textile industries.

## REFERENCES


Abbas, M and Robab H. (2010). Ultrasonic degradation of Rhodamine B in the presence of $H_2O_2$ and some metal oxide. *Ultrasonics Sonochemistry*. 17; pp. 168-172.

Adosinda, M.; Martins, M.; Ferreira, I.C., Santos, I.M.; Wueiroz, M.J. and Lima, N. (2001). Biodegradation of bioaccessible textile azo dyes by Phanerochaete chrysosporium. *Journal of Biotechnology*, 89, pp. 91-98.

Ahmad, A.L. and Pussa, S.W. (2007). Reactive dyes decolorization from an aqueous solution by combined coagulation/micellar-enhanced ultrafiltration process, *Chemical Engineering Journal* 132; pp. 257-265.

Akpan, U.G. and Hameed, B.H., (2009). Parameters affecting the photocatalytic degradation of dyes using $TiO_2$-based photocatalysts: A review, *Journal of hazardous material*, 170, pp. 520-529.

Akpan, U.G. and Hameed, B.H. (2011). Solar degradation of an azo dye, acid red 1, by Ca-Ce-W $TiO_2$ composite catalyst, *Chemical Engineering Journal* 169, pp. 91-99.

Akpan, U.G. and Hameed, B.H. (2011). "Development and photocatalytic activities of $TiO_2$ doped with Ca-Ce-W in the degradation of acid red 1 under visible light irradiation," *Desalination & Water Treatment*, 175: pp. 3769 – 375.

Al-Degs, Y., Khraisheh, M.A.M., Allen, S.J.,and Ahmad, M.N. (2000). "Effect of Carbon Surface Chemistry on the Removal of Reactive Dyes from Textile Effluent", *Water Resources*, 34, pp. 927.

Ali, H. and Muhammad, S.K. (2008). "Biodecolourization of Acid Violet 19 by Alternariasolani," *Journal of African Biotechnology*, 7, pp. 831-833

Al-Momani, F. and Touraud, E. (2002). "Biodegradability Enhancement of Textile Dyes and Textile Wastewater by UV Photolysis", *Journal of Photochemistry. Photobiology. A: Chem*istry, 153, pp. 191.

Andreozzi, R., Caprio, V., Insola, V., Marotta, R. (1999). Advanced oxidation processes (AOP) for water purification and recovery, *Catalysis Today* 53; pp. 51–59.

Anliker, R. and Clarke E. A. (1982). International regulation of chemicals-implications for organic colorants. *Journal of Society of Dyers and Colourist*. 98, pp. 42±55.

Arana, J., Rend´on, E.T., Rodr´ıguez, J.M.D., Meli´an, J.A.H., D´ıaz, O.G., and Pe˜na, J.P. (2001). Highly concentrated phenolic wastewater treatment by the photo-Fenton reaction, mechanism study by FTIR-ATR, *Chemosphere* 44; pp. 1017–1023.

Baran, W., Makowski, A., Wardas, W. (2008). The effect of UV radiation absorption of cationic and anionic dye solutions on their photocatalytic degradation in the presence of $TiO_2$, *Dyes Pigment.* 76; pp. 226–230.

Bogan, B.W. and Lamar, R.T. (1995). One-electron oxidation in the degradation of creosote polycyclic aromatic hydrocarbons by Phanerochaete chrysosporium. *Applied and Environmental Microbiology*, 61, pp. 2631-2635.

Borker, P., Salker, A.V. (2006). Photocatalytic degradation of textile azo dye over $Ce1-xSnxO_2$ series, *Journal of Material Science Engineering. B* 133; pp. 55–60.

Box, G.E.P, Hunter W.G. and Hunter, J.S. (1987). Statistics for Experimenters, Wiley Interscience, John Wiley & Sons, Inc.

Brown, M. A. and De Vito S. C. (1993)."Predicting azo dye toxicity." Critical Reviews in *Environmental Science and Technology* 23(3): pp. 249-324.

Cancer, W. H. O.-I.A. f. R. o. (2010)."General Introduction to the Chemistry of Dyes." IARC Monographs on the Evaluation of Carcinogenic Risks to Humans 99: pp. 55-67.

Carp, O., Huisman, C.L., and Reller, A. (2004). Photoinduced reactivity of titanium oxide photoinduced reactivity of titanium oxide, *Solid State Chemistry*. 32; pp. 33–177.

Chagas, E.P. and Durrant, L. R. (2001). Decolorization of azo dyes by Phanerochaete chrysosporium and Pleurotus sajorcaju. *Enzyme and Microbial Technology*, 29, pp. 474-477.

Chakrabarti, S., and Dutta, B.K. (2004). Photocatalytic degradation of model textile dyes in wastewater using ZnO as semiconductor catalyst, *Journal of Hazardous Materials. B.* 112; pp. 269–278.

Chen, L.C., Huang, C.M., and Tsai, F.R. (2007). Characterization and photocatalytic activity of K+-doped $TiO_2$ photocatalysts, *Journal of Molecular Catalysis. A: Chemistry*. 265 pp. 133–140.

Christie, R.M. (2001). “Colour Chemistry”. Royal Society of Chemistry, Cambridge, UK.

Cooper, P. (1993). Removing colour from dyehouse wastewaters – a critical review of technology available. *Journal of Society of Dyers and Colourist.* 109; pp. 97 – 100.

d’Hennezel, O., Pichat P. and Ollis, D.F. (1998). A: Chem. 118; 197–204.

Daneshvar, N., Salari, D., Khataee,A.R. (2003). *Journal of Photochemistry and Photobiology. A: Chemistry.* 157; pp. 111.

Davis, R.J., Gainer, J.L., O'Neal, G., Wu, I., (1994). Photocatalytic decolorization of wastewater dyes. *Water and Environmental Research* 66, pp. 50–53.

Do J.S, and Chen M.L. (1994). Decolourization of dye-containing solutions by electrocoagulation. *Journal of Applied Electrochemistry*. 24: pp. 785–790.

Earle, M.D. (1942). The electrical conductivity of titanium dioxide. Physical review 61(1-2): pp. 51.

Fernandez, A., Lassaletta, G., Jimenez, V.M., Justo, A., Gonzalez-Elipe, A.R., Herrman, J.M.,Tahiri, H. and AîtIchou, Y. (1995). "Preparation and Characterization of $TiO_2$ Photocatalysts Supported on Various Rigid Supports (Glass,Quartz and Stainless Steel). Comparative Studies of Photocatalytic Activity in Water Purification", *Applied Catalysis. B Environment.***7**, pp. 49.

Fox, M.A. and Dulay, M.T. (1993). Heterogeneous photocatalysis. Chemistry. Reviewed. 93; pp. 341–357

Gaya, U.I. and Abdullah, A.H. (2008). Heterogeneous photocatalytic degradation of organic contaminants over titanium dioxide: a review of fundamentals, progress and problems, *Journal of Photochemistry and Photobiology. C: Photochemistry.* Reviewed. 9; pp. 1–12

Giwa, A., Nkeonye, P.O., Bello, K.A., and Kolawole, E.G. (2012). "Photocatalytic Decolourization and Degradation of C. I. Basic Blue 41 Using $TiO_2$ Nanoparticles," *Journal of Environmental Protection*, 3, pp. 1063-1069. doi:10.4236/jep.2012.39124

Golob, V. and Tusek, L. (1999). Visible absorption spectrophotometry of disperse dyes. Dyes and Pigments; 40: pp. 211–7.

Goncalves, M.S.T., Oliveira-Campos, A.M.F., Pinto, E.M.M.S.,Plasencia, P.M.S., Queiroz, M.J.R.P.(1999). Photochemical treatment of solutions of azo dyes containing $TiO_2$. *Chemosphere* 39, pp. 781–786.

Guillard, C., Lachheb, H., Houas, A., Ksibi, M., Elaloui, E. and Herrmann, J.M. (2003b)."Influence of Chemical Structure of Dyes, of pH and of Inorganic Salts on Their Photocatalytic Degradation by $TiO_2$ Comparison of the Efficiency of Powder and $TiO_2$",*Journal of Photochemistry and Photobiology. A: Chemistry*., 158, pp. 27.

Hao, O. J.; Hyunook, K.; Chiang P. (2000). Decolorization of wastewater. *Critical reviews in environmental science and technology*, 30, pp. 449-505, ISSN 1064-3389.

Herbst, W. and Hunger, K. (1997). Industrial Organic Pigments: Production, Properties and Applications, 2nd edition., VCH, Weinheim.

Hou, H.; Zhou, J.; Wang, J.; Du, C.; and Yan, B. (2003). Enhancement of laccase production by Pleurotus ostreatus and its use for the decolorization of anthraquinone dye. Process Biochemistry, 39, pp. 1415-1419.

Huang, M., Xu, C., Wu, Z., Huang, Y., Lin, J., and Wu, J. (2008). Photocatalytic discolorization of methyl orange solution by Pt modified $TiO_2$ loaded on natural zeolite, *Journal of Dyes Pigment*. 77, pp. 327–334.

Japan Nanonet Bulletin,(2005) "Discovery and applications of photocatalysis — Creating a comfortable future by making use of light energy". Issue 44.

Kaludjerski, M., Gurol, M.D. (2004). Assessment of enhancement in biodegradability of dichlorodiethyl ether (DCDE) by pre-oxidation, *Journal of Water Resources 38; pp. 1595–1603.*

Kang, S.F., Liao, C.H., and Chen, M.C. (2002). Pre-oxidation and coagulation of textile wastewater by the Fenton process, *Chemosphere* 46; pp. 923–928.

Kaur, S. (2007). Light induced oxidative degradation studies of organic dyes and their intermediates-Ph.D research dissertation. School of Chemistry and Biochemistry, Thapar University, India.

Kitis, M., Adams, C.D., and Daigger, G.T. (1999). The effects of Fenton's reagent pretreatmenton the biodegradability of non ionic surfactants, *Journal of Water Resources.* 33 (11). pp. 2561–2568.

Knapp, J.S., Newby, P.S. and Reece, L.P. (1995). Decolorization of dyes by wood-rotting basidiomycete fungi. *Enzyme and Microbiological Technology*, 17,pp. 664-668.

Koleske, J. V. (1995). Paint and Coating Testing Manual. ASTM International. pp. 232 ISBN 978-0-8031-2060-0.

Konstantinou, K.I. and Albanis, T.A. (2004). "$TiO_2$-assisted photocatalytic degradation of azo dyes in aqueous solution: kinetic, and mechanistic investigations: A review,"*Journal of Applied Catalysis B: Environmental*, vol. 49, pp. 1-14.

Kuo, W.G. (1992). Decolourising dye wastewater with Fenton's reagent, *Journal of Water Resources*. 26 (7): pp. 881–886.

Kurtoglu, M. E., Longenbach, T., and Gogotsi, Y. (2011). "Preventing Sodium Poisoning of Photocatalytic $TiO_2$ Films on Glass by Metal Doping". *International Journal of Applied Glass Science* 2 (2): pp. 108–116.

Lachheb, H.,Puzenat, E., Houas, A., Ksibi, M., Elaloui, E., Guillard, C. and Herrmann, J.M. (2002). "Photocatalytic Degradation of Various Types of Dyes (Alizarin S, Crocein Orange G, Methyl Red, Congo Red, Methylene Blue) in Water by UV-Irradiated Titania", *Applied Catalysis B: Environment*.,39, pp. 75.

Lance, P.G. and Barbano, D.M. (1997). "The Influence of Fat Substitutes Based on Protein and Titanium Dioxide on the Sensory Properties of Lowfat Milk". *Journal of Dairy Science* 80 (11): pp. 2726.

Lea, J., and Adesina, A.A. (1998). The photo-oxidative degradationof sodium dodecyl sulfate in aerated aqueous TiO2 suspension. *Journal of Photochemistry and Photobiology A: Chemistry* 118: pp. 111–122.

Leena, R. and Selva Raj D. (2008)."Bio-decolourization of textile effluent containing Reactive Black-B by effluent-adapted and non-adapted bacteria," *Journal of African Biotechnology,* 7, pp. 3309-3313.

Legrini, O., Oliveros, E. and Braun, A.M. (1993). "Photochemical Processes for Water Treatment", *Journal of Chemistry. Reviewed*., 93, pp. 671.

Li, Y., Sun, S., Ma, M., Ouyang, Y. and Yan, W. (2008). Kinetic study and model of the photocatalytic degradation of rhodamine B (RhB) by a $TiO_2$-coated activated carbon catalyst: effects of initial RhB content, light intensity and $TiO_2$ content in the catalyst. *Chemical Engineering Journal*. 142: pp. 147–155.

Lin, S.H. and Peng, C.F. (1996). Continous treatment of textile wastewaters by combined coagulation, electrochemical oxidation and activated sludge. *Water Resources,* 30: pp. 587-592

Liu, C.-C., Y.-H. and Hsieh, Y.-H. (2006a). "Photodegradation treatment of azo dye wastewater by UV/$TiO_2$ process." *Dyes and Pigments* 68 (2–3): pp. 191-195.

Liu, S., Yang, J.-H., and Choy, J.-H. (2006b). Microporous $SiO_2$-$TiO_2$ nanosols pillared montmorillonite for photocatalytic decomposition of methyl orange, *Journal of . Photochemistry and Photobiology. A: Chemistry*. 179: pp. 75–80.

Lunar, L., Sicilia, D., Rubio, S., Perez-Bendito, D. and Nickel, U. (2000). Degradation ofphotographic developers by Fenton's reagent: condition optimization and kinetics for metal oxidation, *Journal of Water Resources*. 34 (6): pp. 1791–1802.

Malato, S., Blanco, J., Vidal, A. and Richter, C.(2002). Photocatalysis with solar energy at a pilotplant scale: an overview. *Applied Catalysis. B: Environment*., 37, pp.1-15.

Mamdouh, M., Nassar, and YehiaMagdy, H. (1997)."Removal of different basic dyes from aqueous solutions by adsorption on palm fruit bunch particles," *Journal of Chemical Engineering*, 66, pp. 223-226.

Marchand, R., Brohan, L., and Tournoux, M. (1980). "A new form of titanium dioxide and the potassium octatitanate $K_2Ti_8O_{17}$". *Materials Research Bulletin* 15 (8): pp. 1129– 1133. doi:10.1016/0025-5408(80)90076-8.

Martinez, N.S.S., Fernandez, J.F., Segura, X.F., and Ferrer, A.S., (2003). Pre-oxidation of an extremely polluted industrial wastewater by the Fenton's reagent, *Journal of Hazardous Material*. B 101, pp. 315–322.

Meric, S., Kaptan, D. and Lmez, T. (2004). Colour and COD removal from wastewater containing reactive Black 5 using Fenton's oxidation process, *Chemosphere* 54 (3) pp. 435–441.

Mester, T. and Tien, M. (2000). Oxidation mechanism of ligninolytic enzymes involved in the degradation of environmental pollutants. *International Biodeterioration & Biodegradation*, 46, pp. 51-59.

Meyer U. (1981). Biodegradation of synthetic organic colorants. In Microbial Degradation of Xenobiotics and Recalcitrant Compounds, FEMS Symposium 12. pp.371±378. Academic Press, New York.

Mills, A. and Hunte, L. (1997). An overviewof semiconductor photocatalysis, Journal of Photochemistry and Photobiology A: Chemistry. 108; pp. 1–35.

Moraes, S., Freire, R.S. and Duran, N. (2000).“Degradation and Toxicity Reduction of Textile Effluent by Combined Photocatalytic and Ozonation Processes”, *Chemosphere*, 40, pp. 369.

Moreira, M.T.; Mielgo, I.; Feijoo, G. and Lema, J.M. (2000). Evaluation of different fungal strains in the decolorisation of synthetic dyes. *Biotechnology letters*, 22, pp. 1499-1503.

Munoz, I., Rieradevall, J., Torrades, F., Peral, J. and Domenech, X. (2005).“Environmental Assessment of Different Solar Driven Advanced Oxidation Processes”, *Solar Energy***,** 79: pp. 369.

Munter, R. (2001). “Advanced Oxidation Processes–Current Status and prospects.” *Proceedings of the Estonian Academy of Sciences Chemistry,* 50 (2): pp. 59–80

Neppolian, B., Choi, H.C., Sakthivel, S., Arabindoo, B. and Murugesan, V. (2002). *Journal of Hazardous Materials.* B 89: pp. 303.

Neyens, E. and Baeyens, J. (2003). A review of classic Fenton's peroxidation as an advanced oxidation technique, *Journal of Hazardous Materials* B 98; pp. 33–50.

Nishio, J., Tokumura, M., Znad, H.T. and Kawase, Y. (2006)**.** Photocatalytic decolorization of azo dye with zinc oxide powder in an external UV light irradiation slurry photoreactor. *Journal of Hazardous Materials*, 138(1): pp. 106-115.

Nkeonye , P.O, and Olivera – Campos, A.M.F. (2005). Degradation of C.I. Reactive Orange 4 and its Simulated Dyebath Wastewater by Heterogeneous Photocatalysis. *Dyes and Pigments*. 64, pp. 135-139.

Nkeonye, P.O. (2012). "Chemistry and application of pigments". Lecture manual for Postgraduate students, 2011/2012 session. ABU press, Zaria.

Ollis, D.F., Pelizzetti, E. and Serpone, N. (1989). Heterogeneous Photocatalysis in the Environment: Application to Water Purification. Photocatalysis: Fundamentals and Applications, Wiley, New York.

Olukanni, O.D., Osuntoki, A.A. and Gbenle, G.A. (2006)."Textile effluent biodegradation potentials of textile effluent-adapted and non-adapted bacteria," *Journal of African Biotechnology*, 5, pp. 1980-1984.

P´erez, M., Torrades, F., Dom`enech, X. and Peral, J. (2002). Fenton and photo-Fenton oxidation of textile effluents, *Water Resources*. 36; pp. 2703–2710.

Parsons, S. (2004) Advanced Oxidation Processes for Water and Wastewater Treatment. IWA Publishing, London.

Paschotta, R. (2009). "Bragg Mirrors". *Encyclopedia of Laser Physics and Technology*. RP Photonics.

Pehlivan, E., Altun, T. and Parlayici, S. (2008). Utilizartion of barley straws as biosorbents for $Cu^{2+}$and $Pb^{2+}$ ions, Journal of Hazardous Materials. 164, pp. 982-986

Pinheiro, H. M. and E. Touraud (2004). "Aromatic amines from azo dye reduction: status review with emphasis on direct UV spectrophotometric detection in textile industry wastewaters." *Dyes andPigments* 61(2): pp. 121-139.

Pizarro, P. and Guillard, C. (2005). "Photocatalytic degradation of imazapyr in water: Comparison of activities of different supported and unsupported $TiO_2$-based catalysts." *Catalysis Today* 101(3–4): pp. 211-218.

Poulios, I. and Aetopoulou, I. (1999). Environmental Technology. 20; pp. 479.

Raju,N.S.,Venkataraman,G.V., Girish, S.T., Raghavendra, V.B. and Shivashankar, P. (2007)."Isolation and Evaluation of Indigenous soil fungi for Decolourization of Textile Dyes,"*Journal of Applied Sciences*, 7, pp. 298-301.

Ralph,W. and Matthews, (1992). "Photocatalytic oxidation of organic contaminants in water: An aid to environmental preservation," *Journal of pure & applied chemistry*, 64, pp. 1285-1290.

Rashidi, S., Nikazar, M., Yazdi, A.V. and Fazaeli, R. (2014). "Optimized photocatalytic degradation of reactive blue 2 by $TiO_2$/UV process," *Journal of Environmental Science and Health, Part A*, 49, pp. 452–462.

Rathi, A., Rajor, H.K., Sharma, R.K. (2003). Photodegradation of direct yellow-12 using UV/H2O2/$Fe^{2+}$, *Journal of Hazardous Materials*. B 102; pp. 231–241.

Rauf, M. A., Ashraf, S.S. and Alhadrami, S.N. (2005): Photolytic Oxidation of Coomasie. *Chemical Engineering Journal,89:185 – 192.*

Rauf, M.A., Bukallah, S.B., Hamadi, A., Sulaiman, A. and Hammadi, F. (2007). Photodegradation of textile dyes. *Journal of Chemical Engineering.* 129, pp.167–172

Rauf, M.A., Meetani, M.A. and Hisaindee, S. (2011). An overview on the photocatalytic degradation of azo dyes in the presence of $TiO_2$ doped with selective transition metals. *Desalination*. 276(1-3): pp. 13-27.

Reutergådh, L. B. and Iangphasuk, M. (1997). "Photocatalytic decolourization of reactive azo dye: A comparison between $TiO_2$ and us photocatalysis." *Chemosphere* 35(3): pp. 585-596.

Robinson, T., McMullan, G., Marchant, R. and Nigam, P. (2001). Remediation of dyes in textile effluent: a critical review on current treatment technologies with a proposed alternative, *Bioresources and Technology*. 77; pp. 247–255.

Roger, W. H and Ronald, D. S. (2002). Statistical Thinking: Improving Business Performance, Duxbury Press.

Sahel, K.; Perol, N., Chermette, H., Bordes, C., Derriche, Z., and Guillard, C. (2007): Photocatalytic decoloration of Remazol Black (RB5) and Procion Red MX-5B Isotherm of adsorption, kinetic of decoloration and mineralization, *Applied Catalysis B: Environmenta*l 77: pp. 100-109.

Sakthivel, S., Neppolian, B., Palanichamy, M., Arabindoo, B., Murugesan, V. (1999). *Indian Journal of Chemical Technology*. 6; pp. 161.

Sakthivel, S., Neppolian, B., Shankar, M.V., Arabindoo, B., Palanichamy, M., Murugesan, V. (2003). *Solar Energy Material. Solar Cells* 77; pp. 65.

Saquib, M., Muneer, M. (2003). *Dyes Pigments* 56; pp. 37–49.

Saquiba, M., Tariqa, M.A., Faisala, M. and Muneer, M. (2008). Photocatalytic degradation of two selected dye derivatives in aqueous suspensions of titanium dioxide, *Desalination* 219, pp. 301–311.

Science dialy, (2011). Clean, Cheap Ways to Produce Hydrogen for use in fuel cells. A dash of disorder yields a very efficient photocatalyst.

Serpone, N., Terzian, R., Minero C. and Pelizzetti, E. (1993). American Chemical Society, New York, pp. 281–314.

Shakir, K.; Elkafrawy, A. F.; Ghoneimy, H. F.; Behir, S. G. E. and Refaat, M. (2010). Removal of rhodamine B (a basic dye) and thoron (an acidic dye) from dilute aqueous solutionsand wastewater simulants by ion flotation. *Water research*, 44, pp. 1449-1461. ISSN 0043-1354

Sharma, A., Rao, P., Mathur, R.P., Ametha, S.C., (1995). Journal of Photochemistry and Photobiology. A 86; pp. 97.

Shaw, T., Simpson, B., Wilson, B., Oostman, H., Rainey, D., and Storrs, F. (2010). "True photoallergy to sunscreens is rare despite popular belief". *Dermatitis* 21 (4): pp. 185-198.

Shaylinda, N. ( 2005). Decolourisation of dye solution containing azo acid orange 7 by electricity, PhD. Thesis, Faculty of Civil Engineering Universiti Teknologi Malaysia

Shourong, Z., Qingguo, H., Jun, Z. and Bingkun, W. (1997). *Journal of Photochemistry and Photobiology. A: Chemical*. 108; pp. 235.

Siddiqui, M.F., Andleeb, S.; Ali, N.,Ghumro, P.B. and Ahmed, S. (2009). "Up-flow immobilized fungal Column Reactor for the Treatment of Anthraquinone dye Drimarene blue K2RL," *Journal of African Biotechnology*, 8, pp. 5570-5577

Skoeb, E.V., Ustinovich, E.A., Kulak, A.I. and Sviridov, D.V. (2008): Photocatalytic activity of $TiO_2$ : $In_2O_3$ nanocomposite films towards the degradation of arylmethane and azo dyes, *Journal of Photochemistry and Photobiology A: Chemistry* 193: pp. 97-102.

Skooge, D.A, West D.M, Holler F.J. (1992). Fundamentals of Analytical Chemistry. 6th ed. Philadelphia: Saunders College Publishing.

Szpyrkowicz, L., Juzzolino, C., Kaul, S.N., Daniele, S., and De Faveri, M.D. (2000) Electrochemical oxidation of dyeing baths bearing disperse dyes. *Indian Journal of Engineering and Chemical Resources.* 39: pp. 3241–3248
.

Staff, N. (2009). "Titanium Dioxide ($TiO_2$) Nanoparticles In Household Products Linked To Cancer In Mice."

Sun, J., Wang, X., Sun, J., Sun, R., Sun, S., Qiao, L. (2006). Photocatalyticdegradation and kinetics of Orange G using nano-sized Sn(IV)/$TiO_2$/AC photocatalyst, *Journal of Molecular. Catalysis. A: Chemistry*. 260; pp. 241–246.

Sun, J., Qiao, L., Sun, S., Wang, G. (2008). Photocatalytic degradation of Orange G on nitrogen-doped $TiO_2$ catalysts under visible light and sunlight irradiation, *Journal of Hazardous Materials.* 155, pp. 312–319.

Tanaka, K., Padermpole, K. and Hisanaga, T. (2000). *Water Resources*. 34, pp. 327–333.

Tang, W. Z. and A. Huren (1995). "UV/$TiO_2$ photocatalytic oxidation of commercial dyes in aqueous solutions." *Chemosphere* 31(9): pp. 4157-4170.

Tang, W.Z., An, H. (1995). *Chemosphere* 31; pp. 4157

Thiruvenkatachari, R. and Vigneswaran, S. (2008). "A review on UV/TiO <sub & gt;2</sub & gt; photocatalytic oxidation process (Journal Review)." *Korean Journal of Chemical Engineering* 25(1): pp. 64-72.

Tunesi, S., and Anderson, M., (1991). Influence of chemisorption on the photodecompositionof salicylic acid and related compounds using suspended titania ceramic membranes, *Journal of Physical Chemistry*. 95: pp. 3399–3405.

Vautier, M., Herrmann, J.M., and Guillard,C. (2001). "Photocatalytic Degradation of Dyes inWater: Case Study of Indigo and of Indigo Carmine", *Journal of Catalysis*., 201, pp. 46.

Venkataraman, K. (1978). The Chemistry of Synthetic Dyes, vol. 1-8. Academic Press, London,

Wang, C.T. (2007): Photocatalytic activity of nanoparticles gold/iron oxide aerogels for azo dye degradation, *Journal of Non-Crystalline Solids* 353: pp. 1126-1133.

Wang, G.S., Hsieh, S.T., Hong, C.S. (2000). Destruction of humic acid in water by UV light-catalysed oxidation with hydrogen peroxide. *Journal of Water Resources,* 34, pp. 3882-3887.

Wang, X., Yao, Z., Wang, J., Guo, W. and Li, G. (2008). Degradation of reactive brilliant red in aqueous solution by ultrasonic cavitation. *Ultrasonics Sonochemistry.* 15: pp. 43–48.

Weinberg, H.S., and Glaze, W.H. (1997). A unified approach to the analysis of polar organic by-products of oxidation in aqueous matrices, *Journal of Water Resources.* 31; pp. 1555–1572.

Wesenberg, D.; Kyriakides, I.; and Agathos, S.N. (2003). White-rot fungi and their enzymes for the treatment of industrial dye effluents. Biotechnology Advances, 22, pp. 161-187.

Winkler, J. (2003). Titanium dioxide Hannover. Vincentz Network. pp. 5, ISBN 3-87870-148-9.

Xiao, Q., Zhang, J., Xiao, C., and Tan, X. (2007). Photocatalytic decolorization of methylene blue over Zn1−xCoxO under visible light irradiation, *Journal of Science and Engineering.* B 142: pp. 121–125.

Xiaodan, Y., Qingyin, W., Shicheng, J., and Yihang, G. (2006). Nanoscale ZnS/$TiO_2$ composites: Preparation, characterization, and visible-light photocatalytic activity. 57(4-5): pp. 333-341.

Yizhong, W. (2000).“Solar photocatalytic degradation of eight commercial dyes in $TiO_2$ suspension,” *Journal of Water Resources.* 34, pp. 990-994.

Yoon, J., Lee, Y., Kim, S. (2001). Investigation of the reaction pathway of OH radicals produced by Fenton oxidation in the conditions of wastewater treatment,Water Sci. Technol. 44 (5): pp. 15–21.

Yu, X. Wu, Q. Jiang S. and Guo, Y.(2006). “Nano scale ZnS/TiO2 composites: Preparation, characterization, and visible-light photocatalytic activity,” *Journal of Materials Characterization*, 57, pp.333-341.

Zapanta, L.S. and Tien, M. (1997). The roles of veratryl alcohol and oxalate in fungal lignin degradation. *Journal of Biotechnology*, 53, pp. 93-102.

Zhang, L., Liu,C.Y. and Ren, X.M. (1995). *Journal of Photochemistry and Photobiology*. A 85; pp. 239.

Zhang, T., Oyama, T., Horikoshi, S., Hidaka, H., Zhao, J. and Serpone, N. (2002). Photocatalyzed N-demethylation and degradation of methylene blue in titania dispersions exposed to concentrated sunlight, Solar Energy Materials. Solar Cells 73; pp. 287–303.

Zhao, M. and Zhang J. (2008).“Wastewater treatment by photocatalytic oxidation of Nano-ZnO, *Journal of Global Environmental Policy in Japan*, 12, pp. 1-9.

## LIST OF APPENDICE

APPENDICE A: Infra red spectra of synthesized azo pigments

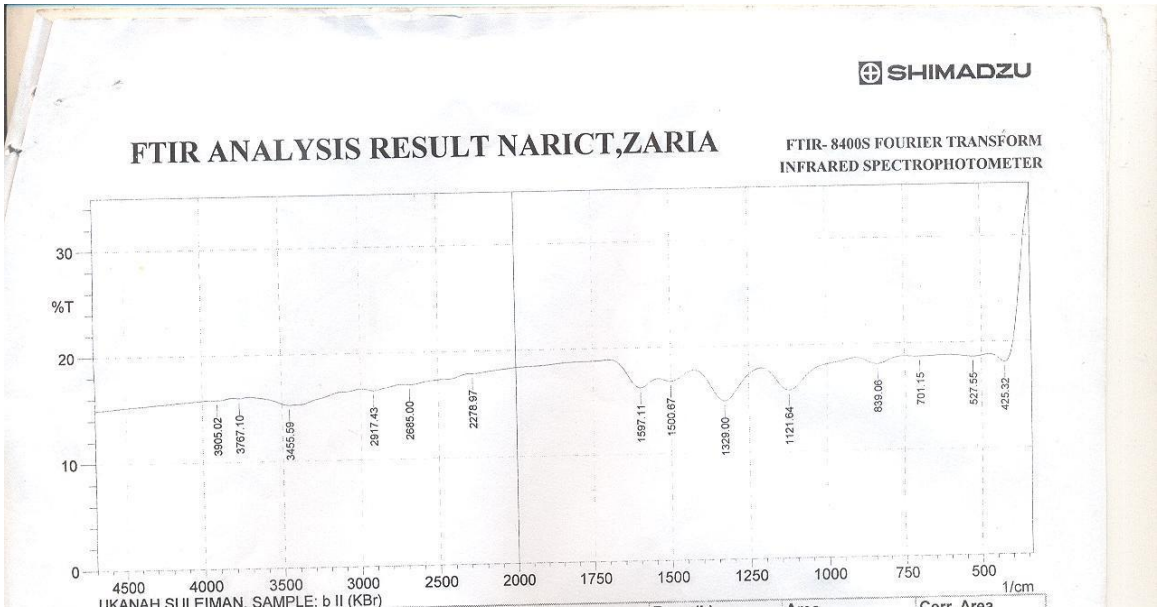


IR spectra of AP1

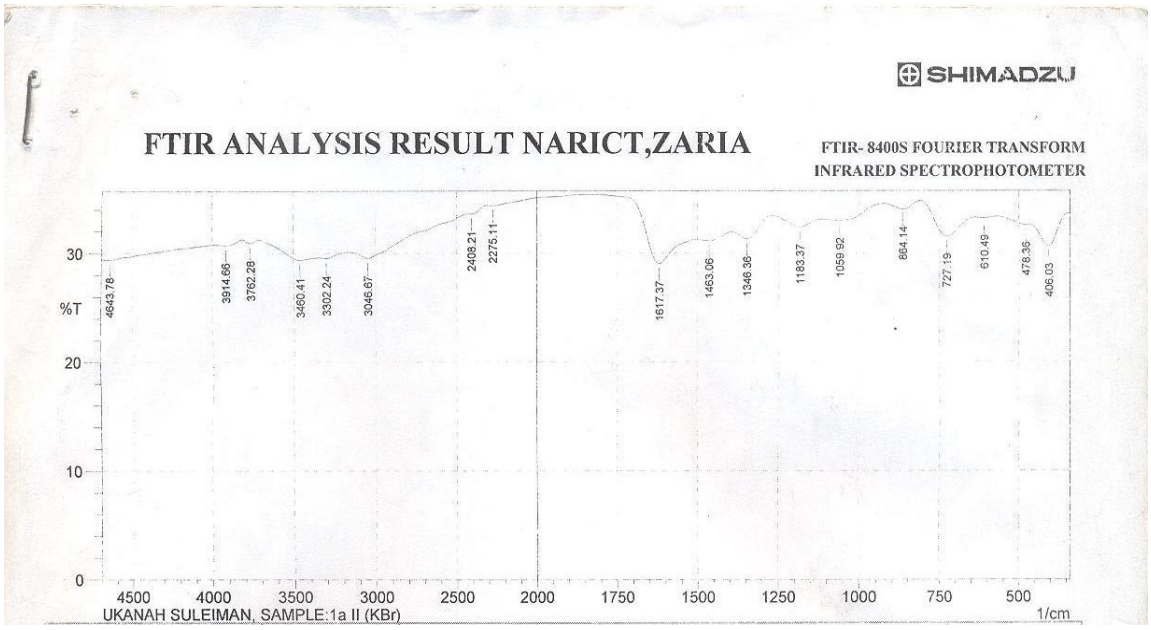


IR Spectra of AP2

APPENDICE B: Gas Chromatography-Mass Spectroscopy of synthesized azo pigment (AP1)

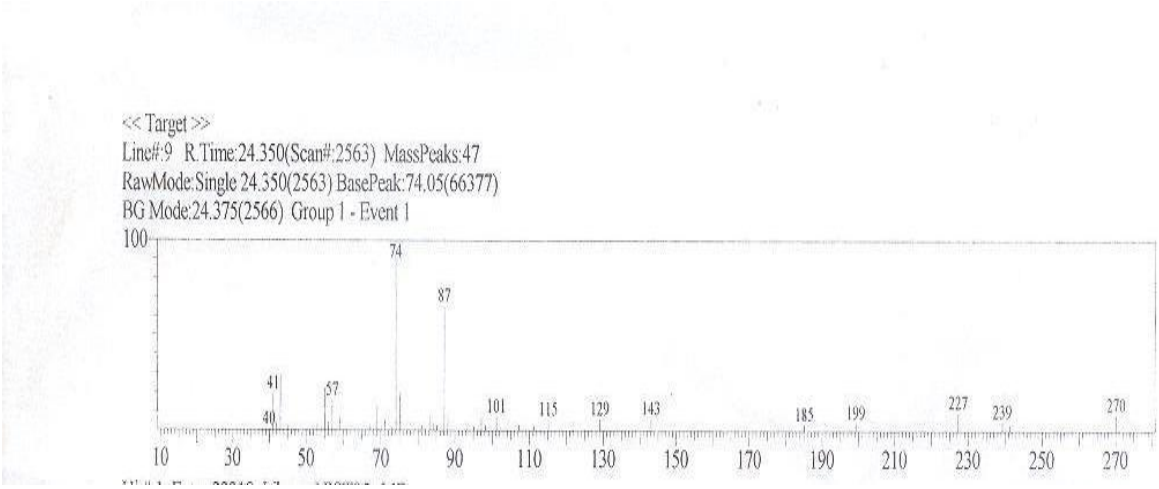


GC-MS of AP1

APPENDICE C: Absorbance and Concentration of Pigments samples

| **Concentration (mg/L)** | **Absorbance** | | | |
|---|---|---|---|---|
| | AP1 | AP2 | VP1 | VP2 |
| **0.001** | 0.035 | 0.025 | 0.048 | 0.038 |
| **0.002** | 0.065 | 0.048 | 0.083 | 0.072 |
| **0.003** | 0.093 | 0.073 | 0.109 | 0.098 |
| **0.004** | 0.126 | 0.096 | 0.134 | 0.123 |
| **0.005** | 0.155 | 0.122 | 0.171 | 0.148 |
| **0.006** | 0.183 | 0.145 | 0.195 | 0.176 |
| **0.007** | 0.211 | 0.171 | 0.221 | 0.204 |
| **0.008** | 0.283 | 0.196 | 0.248 | 0.228 |
| **0.009** | 0.262 | 0.218 | 0.272 | 0.245 |
| **0.01** | 0.288 | 0.232 | 0.298 | 0.263 |

APPENDICE D: Box-Beckhen design for commercial vat and synthesized azo pigment

## Box-Behnken Design For Khaki 2G (VP1)

```
Factors:       4     Replicates:     1
Base runs:    27     Total runs:    27
Base blocks:   1     Total blocks:   1

Center points: 3

MTB > Name C12 "FITS1" C13 "RESI1" C14 "SRES1" C15 "PFit1" C16 "PSEFit1" C17
"CLimLo1" &
CONT> C18 "CLimHi1" C19 "PLimLo1" C20 "PLimHi1"
MTB > RSRegress '%Degradation' = C5 C6 C7 C8 C5*C5 C6*C6 C7*C7 C8*C8 C5*C6 C5*C7
C5*C8 &
CONT> C6*C7 C6*C8 C7*C8;
SUBC>   Order C1;
SUBC>   InUnit 1 0;
SUBC>   Levels 5 20 0 2 0 90 7 9;
SUBC>   GHistogram;
SUBC>   GNormal;
SUBC>   GFits;
SUBC>   GOrder C2;
SUBC>   Brief 2;
SUBC>   Predict C5 C6 C7 C8;
SUBC>     Confidence 95;
SUBC>     PFit 'PFit1';
SUBC>     PSEFit 'PSEFit1';
SUBC>     CLimits 'CLimLo1' 'CLimHi1';
SUBC>     PLimits 'PLimLo1' 'PLimHi1';
SUBC>   Fits 'FITS1';
SUBC>   Residuals 'RESI1';
SUBC>   SResiduals 'SRES1'.
```

## Response Surface Regression: %Degradation versus Pigment Conc, Catalyst Loa, ..

```
The analysis was done using coded units.

Estimated Regression Coefficients for %Degradation

Term                                    Coef  SE Coef        T      P
Constant                             97.6885    3.375   28.944  0.000
Pigment Concentration (mg/L)          3.3557    1.834    1.829  0.092
Catalyst Loading (g/L)               11.3045    1.869    6.048  0.000
Time of exposure                     46.4307    1.688   27.514  0.000
pH                                    0.6517    1.719    0.379  0.711
Pigment Concentration (mg/L)*        -2.1510    2.648   -0.812  0.433
  Pigment Concentration (mg/L)
Catalyst Loading (g/L)*             -12.0435    2.648   -4.547  0.001
  Catalyst Loading (g/L)
Time of exposure*Time of exposure   -46.2082    2.532  -18.251  0.000
pH*pH                                -0.9543    2.604   -0.367  0.720
Pigment Concentration (mg/L)*        -4.9221    3.544   -1.389  0.190
  Catalyst Loading (g/L)
Pigment Concentration (mg/L)*         0.6003    2.811    0.214  0.835
  Time of exposure
Pigment Concentration (mg/L)*pH      -0.1475    2.977   -0.050  0.961
Catalyst Loading (g/L)*               7.0128    2.811    2.494  0.028
  Time of exposure
Catalyst Loading (g/L)*pH            -1.4050    2.977   -0.472  0.645
Time of exposure*pH                   0.3025    2.977    0.102  0.921
S = 5.95431    PRESS = 2398.95
```

R-Sq = 98.98%  R-Sq(pred) = 94.23%  R-Sq(adj) = 97.78%

Analysis of Variance for %Degradation

| Source | DF | Seq SS |
|---|---|---|
| Regression | 14 | 41184.5 |
| Linear | 4 | 26461.7 |
| Pigment Concentration (mg/L) | 1 | 151.3 |
| Catalyst Loading (g/L) | 1 | 1992.9 |
| Time of exposure | 1 | 24312.4 |
| pH | 1 | 5.1 |
| Square | 4 | 14368.4 |
| Pigment Concentration (mg/L)*Pigment Concentration (mg/L) | 1 | 154.8 |
| Catalyst Loading (g/L)*Catalyst Loading (g/L) | 1 | 260.3 |
| Time of exposure*Time of exposure | 1 | 13950.4 |
| pH*pH | 1 | 2.9 |
| Interaction | 6 | 354.4 |
| Pigment Concentration (mg/L)*Catalyst Loading (g/L) | 1 | 115.8 |
| Pigment Concentration (mg/L)*Time of exposure | 1 | 9.6 |
| Pigment Concentration (mg/L)*pH | 1 | 0.1 |
| Catalyst Loading (g/L)*Time of exposure | 1 | 220.6 |
| Catalyst Loading (g/L)*pH | 1 | 7.9 |
| Time of exposure*pH | 1 | 0.4 |
| Residual Error | 12 | 425.4 |
| Lack-of-Fit | 10 | 425.4 |
| Pure Error | 2 | 0.0 |
| Total | 26 | 41609.9 |

| Source | Adj SS | Adj MS |
|---|---|---|
| Regression | 41184.5 | 2941.7 |
| Linear | 27982.4 | 6995.6 |
| Pigment Concentration (mg/L) | 118.6 | 118.6 |
| Catalyst Loading (g/L) | 1297.0 | 1297.0 |
| Time of exposure | 26838.7 | 26838.7 |
| pH | 5.1 | 5.1 |
| Square | 13643.1 | 3410.8 |
| Pigment Concentration (mg/L)*Pigment Concentration (mg/L) | 23.4 | 23.4 |
| Catalyst Loading (g/L)*Catalyst Loading (g/L) | 733.1 | 733.1 |
| Time of exposure*Time of exposure | 11809.3 | 11809.3 |
| pH*pH | 4.8 | 4.8 |
| Interaction | 354.4 | 59.1 |
| Pigment Concentration (mg/L)*Catalyst Loading (g/L) | 68.4 | 68.4 |
| Pigment Concentration (mg/L)*Time of exposure | 1.6 | 1.6 |
| Pigment Concentration (mg/L)*pH | 0.1 | 0.1 |
| Catalyst Loading (g/L)*Time of exposure | 220.6 | 220.6 |
| Catalyst Loading (g/L)*pH | 7.9 | 7.9 |
| Time of exposure*pH | 0.4 | 0.4 |
| Residual Error | 425.4 | 35.5 |
| Lack-of-Fit | 425.4 | 42.5 |
| Pure Error | 0.0 | 0.0 |
| Total | | |

| Source | F |
|---|---|
| Regression | 82.97 |
| Linear | 197.32 |
| Pigment Concentration (mg/L) | 3.35 |
| Catalyst Loading (g/L) | 36.58 |
| Time of exposure | 757.00 |
| pH | 0.14 |
| Square | 96.20 |
| Pigment Concentration (mg/L)*Pigment Concentration (mg/L) | 0.66 |
| Catalyst Loading (g/L)*Catalyst Loading (g/L) | 20.68 |
| Time of exposure*Time of exposure | 333.09 |

| | | |
|---|---|---|
| pH*pH | | 0.13 |
| Interaction | | 1.67 |
| Pigment Concentration (mg/L)*Catalyst Loading (g/L) | | 1.93 |
| Pigment Concentration (mg/L)*Time of exposure | | 0.05 |
| Pigment Concentration (mg/L)*pH | | 0.00 |
| Catalyst Loading (g/L)*Time of exposure | | 6.22 |
| Catalyst Loading (g/L)*pH | | 0.22 |
| Time of exposure*pH | | 0.01 |
| Residual Error | | |
| Lack-of-Fit | 1276336.59 | |
| Pure Error | | |
| Total | | |

| Source | P |
|---|---|
| Regression | 0.000 |
| Linear | 0.000 |
| Pigment Concentration (mg/L) | 0.092 |
| Catalyst Loading (g/L) | 0.000 |
| Time of exposure | 0.000 |
| pH | 0.711 |
| Square | 0.000 |
| Pigment Concentration (mg/L)*Pigment Concentration (mg/L) | 0.433 |
| Catalyst Loading (g/L)*Catalyst Loading (g/L) | 0.001 |
| Time of exposure*Time of exposure | 0.000 |
| pH*pH | 0.720 |
| Interaction | 0.213 |
| Pigment Concentration (mg/L)*Catalyst Loading (g/L) | 0.190 |
| Pigment Concentration (mg/L)*Time of exposure | 0.835 |
| Pigment Concentration (mg/L)*pH | 0.961 |
| Catalyst Loading (g/L)*Time of exposure | 0.028 |
| Catalyst Loading (g/L)*pH | 0.645 |
| Time of exposure*pH | 0.921 |
| Residual Error | |
| Lack-of-Fit | 0.000 |
| Pure Error | |
| Total | |

Unusual Observations for %Degradation

| Obs | StdOrder | %Degradation | Fit | SE Fit | Residual | St Resid | |
|---|---|---|---|---|---|---|---|
| 11 | 1 | 54.370 | 63.912 | 4.042 | -9.542 | -2.18 | R |
| 25 | 13 | 0.000 | -11.286 | 4.648 | 11.286 | 3.03 | R |

R denotes an observation with a large standardized residual.

Estimated Regression Coefficients for %Degradation using data in uncoded units

| Term | Coef |
|---|---|
| Constant | -107.131 |
| Pigment Concentration (mg/L) | 2.13701 |
| Catalyst Loading (g/L) | 47.8223 |
| Time of exposure | 2.85364 |
| pH | 17.2686 |
| Pigment Concentration (mg/L)* Pigment Concentration (mg/L) | -0.0382403 |
| Catalyst Loading (g/L)* Catalyst Loading (g/L) | -12.0435 |
| Time of exposure*Time of exposure | -0.0228189 |
| pH*pH | -0.954289 |
| Pigment Concentration (mg/L)* Catalyst Loading (g/L) | -0.656283 |

```
Pigment Concentration (mg/L)*      0.00177863
  Time of exposure
Pigment Concentration (mg/L)*pH    -0.0196667
Catalyst Loading (g/L)*              0.155840
  Time of exposure
Catalyst Loading (g/L)*pH            -1.40500
Time of exposure*pH                0.00672222
```

Predicted Response for New Design Points Using Model for %Degradation

| Point | Fit | SE Fit | 95% CI | 95% PI |
|---|---|---|---|---|
| 1 | 75.443 | 4.68814 | ( 65.2283, 85.657) | ( 58.9309, 91.955) |
| 2 | 95.242 | 4.55544 | ( 85.3164, 105.167) | ( 78.9072, 111.577) |
| 3 | 96.003 | 4.59261 | ( 85.9962, 106.009) | ( 79.6186, 112.387) |
| 4 | 99.716 | 4.64815 | ( 89.5886, 109.844) | ( 83.2579, 116.174) |
| 5 | 97.435 | 4.66762 | ( 87.2649, 107.605) | ( 80.9504, 113.919) |
| 6 | 104.185 | 4.54255 | ( 94.2875, 114.082) | ( 87.8672, 120.502) |
| 7 | 71.330 | 4.68814 | ( 61.1150, 81.544) | ( 54.8176, 87.842) |
| 8 | 4.444 | 4.60652 | ( -5.5923, 14.481) | (-11.9581, 20.847) |
| 9 | 67.550 | 4.25522 | ( 58.2790, 76.822) | ( 51.6046, 83.496) |
| 10 | 97.911 | 4.59261 | ( 87.9045, 107.917) | ( 81.5269, 114.295) |
| 11 | 63.912 | 4.04232 | ( 55.1042, 72.719) | ( 48.2312, 79.592) |
| 12 | 92.027 | 4.54841 | ( 82.1165, 101.937) | ( 75.7013, 108.352) |
| 13 | 91.804 | 4.01402 | ( 83.0583, 100.550) | ( 76.1581, 107.450) |
| 14 | -2.702 | 4.48108 | (-12.4657, 7.061) | (-18.9390, 13.535) |
| 15 | 97.689 | 3.37510 | ( 90.3348, 105.042) | ( 82.7760, 112.601) |
| 16 | 97.689 | 3.37510 | ( 90.3348, 105.042) | ( 82.7760, 112.601) |
| 17 | 98.443 | 4.66762 | ( 88.2732, 108.613) | ( 81.9588, 114.927) |
| 18 | 96.365 | 5.03836 | ( 85.3873, 107.343) | ( 79.3703, 113.359) |
| 19 | 3.746 | 4.60652 | ( -6.2906, 13.783) | (-12.6564, 20.149) |
| 20 | 56.521 | 4.48272 | ( 46.7542, 66.288) | ( 40.2823, 72.760) |
| 21 | 90.428 | 4.54841 | ( 80.5182, 100.338) | ( 74.1030, 106.754) |
| 22 | 0.143 | 4.54255 | ( -9.7542, 10.041) | (-16.1745, 16.461) |
| 23 | 96.749 | 4.55544 | ( 86.8231, 106.674) | ( 80.4139, 113.083) |
| 24 | 97.689 | 3.37510 | ( 90.3348, 105.042) | ( 82.7760, 112.601) |
| 25 | -11.286 | 4.64815 | (-21.4131, -1.158) | (-27.7438, 5.173) |
| 26 | 93.232 | 4.52063 | ( 83.3825, 103.082) | ( 76.9434, 109.521) |
| 27 | 5.654 | 4.64356 | ( -4.4634, 15.771) | (-10.7980, 22.106) |

Regression equation data for Caledon Khaki 2G (VP1)

| Predictor | Coef | SE Coef | T | P |
|---|---|---|---|---|
| Constant | -3.79 | 62.90 | -0.06 | 0.952 |
| Pigment Concentration (mg/L) | 0.565 | 1.033 | 0.55 | 0.590 |
| Catalyst Loading (g/L) | 16.222 | 7.702 | 2.11 | 0.047 |
| Time of exposure | 0.9674 | 0.1628 | 5.94 | 0.000 |
| pH | 0.652 | 7.575 | 0.09 | 0.932 |

S = 26.2404  R-Sq = 63.6%  R-Sq(adj) = 57.0%

Analysis of Variance

| Source | DF | SS | MS | F | P |
|---|---|---|---|---|---|
| Regression | 4 | 26461.7 | 6615.4 | 9.61 | 0.000 |
| Residual Error | 22 | 15148.3 | 688.6 | | |
| Total | 26 | 41609.9 | | | |

| Source | DF | Seq SS |
|---|---|---|
| Pigment Concentration (mg/L) | 1 | 151.3 |
| Catalyst Loading (g/L) | 1 | 1992.9 |
| Time of exposure | 1 | 24312.4 |
| pH | 1 | 5.1 |

| Obs | Pigment Concentration (mg/L) | %Degradation | Fit | SE Fit | Residual | St Resid |
|---|---|---|---|---|---|---|
| 1 | 12.5 | 74.24 | 52.66 | 12.01 | 21.58 | 0.92 |
| 2 | 12.5 | 96.65 | 85.11 | 11.87 | 11.54 | 0.49 |
| 3 | 12.5 | 97.28 | 111.11 | 11.55 | -13.83 | -0.59 |
| 4 | 20.0 | 99.31 | 116.00 | 12.32 | -16.69 | -0.72 |
| 5 | 20.0 | 98.11 | 71.82 | 12.32 | 26.29 | 1.13 |
| 6 | 12.5 | 97.42 | 127.99 | 11.89 | -30.57 | -1.31 |
| 7 | 12.5 | 68.97 | 51.36 | 12.01 | 17.61 | 0.75 |
| 8 | 12.5 | 0.00 | 25.35 | 11.85 | -25.35 | -1.08 |
| 9 | 12.5 | 67.76 | 95.54 | 11.37 | -27.78 | -1.17 |
| 10 | 12.5 | 98.49 | 112.42 | 11.55 | -13.93 | -0.59 |
| 11 | 5.0 | 54.37 | 47.78 | 10.90 | 6.59 | 0.28 |
| 12 | 5.0 | 95.47 | 64.65 | 11.60 | 30.82 | 1.31 |
| 13 | 5.0 | 95.30 | 107.53 | 10.97 | -12.23 | -0.51 |
| 14 | 12.5 | 0.00 | 40.92 | 11.53 | -40.92 | -1.74 |
| 15 | 12.5 | 97.96 | 68.23 | 5.09 | 29.73 | 1.15 |
| 16 | 12.5 | 97.96 | 68.23 | 5.09 | 29.73 | 1.15 |
| 17 | 20.0 | 98.66 | 73.12 | 12.32 | 25.54 | 1.10 |
| 18 | 5.0 | 93.60 | 80.22 | 12.42 | 13.38 | 0.58 |
| 19 | 12.5 | 0.00 | 24.05 | 11.85 | -24.05 | -1.03 |
| 20 | 5.0 | 58.13 | 91.31 | 12.42 | -33.18 | -1.44 |
| 21 | 5.0 | 94.33 | 63.35 | 11.60 | 30.98 | 1.32 |
| 22 | 5.0 | 0.00 | 20.47 | 11.89 | -20.47 | -0.87 |
| 23 | 12.5 | 97.00 | 83.80 | 11.87 | 13.20 | 0.56 |
| 24 | 12.5 | 97.95 | 68.23 | 5.09 | 29.72 | 1.15 |
| 25 | 12.5 | 0.00 | 8.48 | 12.32 | -8.48 | -0.37 |
| 26 | 20.0 | 98.40 | 88.69 | 11.52 | 9.71 | 0.41 |
| 27 | 20.0 | 0.00 | 28.94 | 12.02 | -28.94 | -1.24 |

## Box-Behnken Design For Caledon Green 2G

```
Factors:       4     Replicates:     1
Base runs:    27     Total runs:    27
Base blocks:   1     Total blocks:   1

Center points: 3

MTB > Name C12 "FITS1" C13 "RESI1" C14 "SRES1" C15 "PFit1" C16 "PSEFit1" C17
"CLimLo1" &
CONT> C18 "CLimHi1" C19 "PLimLo1" C20 "PLimHi1"
MTB > RSRegress '%Degradation' = C5 C6 C7 C8 C5*C5 C6*C6 C7*C7 C8*C8 C5*C6 C5*C7
C5*C8 &
CONT> C6*C7 C6*C8 C7*C8;
SUBC>   Order C1;
SUBC>   InUnit 1 0;
SUBC>   Levels 5 20 0 2 0 90 7 9;
SUBC>   GHistogram;
SUBC>   GNormal;
SUBC>   GFits;
SUBC>   GOrder C2;
SUBC>   Brief 2;
SUBC>   Predict C5 C6 C7 C8;
SUBC>     Confidence 95;
SUBC>     PFit 'PFit1';
SUBC>     PSEFit 'PSEFit1';
SUBC>     CLimits 'CLimLo1' 'CLimHi1';
SUBC>     PLimits 'PLimLo1' 'PLimHi1';
SUBC>   Fits 'FITS1';
SUBC>   Residuals 'RESI1';
```

```
SUBC>   SResiduals 'SRES1'.
```

## Response Surface Regression: %Degradation versus Pigment Conc, Catalyst Loa, ..

```
The analysis was done using coded units.

Estimated Regression Coefficients for %Degradation

Term                                    Coef  SE Coef        T      P
Constant                             98.6067    3.720   26.504  0.000
Pigment Concentration (mg/L)          4.0538    2.211    1.834  0.092
Catalyst Loading (g/L)               14.1887    2.038    6.961  0.000
Time of exposure                     45.5872    1.916   23.795  0.000
pH                                   -0.9642    2.121   -0.455  0.658
Pigment Concentration (mg/L)*        -3.1558    3.053   -1.034  0.322
  Pigment Concentration (mg/L)
Catalyst Loading (g/L)*             -14.2441    3.130   -4.551  0.001
  Catalyst Loading (g/L)
Time of exposure*Time of exposure   -45.6948    2.793  -16.360  0.000
pH*pH                                -4.5745    2.987   -1.531  0.152
Pigment Concentration (mg/L)*        -4.0401    3.946   -1.024  0.326
  Catalyst Loading (g/L)
Pigment Concentration (mg/L)*         0.2470    3.138    0.079  0.939
  Time of exposure
Pigment Concentration (mg/L)*pH       3.7637    3.921    0.960  0.356
Catalyst Loading (g/L)*               8.0715    2.979    2.710  0.019
  Time of exposure
Catalyst Loading (g/L)*pH            -0.3605    3.187   -0.113  0.912
Time of exposure*pH                  -1.7739    3.572   -0.497  0.628


S = 6.63592    PRESS = 3436.55
R-Sq = 98.74%  R-Sq(pred) = 91.82%  R-Sq(adj) = 97.27%


Analysis of Variance for %Degradation

Source                                                          DF   Seq SS
Regression                                                      14  41458.4
  Linear                                                         4  26886.9
    Pigment Concentration (mg/L)                                 1    211.7
    Catalyst Loading (g/L)                                       1   3726.9
    Time of exposure                                             1  22515.3
    pH                                                           1    433.0
  Square                                                         4  14117.7
    Pigment Concentration (mg/L)*Pigment Concentration (mg/L)    1    208.9
    Catalyst Loading (g/L)*Catalyst Loading (g/L)                1    626.7
    Time of exposure*Time of exposure                            1  13242.3
    pH*pH                                                        1     39.8
  Interaction                                                    6    453.8
    Pigment Concentration (mg/L)*Catalyst Loading (g/L)          1     80.7
    Pigment Concentration (mg/L)*Time of exposure                1      9.8
    Pigment Concentration (mg/L)*pH                              1     39.0
    Catalyst Loading (g/L)*Time of exposure                      1    311.4
    Catalyst Loading (g/L)*pH                                    1      2.0
    Time of exposure*pH                                          1     10.9
Residual Error                                                  12    528.4
  Lack-of-Fit                                                    9    517.8
  Pure Error                                                     3     10.6
Total                                                           26  41986.9

Source                                                      Adj SS   Adj MS
```

| | | |
|---|---|---|
| Regression | 41458.4 | 2961.3 |
| Linear | 27732.7 | 6933.2 |
| Pigment Concentration (mg/L) | 148.0 | 148.0 |
| Catalyst Loading (g/L) | 2133.9 | 2133.9 |
| Time of exposure | 24933.9 | 24933.9 |
| pH | 9.1 | 9.1 |
| Square | 12448.0 | 3112.0 |
| Pigment Concentration (mg/L)*Pigment Concentration (mg/L) | 47.1 | 47.1 |
| Catalyst Loading (g/L)*Catalyst Loading (g/L) | 912.0 | 912.0 |
| Time of exposure*Time of exposure | 11786.7 | 11786.7 |
| pH*pH | 103.3 | 103.3 |
| Interaction | 453.8 | 75.6 |
| Pigment Concentration (mg/L)*Catalyst Loading (g/L) | 46.2 | 46.2 |
| Pigment Concentration (mg/L)*Time of exposure | 0.3 | 0.3 |
| Pigment Concentration (mg/L)*pH | 40.6 | 40.6 |
| Catalyst Loading (g/L)*Time of exposure | 323.3 | 323.3 |
| Catalyst Loading (g/L)*pH | 0.6 | 0.6 |
| Time of exposure*pH | 10.9 | 10.9 |
| Residual Error | 528.4 | 44.0 |
| Lack-of-Fit | 517.8 | 57.5 |
| Pure Error | 10.6 | 3.5 |
| Total | | |

| Source | F | P |
|---|---|---|
| Regression | 67.25 | 0.000 |
| Linear | 157.45 | 0.000 |
| Pigment Concentration (mg/L) | 3.36 | 0.092 |
| Catalyst Loading (g/L) | 48.46 | 0.000 |
| Time of exposure | 566.22 | 0.000 |
| pH | 0.21 | 0.658 |
| Square | 70.67 | 0.000 |
| Pigment Concentration (mg/L)*Pigment Concentration (mg/L) | 1.07 | 0.322 |
| Catalyst Loading (g/L)*Catalyst Loading (g/L) | 20.71 | 0.001 |
| Time of exposure*Time of exposure | 267.66 | 0.000 |
| pH*pH | 2.35 | 0.152 |
| Interaction | 1.72 | 0.200 |
| Pigment Concentration (mg/L)*Catalyst Loading (g/L) | 1.05 | 0.326 |
| Pigment Concentration (mg/L)*Time of exposure | 0.01 | 0.939 |
| Pigment Concentration (mg/L)*pH | 0.92 | 0.356 |
| Catalyst Loading (g/L)*Time of exposure | 7.34 | 0.019 |
| Catalyst Loading (g/L)*pH | 0.01 | 0.912 |
| Time of exposure*pH | 0.25 | 0.628 |
| Residual Error | | |
| Lack-of-Fit | 16.31 | 0.021 |
| Pure Error | | |
| Total | | |

Unusual Observations for %Degradation

| Obs | StdOrder | %Degradation | Fit | SE Fit | Residual | St Resid | |
|---|---|---|---|---|---|---|---|
| 5 | 13 | 0.000 | -13.036 | 5.338 | 13.036 | 3.31 | R |

R denotes an observation with a large standardized residual.

Estimated Regression Coefficients for %Degradation using data in uncoded units

| Term | Coef |
|---|---|
| Constant | -286.826 |
| Pigment Concentration (mg/L) | -1.56577 |
| Catalyst Loading (g/L) | 44.2231 |
| Time of exposure | 3.17077 |
| pH | 68.0888 |

```
Pigment Concentration (mg/L)*       -0.0561026
  Pigment Concentration (mg/L)
Catalyst Loading (g/L)*               -14.2441
  Catalyst Loading (g/L)
Time of exposure*Time of exposure   -0.0225653
pH*pH                                 -4.57446
Pigment Concentration (mg/L)*        -0.538677
  Catalyst Loading (g/L)
Pigment Concentration (mg/L)*      0.000731985
  Time of exposure
Pigment Concentration (mg/L)*pH       0.501823
Catalyst Loading (g/L)*               0.179367
  Time of exposure
Catalyst Loading (g/L)*pH            -0.360541
Time of exposure*pH                 -0.0394197


Predicted Response for New Design Points Using Model for %Degradation

Point      Fit   SE Fit         95% CI               95% PI
    1   98.607  3.72049  ( 90.5005, 106.713)  ( 82.0309, 115.183)
    2   58.924  4.64509  ( 48.8035,  69.045)  ( 41.2756,  76.573)
    3    1.941  5.35079  ( -9.7178,  13.599)  (-16.6326,  20.514)
    4   92.652  4.61272  ( 82.6019, 102.702)  ( 75.0438, 110.260)
    5  -13.036  5.33764  (-24.6662,  -1.407)  (-31.5917,   5.519)
    6   98.842  5.51796  ( 86.8196, 110.865)  ( 80.0382, 117.646)
    7   98.607  3.72049  ( 90.5005, 106.713)  ( 82.0309, 115.183)
    8   64.996  5.50740  ( 52.9963,  76.995)  ( 46.2066,  83.785)
    9   -0.802  5.04212  (-11.7880,  10.184)  (-18.9608,  17.356)
   10   66.203  5.28981  ( 54.6777,  77.729)  ( 47.7131,  84.693)
   11    7.976  5.21548  ( -3.3878,  19.339)  (-10.4138,  26.365)
   12   50.498  5.04794  ( 39.4997,  61.497)  ( 32.3319,  68.664)
   13   95.302  5.01000  ( 84.3857, 106.217)  ( 77.1852, 113.418)
   14   95.409  5.15072  ( 84.1868, 106.632)  ( 77.1066, 113.712)
   15   61.995  4.86796  ( 51.3885,  72.601)  ( 44.0633,  79.926)
   16   95.382  5.77718  ( 82.7944, 107.969)  ( 76.2118, 114.552)
   17   99.644  5.25019  ( 88.2051, 111.083)  ( 81.2079, 118.081)
   18   92.131  5.71995  ( 79.6681, 104.594)  ( 73.0425, 111.219)
   19   98.607  3.72049  ( 90.5005, 106.713)  ( 82.0309, 115.183)
   20   96.663  5.08386  ( 85.5860, 107.740)  ( 78.4490, 114.877)
   21   91.042  4.64984  ( 80.9114, 101.174)  ( 73.3879, 108.697)
   22  106.515  4.56798  ( 96.5625, 116.468)  ( 88.9623, 124.068)
   23   97.730  5.14820  ( 86.5128, 108.947)  ( 79.4305, 116.029)
   24    0.362  5.21938  (-11.0098,  11.734)  (-18.0326,  18.757)
   25    3.560  5.29928  ( -7.9861,  15.106)  (-14.9429,  22.063)
   26   91.551  4.06302  ( 82.6980, 100.403)  ( 74.5972, 108.504)
   27   91.551  4.06302  ( 82.6980, 100.403)  ( 74.5972, 108.504)
Regression equation data for Caledon Green 2G (VP2)

Predictor                      Coef  SE Coef      T      P
Constant                      46.94    61.07   0.77  0.450
Pigment Concentration (mg/L)  0.728    1.043   0.70  0.493
Catalyst Loading (g/L)       17.148    7.395   2.32  0.030
Time of exposure             0.9310   0.1622   5.74  0.000
pH                           -6.132    7.721  -0.79  0.436


S = 26.1985   R-Sq = 64.0%   R-Sq(adj) = 57.5%
Analysis of Variance

Source          DF       SS      MS     F      P
Regression       4  26886.9  6721.7  9.79  0.000
Residual Error  22  15100.0   686.4
```

```
Total           26  41986.9


Source                          DF   Seq SS
Pigment Concentration (mg/L)     1    211.7
Catalyst Loading (g/L)           1   3726.9
Time of exposure                 1  22515.3
pH                               1    433.0

           Pigment
     Concentration
Obs          (mg/L)  %Degradation     Fit  SE Fit  Residual  St Resid
  1            12.5         98.90   66.02    5.12     32.88      1.28
  2             5.0         51.14   43.41   11.03      7.73      0.33
  3            12.5          0.00   30.25   11.52    -30.25     -1.29
  4            12.5         98.35   77.03   11.64     21.32      0.91
  5            12.5          0.00    6.97   11.94     -6.97     -0.30
  6            12.5         97.98  118.93   13.50    -20.95     -0.93
  7            12.5         98.90   66.02    5.12     32.88      1.28
  8            12.5         62.56   42.74   12.70     19.82      0.87
  9            12.5          0.00   41.27   11.52    -41.27     -1.75
 10            12.5         59.72   55.00   11.46      4.72      0.20
 11            20.0          0.00   29.58   11.97    -29.58     -1.27
 12             5.0         53.16   85.31   12.80    -32.15     -1.41
 13            12.5         96.09   89.30   11.57      6.79      0.29
 14            20.0         98.61   88.62   11.23      9.99      0.42
 15            12.5         63.00   90.76   11.73    -27.76     -1.19
 16             5.0         93.46   77.71   12.09     15.75      0.68
 17            20.0         99.24  113.37   12.42    -14.13     -0.61
 18            20.0         96.15   77.61   12.84     18.54      0.81
 19            12.5         98.92   66.02    5.12     32.90      1.28
 20            12.5         97.42  114.04   11.39    -16.62     -0.70
 21             5.0         95.59  102.46   10.97     -6.87     -0.29
 22            12.5         98.81  125.06   11.13    -26.25     -1.11
 23            20.0         98.89   65.34   12.06     33.55      1.44
 24             5.0          0.00   18.67   12.03    -18.67     -0.80
 25            12.5          0.00   17.99   12.34    -17.99     -0.78
 26             5.0         90.68   66.69   10.65     23.99      1.00
 27             5.0         95.28   66.69   10.65     28.59      1.19
```

## Box-Behnken Design For AP1

```
Factors:       4     Replicates:     1
Base runs:    27     Total runs:    27
Base blocks:   1     Total blocks:   1

Center points: 3

MTB > Name C16 "FITS1" C17 "RESI1" C18 "SRES1" C19 "PFit1" C20 "PSEFit1" C21
"CLimLo1" &
CONT> C22 "CLimHi1" C23 "PLimLo1" C24 "PLimHi1"
MTB > RSRegress '%Degradation' = C5 C6 C7 C8 C5*C5 C6*C6 C7*C7 C8*C8 C5*C6 C5*C7
C5*C8 &
CONT> C6*C7 C6*C8 C7*C8;
SUBC>   Order C12;
SUBC>   InUnit 1 0;
SUBC>   Levels 5 20 0 2 0 90 8 10;
SUBC>   GHistogram;
SUBC>   GNormal;
SUBC>   GFits;
SUBC>   GOrder C13;
SUBC>   Brief 2;
```

```
SUBC>   Predict C5 C6 C7 C8;
SUBC>     Confidence 95;
SUBC>     PFit 'PFit1';
SUBC>     PSEFit 'PSEFit1';
SUBC>     CLimits 'CLimLo1' 'CLimHi1';
SUBC>     PLimits 'PLimLo1' 'PLimHi1';
SUBC>   Fits 'FITS1';
SUBC>   Residuals 'RESI1';
SUBC>   SResiduals 'SRES1'.
```

## Response Surface Regression: %Degradation versus Pigment Conc, Catalyst Loa, ..

The analysis was done using coded units.

Estimated Regression Coefficients for %Degradation

| Term | Coef | SE Coef | T | P |
|---|---|---|---|---|
| Constant | 97.8880 | 3.692 | 26.510 | 0.000 |
| Pigment Concentration (mg/L) | 5.2292 | 2.007 | 2.606 | 0.023 |
| Catalyst Loading (g/L) | 9.0788 | 2.045 | 4.440 | 0.001 |
| Time of exposure (min.) | 47.3025 | 1.880 | 25.155 | 0.000 |
| pH | 1.2682 | 1.846 | 0.687 | 0.505 |
| Pigment Concentration (mg/L)* Pigment Concentration (mg/L) | -2.9893 | 2.897 | -1.032 | 0.323 |
| Catalyst Loading (g/L)* Catalyst Loading (g/L) | -9.4518 | 2.897 | -3.262 | 0.007 |
| Time of exposure (min.)* Time of exposure (min.) | -46.0999 | 2.848 | -16.185 | 0.000 |
| pH*pH | -1.0159 | 2.770 | -0.367 | 0.720 |
| Pigment Concentration (mg/L)* Catalyst Loading (g/L) | -9.1851 | 3.877 | -2.369 | 0.035 |
| Pigment Concentration (mg/L)* Time of exposure (min.) | 1.4875 | 3.257 | 0.457 | 0.656 |
| Pigment Concentration (mg/L)*pH | -1.3720 | 3.076 | -0.446 | 0.663 |
| Catalyst Loading (g/L)* Time of exposure (min.) | 3.8350 | 3.257 | 1.177 | 0.262 |
| Catalyst Loading (g/L)*pH | -2.1495 | 3.076 | -0.699 | 0.498 |
| Time of exposure (min.)*pH | 0.4000 | 3.257 | 0.123 | 0.904 |

S = 6.51416  PRESS = 2942.24
R-Sq = 98.79%  R-Sq(pred) = 93.00%  R-Sq(adj) = 97.37%

Analysis of Variance for %Degradation

| Source | DF | Seq SS |
|---|---|---|
| Regression | 14 | 41499.1 |
| Linear | 4 | 28675.9 |
| Pigment Concentration (mg/L) | 1 | 265.5 |
| Catalyst Loading (g/L) | 1 | 1542.3 |
| Time of exposure (min.) | 1 | 26850.3 |
| pH | 1 | 17.8 |
| Square | 4 | 12439.8 |
| Pigment Concentration (mg/L)*Pigment Concentration (mg/L) | 1 | 243.7 |
| Catalyst Loading (g/L)*Catalyst Loading (g/L) | 1 | 1.3 |
| Time of exposure (min.)*Time of exposure (min.) | 1 | 12183.4 |
| pH*pH | 1 | 11.4 |
| Interaction | 6 | 383.4 |
| Pigment Concentration (mg/L)*Catalyst Loading (g/L) | 1 | 282.2 |
| Pigment Concentration (mg/L)*Time of exposure (min.) | 1 | 8.9 |
| Pigment Concentration (mg/L)*pH | 1 | 12.1 |
| Catalyst Loading (g/L)*Time of exposure (min.) | 1 | 58.8 |

| | | |
|---|---|---|
| Catalyst Loading (g/L)*pH | 1 | 20.7 |
| Time of exposure (min.)*pH | 1 | 0.6 |
| Residual Error | 12 | 509.2 |
| Lack-of-Fit | 10 | 509.1 |
| Pure Error | 2 | 0.1 |
| Total | 26 | 42008.3 |

| Source | Adj SS | Adj MS |
|---|---|---|
| Regression | 41499.1 | 2964.2 |
| Linear | 28267.7 | 7066.9 |
| Pigment Concentration (mg/L) | 288.1 | 288.1 |
| Catalyst Loading (g/L) | 836.6 | 836.6 |
| Time of exposure (min.) | 26850.3 | 26850.3 |
| pH | 20.0 | 20.0 |
| Square | 12733.3 | 3183.3 |
| Pigment Concentration (mg/L)*Pigment Concentration (mg/L) | 45.2 | 45.2 |
| Catalyst Loading (g/L)*Catalyst Loading /L) | 451.6 | 451.6 |
| Time of exposure (min.)*Time of exposure (min.) | 11115.9 | 11115.9 |
| pH*pH | 5.7 | 5.7 |
| Interaction | 383.4 | 63.9 |
| Pigment Concentration (mg/L)*Catyst Loading (g/L) | 238.2 | 238.2 |
| Pigment Concentration (mg/L)*Te of exposure (min.) | 8.9 | 8.9 |
| Pigment Concentration (mg/L)H | 8.4 | 8.4 |
| Catalyst Loading (g/L)*Time of exposure (min.) | 58.8 | 58.8 |
| Catalyst Loading (g/L)*pH | 20.7 | 20.7 |
| Time of exposure (min.)*pH | 0.6 | 0.6 |
| Residual Error | 509.2 | 42.4 |
| Lack-of-Fit | 509.1 | 50.9 |
| Pure Error | 0.1 | 0.1 |
| Total | | |

| Source | F | P |
|---|---|---|
| Regression | 69.85 | 0.000 |
| Linear | 166.54 | 0.000 |
| Pigment Concentration (mg/L) | 6.79 | 0.023 |
| Catalyst Loading (g/L) | 19.71 | 0.001 |
| Time of exposure (min.) | 632.75 | 0.000 |
| pH | 0.47 | 0.505 |
| Square | 75.02 | 0.000 |
| Pigment Concentration (mg/L)*Pigment Concentration (mg/L) | 1.06 | 0.323 |
| Catalyst Loading (g/L)*Catalyst Loading (g/L) | 10.64 | 0.007 |
| Time of exposure (min.)*Time of exposure (min.) | 261.96 | 0.000 |
| pH*pH | 0.13 | 0.720 |
| Interaction | 1.51 | 0.257 |
| Pigment Concentration (mg/L)*Catalyst Loading (g/L) | 5.61 | 0.035 |
| Pigment Concentration (mg/L)*Time of exposure (min.) | 0.21 | 0.656 |
| Pigment Concentration (mg/L)*pH | 0.20 | 0.663 |
| Catalyst Loading (g/L)*Time of exposure (min.) | 1.39 | 0.262 |
| Catalyst Loading (g/L)*pH | 0.49 | 0.498 |
| Time of exposure (min.)*pH | 0.02 | 0.904 |
| Residual Error | | |
| Lack-of-Fit | 949.23 | 0.001 |
| Pure Error | | |
| Total | | |

Unusual Observations for %Degradation

| Obs | StdOrder | %Degradation | Fit | SE Fit | Residual | St Resid | |
|---|---|---|---|---|---|---|---|
| 8 | 8 | 0.000 | -10.210 | 5.129 | 10.210 | 2.54 | R |

R denotes an observation with a large standardized residual.

Estimated Regression Coefficients for %Degradation using data in uncoded units

| Term | Coef |
|---|---|
| Constant | -170.084 |
| Pigment Concentration (mg/L) | 4.69860 |
| Catalyst Loading (g/L) | 58.8018 |
| Time of exposure (min.) | 2.87973 |
| pH | 23.5901 |
| Pigment Concentration (mg/L)* Pigment Concentration (mg/L) | -0.0531434 |
| Catalyst Loading (g/L)* Catalyst Loading (g/L) | -9.45181 |
| Time of exposure (min.)* Time of exposure (min.) | -0.0227654 |
| pH*pH | -1.01587 |
| Pigment Concentration (mg/L)* Catalyst Loading (g/L) | -1.22469 |
| Pigment Concentration (mg/L)* Time of exposure (min.) | 0.00440741 |
| Pigment Concentration (mg/L)*pH | -0.182937 |
| Catalyst Loading (g/L)* Time of exposure (min.) | 0.0852222 |
| Catalyst Loading (g/L)*pH | -2.14953 |
| Time of exposure (min.)*pH | 0.00888889 |

Predicted Response for New Design Points Using Model for %Degradation

| Point | Fit | SE Fit | 95% CI | 95% PI |
|---|---|---|---|---|
| 1 | 4.338 | 5.03965 | ( -6.6425, 15.318) | (-13.6068, 22.283) |
| 2 | 99.216 | 5.08520 | ( 88.1362, 110.296) | ( 81.2102, 117.222) |
| 3 | 5.238 | 5.10649 | ( -5.8880, 16.364) | (-12.7962, 23.272) |
| 4 | 102.818 | 5.10649 | ( 91.6920, 113.944) | ( 84.7838, 120.852) |
| 5 | 99.008 | 5.08017 | ( 87.9394, 110.077) | ( 81.0092, 117.007) |
| 6 | 90.570 | 4.94568 | ( 79.7941, 101.345) | ( 72.7495, 108.390) |
| 7 | 99.743 | 5.03965 | ( 88.7625, 110.723) | ( 81.7982, 117.688) |
| 8 | -10.210 | 5.12894 | (-21.3850, 0.965) | (-28.2745, 7.855) |
| 9 | 96.407 | 5.02443 | ( 85.4593, 107.354) | ( 78.4821, 114.331) |
| 10 | 97.888 | 3.69244 | ( 89.8429, 105.933) | ( 81.5733, 114.203) |
| 11 | 0.278 | 4.98377 | (-10.5810, 11.136) | (-17.5929, 18.148) |
| 12 | 97.380 | 4.96966 | ( 86.5525, 108.208) | ( 79.5286, 115.232) |
| 13 | 76.725 | 5.12894 | ( 65.5500, 87.900) | ( 58.6605, 94.790) |
| 14 | -2.245 | 4.97608 | (-13.0873, 8.597) | (-20.1057, 15.615) |
| 15 | 2.602 | 5.02443 | ( -8.3457, 13.549) | (-15.3229, 20.526) |
| 16 | 74.924 | 4.65532 | ( 64.7808, 85.067) | ( 57.4788, 92.369) |
| 17 | 95.618 | 4.90242 | ( 84.9363, 106.299) | ( 77.8544, 113.381) |
| 18 | 102.553 | 4.98377 | ( 91.6940, 113.411) | ( 84.6821, 120.423) |
| 19 | 86.013 | 4.39144 | ( 76.4453, 95.582) | ( 68.8963, 103.130) |
| 20 | 56.148 | 4.90421 | ( 45.4628, 66.833) | ( 38.3824, 73.914) |
| 21 | 81.759 | 5.08520 | ( 70.6795, 92.839) | ( 63.7535, 99.765) |
| 22 | 91.294 | 4.96966 | ( 80.4659, 102.122) | ( 73.4419, 109.146) |
| 23 | 97.888 | 3.69244 | ( 89.8429, 105.933) | ( 81.5733, 114.203) |
| 24 | 97.888 | 3.69244 | ( 89.8429, 105.933) | ( 81.5733, 114.203) |
| 25 | 61.954 | 4.42240 | ( 52.3182, 71.589) | ( 44.7989, 79.109) |
| 26 | 89.385 | 4.97608 | ( 78.5427, 100.227) | ( 71.5243, 107.245) |
| 27 | 98.482 | 5.51209 | ( 86.4718, 110.491) | ( 79.8891, 117.074) |

Regression Equation data for AP1

| Predictor | Coef | SE Coef | T | P |
|---|---|---|---|---|
| Constant | -3.47 | 62.26 | -0.06 | 0.956 |
| Pigment Concentration (mg/L) | 0.3619 | 0.9690 | 0.37 | 0.712 |
| Catalyst Loading (g/L) | 11.414 | 7.226 | 1.58 | 0.128 |
| Time of exposure (min.) | 1.0512 | 0.1579 | 6.66 | 0.000 |

```
pH                            1.179    6.873   0.17  0.865

S = 24.6175   R-Sq = 68.3%   R-Sq(adj) = 62.5%

Analysis of Variance

Source          DF       SS      MS      F      P
Regression       4  28675.9  7169.0  11.83  0.000
Residual Error  22  13332.4   606.0
Total           26  42008.3

Source                          DF   Seq SS
Pigment Concentration (mg/L)     1    265.5
Catalyst Loading (g/L)           1   1542.3
Time of exposure (min.)          1  26850.3
pH                               1     17.8
```

| Obs | Pigment Concentration (mg/L) | %Degradation | Fit | SE Fit | Residual | St Resid |
|---|---|---|---|---|---|---|
| 1 | 12.5 | 0.00 | 24.26 | 11.12 | -24.26 | -1.10 |
| 2 | 20.0 | 99.20 | 71.92 | 11.56 | 27.28 | 1.26 |
| 3 | 20.0 | 0.00 | 25.79 | 11.56 | -25.79 | -1.19 |
| 4 | 20.0 | 99.52 | 120.40 | 11.56 | -20.88 | -0.96 |
| 5 | 20.0 | 99.37 | 74.27 | 11.28 | 25.10 | 1.15 |
| 6 | 20.0 | 98.76 | 84.51 | 10.81 | 14.25 | 0.64 |
| 7 | 12.5 | 98.78 | 118.86 | 11.12 | -20.08 | -0.91 |
| 8 | 12.5 | 0.00 | 11.66 | 11.27 | -11.66 | -0.53 |
| 9 | 12.5 | 97.18 | 116.50 | 10.84 | -19.32 | -0.87 |
| 10 | 12.5 | 97.24 | 70.38 | 4.77 | 26.86 | 1.11 |
| 11 | 12.5 | 0.00 | 34.49 | 11.13 | -34.49 | -1.57 |
| 12 | 12.5 | 96.79 | 80.62 | 11.16 | 16.17 | 0.74 |
| 13 | 12.5 | 81.62 | 106.27 | 11.27 | -24.65 | -1.13 |
| 14 | 5.0 | 0.00 | 20.36 | 10.89 | -20.36 | -0.92 |
| 15 | 12.5 | 0.00 | 21.90 | 10.84 | -21.90 | -0.99 |
| 16 | 12.5 | 74.17 | 57.79 | 10.67 | 16.38 | 0.74 |
| 17 | 12.5 | 98.52 | 82.97 | 10.81 | 15.55 | 0.70 |
| 18 | 12.5 | 96.96 | 129.10 | 11.13 | -32.14 | -1.46 |
| 19 | 5.0 | 93.47 | 66.49 | 10.29 | 26.98 | 1.21 |
| 20 | 5.0 | 51.88 | 55.07 | 11.65 | -3.19 | -0.15 |
| 21 | 12.5 | 80.23 | 60.14 | 11.56 | 20.09 | 0.92 |
| 22 | 5.0 | 94.86 | 68.84 | 11.16 | 26.02 | 1.19 |
| 23 | 12.5 | 97.37 | 70.38 | 4.77 | 26.99 | 1.12 |
| 24 | 12.5 | 96.92 | 70.38 | 4.77 | 26.54 | 1.10 |
| 25 | 5.0 | 53.40 | 56.25 | 10.23 | -2.85 | -0.13 |
| 26 | 5.0 | 93.57 | 114.97 | 10.89 | -21.40 | -0.97 |
| 27 | 5.0 | 93.85 | 79.08 | 11.65 | 14.77 | 0.68 |

## Box-Behnken Design For AP2

```
Factors:       4     Replicates:     1
Base runs:    27     Total runs:    27
Base blocks:   1     Total blocks:   1

Center points: 3

MTB > Name C12 "FITS1" C13 "RESI1" C14 "SRES1" C15 "PFit1" C16 "PSEFit1" C17
"CLimLo1" &
CONT> C18 "CLimHi1" C19 "PLimLo1" C20 "PLimHi1"
MTB > RSRegress '%Degradation' = C5 C6 C7 C8 C5*C5 C6*C6 C7*C7 C8*C8 C5*C6 C5*C7
C5*C8 &
CONT> C6*C7 C6*C8 C7*C8;
```

```
SUBC>   Order C1;
SUBC>   InUnit 1 0;
SUBC>   Levels 5 20 0 2 0 90 8 10;
SUBC>   GHistogram;
SUBC>   GNormal;
SUBC>   GFits;
SUBC>   GOrder C2;
SUBC>   Brief 2;
SUBC>   Predict C5 C6 C7 C8;
SUBC>     Confidence 95;
SUBC>     PFit 'PFit1';
SUBC>     PSEFit 'PSEFit1';
SUBC>     CLimits 'CLimLo1' 'CLimHi1';
SUBC>     PLimits 'PLimLo1' 'PLimHi1';
SUBC>   Fits 'FITS1';
SUBC>   Residuals 'RESI1';
SUBC>   SResiduals 'SRES1'.
```

## Response Surface Regression: %Degradation versus Pigment Conc, Catalyst Loa, ..

```
The analysis was done using coded units.

Estimated Regression Coefficients for %Degradation

Term                                    Coef  SE Coef        T      P
Constant                             97.4719    4.300   22.669  0.000
Pigment Concentration (mg/L)          3.2771    2.337    1.402  0.186
Catalyst Loading (g/L)               15.4948    2.381    6.508  0.000
Time of exposure (min.)              45.4500    2.190   20.755  0.000
pH                                    0.2909    2.150    0.135  0.895
Pigment Concentration (mg/L)*        -1.7197    3.374   -0.510  0.620
  Pigment Concentration (mg/L)
Catalyst Loading (g/L)*             -16.0747    3.374   -4.764  0.000
  Catalyst Loading (g/L)
Time of exposure (min.)*            -45.3750    3.317  -13.680  0.000
  Time of exposure (min.)
pH*pH                                -2.1464    3.226   -0.665  0.518
Pigment Concentration (mg/L)*        -5.0237    4.515   -1.113  0.288
  Catalyst Loading (g/L)
Pigment Concentration (mg/L)*         0.7800    3.793    0.206  0.841
  Time of exposure (min.)
Pigment Concentration (mg/L)*pH       0.2147    3.582    0.060  0.953
Catalyst Loading (g/L)*               9.0725    3.793    2.392  0.034
  Time of exposure (min.)
Catalyst Loading (g/L)*pH            -0.7178    3.582   -0.200  0.845
Time of exposure (min.)*pH            0.0325    3.793    0.009  0.993


S = 7.58566    PRESS = 4214.27
R-Sq = 98.36%  R-Sq(pred) = 89.98%  R-Sq(adj) = 96.44%

Analysis of Variance for %Degradation

Source                                                        DF   Seq SS
Regression                                                    14  41354.7
  Linear                                                       4  28326.7
    Pigment Concentration (mg/L)                               1    205.4
    Catalyst Loading (g/L)                                     1   3332.9
    Time of exposure (min.)                                    1  24788.4
    pH                                                         1      0.0
  Square                                                       4  12617.3
    Pigment Concentration (mg/L)*Pigment Concentration (mg/L)  1    624.9
    Catalyst Loading (g/L)*Catalyst Loading (g/L)              1    216.1
```

| | | |
|---|---|---|
| Time of exposure (min.)*Time of exposure (min.) | 1 | 11748.1 |
| pH*pH | 1 | 28.3 |
| Interaction | 6 | 410.6 |
| Pigment Concentration (mg/L)*Catalyst Loading (g/L) | 1 | 76.6 |
| Pigment Concentration (mg/L)*Time of exposure (min.) | 1 | 2.4 |
| Pigment Concentration (mg/L)*pH | 1 | 0.1 |
| Catalyst Loading (g/L)*Time of exposure (min.) | 1 | 329.2 |
| Catalyst Loading (g/L)*pH | 1 | 2.3 |
| Time of exposure (min.)*pH | 1 | 0.0 |
| Residual Error | 12 | 690.5 |
| Lack-of-Fit | 10 | 690.5 |
| Pure Error | 2 | 0.0 |
| Total | 26 | 42045.2 |

| Source | Adj SS | Adj MS |
|---|---|---|
| Regression | 41354.7 | 2953.9 |
| Linear | 27675.6 | 6918.9 |
| Pigment Concentration (mg/L) | 113.1 | 113.1 |
| Catalyst Loading (g/L) | 2436.8 | 2436.8 |
| Time of exposure (min.) | 24788.4 | 24788.4 |
| pH | 1.1 | 1.1 |
| Square | 12690.0 | 3172.5 |
| Pigment Concentration (mg/L)*Pigment Concentration (mg/L) | 14.9 | 14.9 |
| Catalyst Loading (g/L)*Catalyst Loading (g/L) | 1306.1 | 1306.1 |
| Time of exposure (min.)*Time of exposure (min.) | 10769.1 | 10769.1 |
| pH*pH | 25.5 | 25.5 |
| Interaction | 410.6 | 68.4 |
| Pigment Concentration (mg/L)*Catalyst Loading (g/L) | 71.2 | 71.2 |
| Pigment Concentration (mg/L)*Time of exposure (min.) | 2.4 | 2.4 |
| Pigment Concentration (mg/L)*pH | 0.2 | 0.2 |
| Catalyst Loading (g/L)*Time of exposure (min.) | 329.2 | 329.2 |
| Catalyst Loading (g/L)*pH | 2.3 | 2.3 |
| Time of exposure (min.)*pH | 0.0 | 0.0 |
| Residual Error | 690.5 | 57.5 |
| Lack-of-Fit | 690.5 | 69.1 |
| Pure Error | 0.0 | 0.0 |
| Total | | |

| Source | F | P |
|---|---|---|
| Regression | 51.33 | 0.000 |
| Linear | 120.24 | 0.000 |
| Pigment Concentration (mg/L) | 1.97 | 0.186 |
| Catalyst Loading (g/L) | 42.35 | 0.000 |
| Time of exposure (min.) | 430.79 | 0.000 |
| pH | 0.02 | 0.895 |
| Square | 55.13 | 0.000 |
| Pigment Concentration (mg/L)*Pigment Concentration (mg/L) | 0.26 | 0.620 |
| Catalyst Loading (g/L)*Catalyst Loading (g/L) | 22.70 | 0.000 |
| Time of exposure (min.)*Time of exposure (min.) | 187.15 | 0.000 |
| pH*pH | 0.44 | 0.518 |
| Interaction | 1.19 | 0.374 |
| Pigment Concentration (mg/L)*Catalyst Loading (g/L) | 1.24 | 0.288 |
| Pigment Concentration (mg/L)*Time of exposure (min.) | 0.04 | 0.841 |
| Pigment Concentration (mg/L)*pH | 0.00 | 0.953 |
| Catalyst Loading (g/L)*Time of exposure (min.) | 5.72 | 0.03 |
| Catalyst Loading (g/L)*pH | 0.04 | 0.845 |
| Time of exposure (min.)*pH | 0.00 | 0.993 |
| Residual Error | | |
| Lack-of-Fit | 295931.50 | 0.000 |
| Pure Error | | |
| Total | | |

Unusual Observations for %Degradation

| Obs | StdOrder | %Degradation | Fit | SE Fit | Residual | St Resid |
|---|---|---|---|---|---|---|
| 27 | 13 | 0.000 | -15.850 | 5.973 | 15.850 | 3.39 R |

R denotes an observation with a large standardized residual.

Estimated Regression Coefficients for %Degradation using data in uncoded units

| Term | Coef |
|---|---|
| Constant | -212.586 |
| Pigment Concentration (mg/L) | 1.50949 |
| Catalyst Loading (g/L) | 53.4052 |
| Time of exposure (min.) | 2.78966 |
| pH | 39.2534 |
| Pigment Concentration (mg/L)* Pigment Concentration (mg/L) | -0.0305726 |
| Catalyst Loading (g/L)* Catalyst Loading (g/L) | -16.0747 |
| Time of exposure (min.)* Time of exposure (min.) | -0.0224074 |
| pH*pH | -2.14638 |
| Pigment Concentration (mg/L)* Catalyst Loading (g/L) | -0.669826 |
| Pigment Concentration (mg/L)* Time of exposure (min.) | 0.00231111 |
| Pigment Concentration (mg/L)*pH | 0.0286209 |
| Catalyst Loading (g/L)* Time of exposure (min.) | 0.201611 |
| Catalyst Loading (g/L)*pH | -0.717843 |
| Time of exposure (min.)*pH | 0.000722222 |

Predicted Response for New Design Points Using Model for %Degradation

| Point | Fit | SE Fit | 95% CI | 95% PI |
|---|---|---|---|---|
| 1 | 99.884 | 5.94644 | ( 86.9281, 112.840) | ( 78.8836, 120.885) |
| 2 | 95.173 | 5.78711 | ( 82.5635, 107.782) | ( 74.3842, 115.961) |
| 3 | 4.242 | 5.85088 | ( -8.5059, 16.990) | (-16.6308, 25.115) |
| 4 | 97.472 | 4.29980 | ( 88.1034, 106.840) | ( 78.4736, 116.470) |
| 5 | 55.882 | 5.14982 | ( 44.6614, 67.102) | ( 35.9053, 75.859) |
| 6 | 62.747 | 5.42106 | ( 50.9357, 74.559) | ( 42.4327, 83.062) |
| 7 | 96.919 | 6.41877 | ( 82.9337, 110.904) | ( 75.2682, 118.570) |
| 8 | 56.905 | 5.97259 | ( 43.8917, 69.918) | ( 35.8690, 77.941) |
| 9 | 64.765 | 5.92165 | ( 51.8626, 77.667) | ( 43.7974, 85.732) |
| 10 | 96.377 | 5.92165 | ( 83.4751, 109.279) | ( 75.4099, 117.345) |
| 11 | 4.759 | 5.86861 | ( -8.0276, 17.546) | (-16.1375, 25.655) |
| 12 | 52.941 | 5.71089 | ( 40.4984, 65.384) | ( 32.2534, 73.629) |
| 13 | -3.005 | 5.80353 | (-15.6503, 9.639) | (-23.8155, 17.805) |
| 14 | 97.472 | 4.29980 | ( 88.1034, 106.840) | ( 78.4736, 116.470) |
| 15 | 95.724 | 5.86861 | ( 82.9374, 108.511) | ( 74.8275, 116.620) |
| 16 | 7.424 | 5.94644 | ( -5.5319, 20.380) | (-13.5764, 28.425) |
| 17 | 106.040 | 5.80353 | ( 93.3947, 118.684) | ( 85.2295, 126.850) |
| 18 | 90.252 | 5.11377 | ( 79.1105, 101.394) | ( 70.3198, 110.185) |
| 19 | 97.388 | 5.91580 | ( 84.4991, 110.278) | ( 76.4289, 118.348) |
| 20 | 91.770 | 5.79458 | ( 79.1449, 104.395) | ( 70.9720, 112.568) |
| 21 | 93.426 | 5.75918 | ( 80.8775, 105.974) | ( 72.6742, 114.177) |
| 22 | 94.319 | 5.70880 | ( 81.8803, 106.757) | ( 73.6335, 115.004) |
| 23 | 2.430 | 5.79458 | (-10.1951, 15.055) | (-18.3680, 23.228) |
| 24 | 90.405 | 5.78711 | ( 77.7960, 103.014) | ( 69.6167, 111.193) |
| 25 | 97.472 | 4.29980 | ( 88.1034, 106.840) | ( 78.4736, 116.470) |
| 26 | 95.077 | 5.85088 | ( 82.3291, 107.825) | ( 74.2042, 115.950) |

```
   27  -15.850  5.97259  (-28.8633,  -2.837)  (-36.8860,   5.186)
```

Regression equation data for AP2

| Predictor | Coef | SE Coef | T | P |
|---|---|---|---|---|
| Constant | 3.17 | 63.16 | 0.05 | 0.960 |
| Pigment Concentration (mg/L) | 0.1746 | 0.9829 | 0.18 | 0.861 |
| Catalyst Loading (g/L) | 16.904 | 7.330 | 2.31 | 0.031 |
| Time of exposure (min.) | 1.0100 | 0.1602 | 6.30 | 0.000 |
| pH | 0.012 | 6.972 | 0.00 | 0.999 |

S = 24.9713   R-Sq = 67.4%   R-Sq(adj) = 61.4%

Analysis of Variance

| Source | DF | SS | MS | F | P |
|---|---|---|---|---|---|
| Regression | 4 | 28326.7 | 7081.7 | 11.36 | 0.000 |
| Residual Error | 22 | 13718.5 | 623.6 | | |
| Total | 26 | 42045.2 | | | |

| Source | DF | Seq SS |
|---|---|---|
| Pigment Concentration (mg/L) | 1 | 205.4 |
| Catalyst Loading (g/L) | 1 | 3332.9 |
| Time of exposure (min.) | 1 | 24788.4 |
| pH | 1 | 0.0 |

| Obs | Pigment Concentration (mg/L) | %Degradation | Fit | SE Fit | Residual | St Resid |
|---|---|---|---|---|---|---|
| 1 | 20.0 | 98.16 | 114.58 | 11.73 | -16.42 | -0.74 |
| 2 | 12.5 | 96.84 | 84.71 | 11.32 | 12.13 | 0.55 |
| 3 | 12.5 | 0.00 | 22.35 | 10.99 | -22.35 | -1.00 |
| 4 | 12.5 | 97.41 | 67.82 | 4.84 | 29.59 | 1.21 |
| 5 | 5.0 | 49.10 | 49.60 | 10.38 | -0.50 | -0.02 |
| 6 | 12.5 | 56.53 | 50.90 | 10.82 | 5.63 | 0.25 |
| 7 | 5.0 | 94.42 | 83.41 | 11.82 | 11.01 | 0.50 |
| 8 | 12.5 | 60.44 | 96.36 | 11.43 | -35.92 | -1.62 |
| 9 | 12.5 | 58.83 | 50.92 | 11.73 | 7.91 | 0.36 |
| 10 | 20.0 | 98.58 | 69.11 | 11.73 | 29.47 | 1.34 |
| 11 | 12.5 | 0.00 | 22.38 | 11.28 | -22.38 | -1.00 |
| 12 | 5.0 | 52.49 | 49.59 | 11.82 | 2.90 | 0.13 |
| 13 | 12.5 | 0.00 | 39.27 | 11.29 | -39.27 | -1.76 |
| 14 | 12.5 | 97.38 | 67.82 | 4.84 | 29.56 | 1.21 |
| 15 | 12.5 | 97.58 | 113.28 | 11.28 | -15.70 | -0.70 |
| 16 | 20.0 | 0.00 | 23.68 | 11.73 | -23.68 | -1.07 |
| 17 | 12.5 | 96.73 | 130.17 | 11.29 | -33.44 | -1.50 |
| 18 | 5.0 | 94.92 | 66.50 | 10.44 | 28.42 | 1.25 |
| 19 | 20.0 | 99.60 | 69.14 | 11.44 | 30.46 | 1.37 |
| 20 | 5.0 | 95.04 | 111.96 | 11.04 | -16.92 | -0.76 |
| 21 | 20.0 | 98.16 | 86.03 | 10.96 | 12.13 | 0.54 |
| 22 | 12.5 | 96.72 | 84.73 | 10.97 | 11.99 | 0.53 |
| 23 | 5.0 | 0.00 | 21.06 | 11.04 | -21.06 | -0.94 |
| 24 | 5.0 | 94.63 | 66.52 | 11.32 | 28.11 | 1.26 |
| 25 | 12.5 | 97.40 | 67.82 | 4.84 | 29.58 | 1.21 |
| 26 | 12.5 | 97.45 | 113.25 | 10.99 | -15.80 | -0.70 |
| 27 | 12.5 | 0.00 | 5.46 | 11.43 | -5.46 | -0.25 |